Intelligent Control for Distillation Columns

By

YOUSIF AL-DUNAINAWI

A Thesis Submitted

in Partial Fulfilment of the Requirements for the Degree of

DOCTOR OF PHILOSOPHY

Department of Electronic and Computer Engineering

College of Engineering, Design and Physical Sciences

BRUNEL UNIVERSITY LONDON

September 2017

Dedication

I dedicate this thesis to:

- ♡ **My beloved parents, for their prayers and wishes;**
- ♡ **My wife for her patience and steadfast support;**
- ♡ **My sons, Muhab and Hassan, in whose glistening eyes, I can see my own unfulfilled ambitions.**

Declaration

I declare that this thesis is my own work and is submitted for the first time to the Post-Graduate Research Office. The study was originated, composed and reviewed by myself and my supervisor in the Department of Electronic and Computer Engineering, College of Engineering, Design and Physical Sciences, Brunel University London UK. All the information derived from other works has been properly referenced and acknowledged.

Yousif Khalaf Yousif Al-Dunainawi

September 2017

Acknowledgements

First, I would like to express my sincere gratitude to my supervisor Dr Maysam F. Abbod for his ongoing support of my PhD journey, for his patience, inspiration, and immense knowledge. His supervision helped me through the research period and the writing up of this thesis.

I would also like to thank my sponsor, the Iraqi Ministry of Higher Education and Scientific Research, as represented by the Iraqi Cultural Attaché in London, for giving me this opportunity to complete my study and I am also grateful for their unstinting support and care.

Moreover, I am grateful to my friends Ali, Saad, Dhurgam and Dheyaa from Buckingham University for the limitless backing they gave. In addition, I am thankful to my colleagues at Brunel University; Omar, Ann, Raad and Shireen for all the fun and challenging days during this journey.

Last but not the least, I would like to thank my family: my parents and my brothers and sisters for supporting me spiritually throughout writing this thesis and my life in general. Finally, I bless my wife for her patience and support.

Abstract

Nowadays, industrial processes are having to be rapidly developed to meet high standards regarding increases in the production rate and/or improving product quality. Fulfilling these requirements is having to work in tandem with the pressure to reduce energy consumption due to global environmental regulations. Consequently, most industrial processes critically rely on automatic control, which can provide efficient solutions to meet such challenges and prerequisites. For this thesis, an intelligent system design has been investigated for controlling the distillation process, which is characterised by highly nonlinear and dynamic behaviour. These features raise very challenging tasks for control systems designers. Fuzzy logic and artificial neural networks (ANNs) are the main methods used in this study to design different controllers, namely: PI- PD- and PID-like fuzzy controllers, ANN-based NARMA-L2 in addition to a conventional PID controller for comparison purposes. Genetic algorithm (GA) and particle swarm optimisation (PSO) have also been utilised to tune fuzzy controllers by finding the best set of scaling factors. Finally, an intelligent controller is proposed, called ANFIS-based NARMA-L2, which uses ANFIS as an approximation approach for identifying the underlying systems in a NARMA-L2 configuration. The controllers are applied to control two compositions of a binary distillation column, which has been modelled and simulated in MATLAB® and on the Simulink® platform.

Comparative analysis has been undertaken to investigate the controllers' performance, which shows that PID-like FLC outperforms the other tested fuzzy control configurations, i.e. PI- and PD-like. Moreover, PSO has been found to outperform GA in finding the best set of scaling factors and over a shorter time period. Subsequently, the performance of PID-like FLC has been compared with ANN-based NARMA-L2 and the proposed ANFIS-based

NARMA-L2, by subjecting the controlled column to different test scenarios. Furthermore, the stability and robustness of the controllers have been assessed by subjecting the controlled column to inputs variance and disturbances situations. The proposed ANFIS-based NARMA-L2 controller outperforms and demonstrates more tolerance of disturbances than the other controllers.

Finally, the study has involved investigating the control of a multicomponent distillation column due to its significant enhancement in operational efficiency regarding energy saving and recent widespread implementation. That is, Kaibel's distillation column with 4×4 configuration has been simulated also in MATLAB® and on the Simulink® platform with the proposed controller being implemented to control the temperatures of the column and the outcomes subsequently compared with conventional PID controllers. Again, the novel controller has proven its superiority regarding the disturbances tolerance as well as dealing with the high dynamics and nonlinear behaviour.

Table of contents

List of figures

List of tables

List of Abbreviations

ANFIS	Adaptive Network-based Fuzzy Inference System
ANN	Artificial Neural Network
ARMA	Autoregressive-Moving Average Models
ARMAX	Autoregressive–Moving-Average Model with exogenous inputs model
ARX	Autoregressive Exogenous
BP	Backpropagation
BTX	Benzene, Toluene, and the three Xylene isomers
CARIMA	Controlled Auto-Regressive Integrated Moving Average
CPSO	Chaos-based Particle Swarm Optimisation
DMC	Dynamic Matrix Control
EC	Evolutionary Computation average charts
FFANNs	Feedforward Artificial Neural Networks
FIS	Fuzzy Inference System
FL	Fuzzy Logic
FLC	Fuzzy Logic Control
FTCDC	Fully Thermally Coupled Distillation Column

List of abbreviations

GA	Genetic Algorithm
GB	Global Best position
ISE	Integral Squared Error
ITAE	Integral Time-weighted Absolute Error
MA	Moving Average
MF	Membership Function
MIMO	Multiple-Input–Multiple-Output
MPC	Model Predictive Control
MRC	Model Reference Control
MV	Manipulated Variable
NARMA	Nonlinear Autoregressive Moving Average
NF	Neuro-Fuzzy
NPA	Normal Propanol
ODE	Ordinary Differential Equation
LB	Local Best Position
PID	Proportional-Integral-Derivative
PLSR	Partial Least Square Regression
PSO	Particle Swarm Optimisation
PV	Photovoltaic
RBFNN	Radial Basis Function Neural Network
RMSE	Root Mean Squared Errors
SI	Swarm Intelligence
SISO	Single-Input Single-Output
TSK	Takagi-Sugeno-Kang

Chapter 1

Introduction

1.1 Background

As a result of the global ambition for the more reliable attainment of high product quality, more efficient use of energy, tighter safety as well as environmental regulations, industrial processes have evolved over recent years into very complex, highly nonlinear and integrated systems. Rigorous demands like these naturally lead to more difficult and challenging control problems for today's industrial control engineers; problems requiring more efficient solutions than can be achieved only by conventional techniques. It also requires inter- and cross-disciplinary research and development, in addition to collaboration in both industry and academia. Cooperation between control and other disciplines has been consistently fruitful [1].

A big drive has been seen in the academic community to design new control systems, either by traditional or contemporary methods. Introducing an ingenious control system can be the key factor in improving performance as well as for dealing better with the challenging features of nonlinear and complex processes. In general, when implementing conventional control systems, a reasonable performance is attained over a narrow operating range. However, when a wide range of process tasks is a prerequisite, nonlinearity becomes more evident and hence, the control performance may be sacrificed [2].

Intelligence based methods emerged more than two decades ago to act as an effective solution for many applications, with many comprehensive reviews having been written demonstrating its importance across a wide range of applications [3–5]. From a control view-point, when nonlinearity, uncertainty or control difficulties result from dynamic processes, this can bring severe complications to analysis and synthesis. The most commonly applied approaches are ANNs and Fuzzy Logic (FL), which are essential intelligent techniques widely employed to control nonlinear processes. One of the strongest arguments for the use of intelligent based controllers is their ability to exploit the tolerances for uncertainty and nonlinearity, to achieve robustness and controllability, as well as providing affordable solutions [4]. In addition, many intelligent-hybrid approaches have been innovated to provide an efficient solution to a wide range of problems [6–8].

Recent expansions in both ANN and FL controllers have open on to the possibility of adaptation in these schemes as well. Due to, for instance, the ANN's approach to approximate the nonlinear behaviour of systems by a parameterised model, it is an expected development to extend ideas from traditional parameter adaptive control theory to the ANN control system. A comparable method has also been fruitful in FL control. Henceforth, by merging ANN and FL representation concepts with adaptive control methods, the parametric-uncertainty barrier of traditional adaptive control scheme was broken. This produced to the opportunity of presenting an adaptive control design for complex nonlinear processes having unknown functions rather than parameters, which is an essential characteristic of intelligent control [9].

Corresponding to advances in model-based control, is growing consciousness of the advantages provided by the intelligent modelling and control approaches to deliver elegant solutions to modelling and control problems. The term *"intelligent control"* is typically employed to study theory in process control using machine intelligence phenomena [10]. Its aim is to provide understanding by capturing examples of intelligent behaviour, i.e. generalisation, flexibility, learning or adaptive competence and then reproducing these using computers. The design of intelligent controllers has the aim of achieving high performance, even in extreme conditions, such as changing the plant circumstances or the environment or altering the control objectives, without a need for external intervention. This necessitates the controller having the skill to adapt to changes that significantly affecting the operating conditions of the system and such adaptive performance is not characteristically obtainable via conventional control schemes [10].

1.2 Problem Statement and Motivations

In the recent years, there have been outstanding achievements in process control field. However, introducing adequate control is still beset with as yet unsolved serious problems. The most significant challenges to control system design can be concluded as the following:

- **The increasingly complex demands on control systems**
  Progressively, the achievement of robustness and highly dynamic performance is being required for modern control systems to cope with complex demands uncertainty across a wide range of operating processes.

- **Modelling and identification**
  Many advanced control structures are based on modelling and identification of process, and it is commonly considered that capturing the process behaviour is the most exhausting and time-consuming burden when constructing a model- or data-based control design [11].

- **Severe nonlinearities of industrial processes**
  In industry, most of the traditional controllers have applied to linear systems and poor performance has been typical when nonlinearity has been presented, which is the reality for most industrial processes. Consequently, nonlinearity is still a major problem that needs to be tackled by sophisticated control design.

- **Online measurement**
  Many of critical variables are not easily measured nor are any effective tools for measuring them online across several processes. This creates a significant challenge in terms of controlling them and complicates problems, accordingly.

The three above points have been investigated in this thesis by assessing different controllers in regards to robustness and adaptivity by different test scenarios which are carried out on the binary and multicomponent distillation columns, as will be discussed later.

1.3 Thesis Contributions

It will be seen later that different intelligent control designs have been implemented and an extensive investigation has been carried out so as to identify the most efficient intelligent control approach. The distillation process is considered as a case study in this thesis. Distillation columns are the most used units in chemical and petrochemical plants, being characterised as highly nonlinear and having been studied extensively in control and modelling communities. The main contributions of this thesis are listed as follows:

- Conducting validation assessments for the simulated binary and multicomponent distillation columns, Section 4.2.1 on Page 64 and 67;
- Implementing intelligence-based optimisation approaches in MATLAB® and employing them with different controllers for tuning purposes in a Simulink® environment, Section 5.2.2 on Page 83;
- Proposing a new intelligent control for dynamic systems and implementing in for the control distillation process as a case study for both binary and multicomponent scenarios, Section 5.4 on Page 94;
- Introducing a new method for model optimal structure selection by implementing overlapping intelligent-based optimisation approaches, Section 5.4.1 on Page 98 and 99.

The contributions toward handling the nonlinearity and changing the control objectives without a need for external intervention.

1.4 List of Publications

The papers produced from this thesis are listed as follows:

- Y. Al-Dunainawi and M. F. Abbod, "PSO-PD fuzzy control of distillation column," in 2015 SAI Intelligent Systems Conference (IntelliSys), 2015, pp. 554–558.
- Y. Al-Dunainawi and M. F. Abbod, "Hybrid Intelligent Approach for Predicting Product Composition of Distillation column," Int. J. Advance Research Artificial Intelligence, vol. 5, no. 4, pp. 28–34, 2016.
- Y. Al-Dunainawi and M. F. Abbod, "Evolutionary Based Optimisation of Multivariable Fuzzy Control System of a Binary Distillation Column," in UKSim-AMSS 18th International Conference on Computer Modelling and Simulation, 2016, pp. 127–132.
- Y. Al-Dunainawi, M. F. Abbod, and A. Jizany, "A new MIMO ANFIS-PSO based NARMA-L2 controller for nonlinear dynamic systems," Engineering Application of Artificial Intelligence, vol. 62, pp. 265–275, June 2017.

1.5 Thesis Overview

Having provided an introduction, the motivations as well as the contributions in this chapter, the rest of the thesis is organised as follows.

- **Chapter Two:** in this chapter, the background and a literature review regarding intelligent control systems in various applications are discussed. In addition, the various attempts at controlling the distillation process, with different objectives, are outlined in chronologically. A summary at the end of this chapter, stresses the need for intelligent control systems that can deal with the difficulties presented in dynamic systems.
- **Chapter Three:** principles, theory and methods of intelligent control systems are presented in this chapter. There are five sections covering artificial neural networks, fuzzy

logic and an adaptive neuro-fuzzy inference system. In addition, two evolutionary-based optimisation methods, namely, GA and PSO are introduced. All these intelligent-based approaches are employed in this thesis to design various configurations of intelligent controllers.

- **Chapter Four:** this chapter provides a historical background to the distillation process, types of distillation, and its application and importance. The mathematical model of a binary distillation column is also presented as well as the simulation of the column being discussed. At the end of this chapter, a traditional PID controller is implemented to maintain the product compositions of the simulated distillation column.

- **Chapter Five:** several intelligent controllers are applied to control the simulated binary distillation column, including fuzzy controllers, ANN-based NARMA-L2, and the new proposed ANFIS-based NARMA-L2 controller. The performance of these controllers is evaluated and discussed in this chapter under different conditions, including changing set-points and disturbances rejection tests.

- **Chapter Six:** this chapter presents the modelling and control of a multicomponent distillation column. The history and significance of the multicomponent distillation process are explained. The 4-product distillation column is selected to be controlled by the new proposed ANFIS-based NARMA-L2 controller, with a performance comparison being made with a PID controller.

- **Chapter Seven:** provides a summary of the thesis, conclusions and suggestions for future research avenues.

Chapter 2

Background and Literature Review

2.1 Introduction

At the beginning of the 1980s, intelligent control emerged as a significant synergy between computer-aid control systems and the artificial intelligence field. Since then, it has been growing rapidly with great practical importance and potential, the primary helping factor behind its expansion being the advancement of the vital technical and theoretical infrastructures of computer science and real-time computation approaches [12]. Intelligent control pertains to the engineering field where control approaches are designed that endeavour to behave like the intelligent features of the human. These features consist of adaptation, learning and prediction under high uncertainty and deal with large scale data [13]. Such controllers have progressed from traditional control design by the application of artificial intelligence approaches, with an interdisciplinary research approach being required for their further development. In Chapter three, an overview is given about artificial intelligence approaches that are involved in intelligent control design, such as the ANN, FL and intelligent optimisation methods. While this chapter is dedicated to a brief introduction about intelligent control applications in addition to previous work on the subject in different areas. Also, a brief review on the control of the distillation process is provided.

2.2 Applied Control Systems in Industry

Despite the growing body of literature proposing new control systems, these have not had a substantial impact on industrial control in practice. Industry, in general, leans towards being very cautious about implementing any proposed method until it has been confirmed as being effective through heavily endorsed testing. Consequently, most process control designs up to the present time have been based on the classical Proportional-Integral-Derivative (PID) control approach [14].

The most common control systems implemented in the industry nowadays are:

- **PID control design:** for both types, digital and analogue, occasionally featured with specific configurations like feedforward, ratio, cascade, etc.;
- **Statistical process control:** used mainly for quality control; approaches such as classical Shewart charts, cumulative sum charts, exponentially weighted moving average charts and MIMO control charts. (More details about and descriptions of these approaches can be found in [15]);
- **Intelligent modelling and control**: including neural networks and fuzzy controllers.

2.3 Intelligent Control

Three decades ago, Fu and Saridis were the first to introduce the intelligent control concept [16]. Despite the importance and applicability of intelligent control in different areas of science, the concept had not received much attention at that time. Subsequently, intelligent control was developed into one of the most useful and productive fields of research in engineering disciplines with several applications. Chapter three provides an overview of the artificial intelligence approaches that are used in the thesis, including ANN, FL, GA and PSO. It is not practicable to cover all the previous work related to intelligent control and hence, just some of the recent (last ten years) salient papers are reviewed here.

Kamalasadan [17] has proposed a novel intelligent controller using a Radial Basis Function Neural Network (RBFNN) employed in parallel with an implicit model adaptive control system. The proposed controller has been used to control the speed of induction motor and it was found that the controller performed accurately, was feasible as well as effective, particularly when the controlled induction motor was subjected to unfamiliar dynamics. Chen et al. [18] have designed an intelligent adaptive controller for Multiple-Input–Multiple-Output (MIMO) uncertain nonlinear systems. The proposed control design consisted of a so-called Recurrent Cerebellar Model Articulation Controller (RCMAC) in addition to an auxiliary compensator. RCMAC was applied as an approximator with online-tuned parameters using the Lyapunov function as an objective function of the adaptive law. While the compensator was used to diminish the effect of residual error between RCMAC approximation and the perfect controller. The hybrid control design was implemented on a mechanical system, using mass, spring and damper, as well as a Chua's chaotic circuit as MIMO dynamic processes. It was found that the proposed controller was robust with minimum tracking error.

Fu and Chai [19] have implemented a novel intelligent decoupling design to control a transonic wind tunnel system as a case study of a nonlinear MIMO discrete time process. The proposed controller comprised a reinitialised ANN-based adaptive controller and a free-running ANN to act as an adaptive decoupler, alongside multiple models. Simulation and real-time tests proved the efficiency and the practical implementation of the proposed intelligent controller of nonlinear uncertain processes. Lam [20] has investigated and addressed problems that occur when utilising a sampled-data fuzzy based controller in practice. Takagi–Sugeno's (T-S) fuzzy model was implemented to capture the characteristics of the continuous-time process. The proposed controller was applied to a cart-pole inverted pendulum as a nonlinear plant to illustrate the effectiveness of the designed system. Adaryani [21] has proposed applying an ANN-based Nonlinear Autoregressive Moving Average (NARMA-L2) model to control load frequency of a power system adaptively. The performance of the applied controller was compared with proportional integral control (PI) tuned by GA. The superiority of the ANN-based NARMA-L2 controller was proven across a wide range of operating conditions.

Kassem [22] has employed an adaptive ANN-based NARMA-L2 controller to optimise the duty ratio for the optimum photovoltaic of a water pumping system. A step change in irradiation level was used to test the proposed controller alongside a PID controller for comparison purposes. The effectiveness of the designed controller was demonstrated via the results of the simulated performance of the controlled plant. Menghal [23] has presented implementation of a Neuro-Fuzzy (NF) based controller to maintain the speed of an induction motor. The controller was simulated in MATLAB® and a Simulink® environment and its performance was compared with conventional PI and fuzzy controllers. The behaviour of the controlled motor by NF outperformed other methods regarding the raising time and steady state error.

Li et al. [24] have used the T-S fuzzy model to design state-output-feedback sampled data controllers to assure the stability of performance of closed-loop dynamical systems. The behaviour of the controlled uncertain-active vehicle suspension systems was symmetrically stabilised and satisfied the H_∞ disturbance test. The simulation results showed that the designed control performance of the suspension behaviour was improved, thereby demonstrating the effectiveness of the proposed approach. Sallama et al. [25] have used an NF system to design and implement an advanced supervisory power system stability controller. The results showed that the designed controller performed better than other control designs regarding the stability of the system under external disturbances. The NF system was used to identify the process through the offline learning approach.

Darvill et al. [26] have presented a novel approach for improving a PI control scheme. The proposed approach was based on Adaptive Network-based Fuzzy Inference System (ANFIS) to provide a gain scheduling operation. The hybrid method was applied to a boost converter circuit and the simulation results showed that the controlled circuit by an ANFIS-based PI performed better over fuzzy-based PI design in terms of system response parameters. Pan [27] has introduced a novel hybrid fuzzy control scheme based on fractional-order tuned by the PSO method. The plant used in this study was a hybrid power system using several self-governing generation systems, such as a wind turbine, diesel engine, solar photovoltaic, an aqua electrolyser, fuel-cell, etc. Dynamic response and robustness tests were undertaken to validate the proposed control approach in comparison with two different control designs. The performance of the controller was better than other methods regarding disturbances rejection and system variable variations.

Recently, Mahmud [28] has regulated the voltage of grid-tied solar photovoltaics (PV) using a novel cooperative approach including an ANFIS-based storage energy management system and a PV inverter control scheme. The proposed controller dynamically maintained the voltage of the PV inverter by injection or absorbing appropriate reactive power at the node of the mutual coupling, and it showed a robust response when tested on any system with different situations and network faults.

2.4 Control of the Distillation Process

During the past half century, modelling and control of distillation process have been the subject of thousands of papers and books, with it being estimated that many papers are published each year in this field [29]. Undoubtedly, distillation is the most studied process operation in terms of control and comparatively, no other technique has received so much attention in either the academic or industrial sectors [30]. A graphical demonstration of the number of the published materials about distillation control from 1970 to 2016 is shown in Figure 2.1, while Figure 2.2 depicts the number of published materials according to type over the same period. The source of these figures is Scopus®, the comprehensive index search engine provided by Elsevier B.V. There has been a rapidly growing literature on the control distillation process, especially after the energy crisis at the beginning of the 1970s, which indicates that there was a global interest to introduce an effective solution to deal with a catastrophe of this sort. However, it is beyond the scope of this thesis to review all of these publications. The interested reader is recommended to go to the well-written reviews by Skogestad [28], Yildirim [31] and Sharma [32]. As Skogestad stated, whilst notable efforts have been put into listing the publications that are found most useful, it is evident that some good papers in this field have been left out. Distillation columns, which are used to separate and purify several individual chemicals, come in many possible configurations, and no single

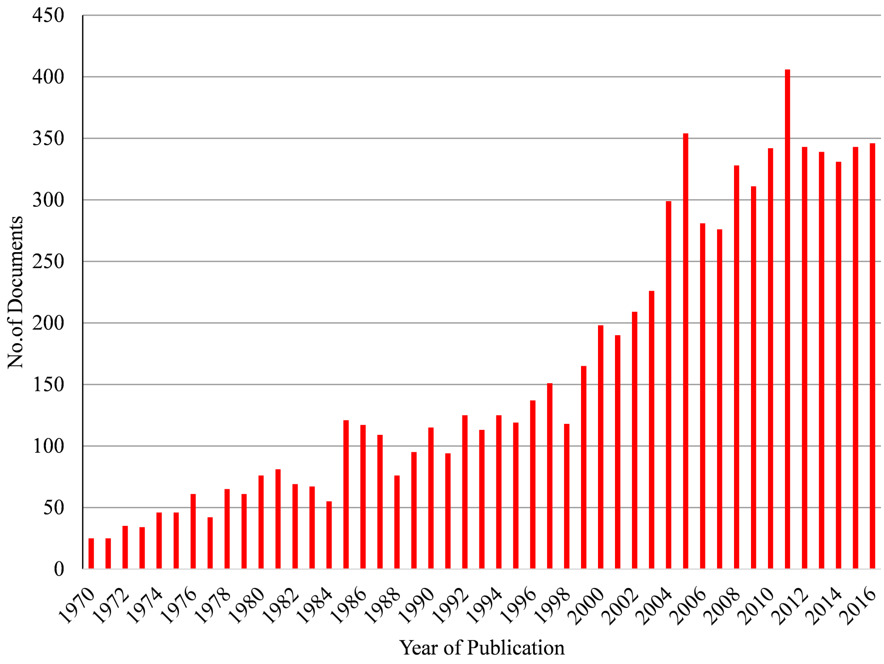

Figure 2.1 Number of published materials about distillation control, from 1970 to 2016 according to Scopus®

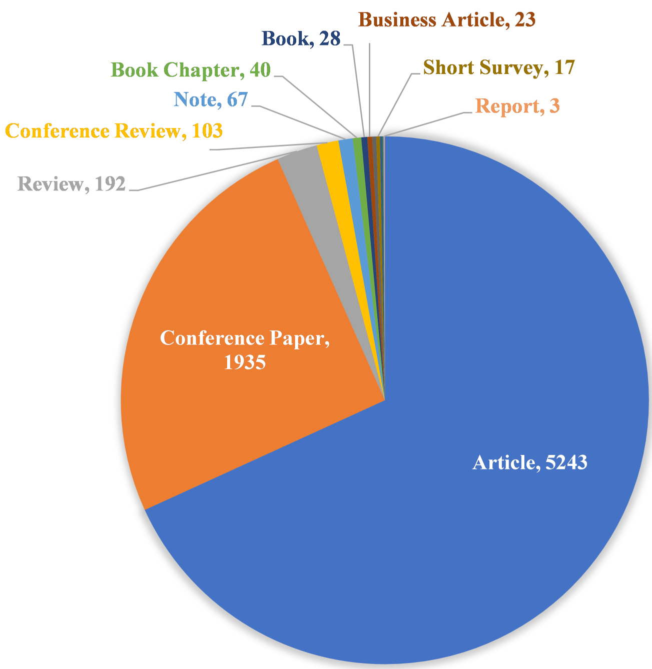

Figure 2.2 Number of published materials according to document type taken from Scopus®

control structure fits all columns. Differences in feed compositions, relative volatilities, product purities, and energy costs impact on the selection of the "optimal" control structure for a given column in a particular plant. More details about the process and operation will be provided in the following chapters.

Many publications in the literature have proposed a specific control configuration or method and applied it to distillation columns, as a case study of a nonlinear MIMO plant. However, a few papers, started with a certain distillation column and compared various structures and configurations of control systems to select the optimal one. Luyben [33] has proposed an indirect method to control the product composition of a distillation column by controlling the difference between two temperature differences in the column. The proposed method offered an attractive alternative control technique over certain ranges. Steady-state errors were less than with the other conventional methods of that time. Three years later [34], he proposed a pioneer configuration by suggesting a profile composition control strategy that allowed for increasing the performance of the controller by greatly reducing the process gain. The main idea of the proposed method was to control the temperature profile location by scanning many thermocouples up and down the column.

Wood and Berry [35] have conducted an experimental work on a pilot-scale binary distillation column and proposed a dual composition control system with two different configurations: a non-interacting and ration control system. The high interaction between the loops of the process was demonstrated and thus, a decoupling control technique was applied to obtain an acceptable performance. A transfer function matrix that describes the dynamic and nonlinearity of the process was also evaluated. Fuentes and Luyben [36] have studied the dynamic behaviour of high-purity distillation columns. Various properties were explored, such as product composition, relative volatility, the sampling time of the composition analyser, and magnitude of the disturbance. The results indicated that distillation columns using low relative volatility respond comparatively slowly. Good performance of the controller can be reached, they suggested, at very high purity levels. Nevertheless, columns with high relative volatility respond so swiftly that significant deviations in product compositions take place before the analyser can react. They concluded that high-purity columns responded much more quickly than predicted by linear analysis. Skogestad et al. [37] have designed a PI controller to maintain the product compositions of a high-purity distillation column. They have reported that the linear control system performance index is reasonable to accept, although model-plant mismatch occurred and it was slow in terms of steady state response. The undesired characteristics like uncertainty and nonlinearity were reduced by the use of logarithmic compositions.

The highly nonlinear behaviour of a distillation column during start-up has been investigated by Ruiz et al. [38] via simulation analysis. They revealed that the most unstable period throughout startup was the so-called semi-continuous phase. They switched the reflux from the total to a specified amount, with the purpose of diminishing instability behaviours and the switching could be conducted in steps. Also, at the end of the phase, the control system designed to derive the column around the specific steady state was switched on. Finco et al. [39] have conducted an analysis of low relative volatility distillation columns. Experimental and simulation were performed for a propylene-propane column at the Sun Refining and Marketing Company's Marcus Hook, PA. The Reflux Ratio-Boilup Ratio (RR-BR) and unorthodox Distillate-Bottoms (D-B) schemes were found as being the two best configurations among various control structures.

Two different distillation systems have been studied by Muhrer [40] via quantitative simulation of the vapour recompression dynamic columns. A mixture of propylene-propane and ethanol-water was considered as a feed to the columns. However, the conclusions drawn from these cases were generic. A Single-Input Single-Output (SISO) conventional control system was used to maintain both compositions, distillate and bottoms, in addition to column pressure. The compositions loops were found to be slower than the pressure loop and so the researchers concluded they could be tuned separately.

Principal component regression in addition to partial least squares approaches were used as prediction methods to estimate the product compositions of a binary distillation column by Mejdell et al. [41]. Steady state data of the column was used as a dataset to achieve a simple linear calibration process for the proposed model. The obtained results were compared with various methods, such as singular value decompositions and generalised least squares;

the findings of estimations were found to be acceptable with minimal modelling effort. Single-point control configuration was implemented by Fruehauf [42] to control product compositions of different distillation columns. The tray temperatures were used for inferring the product compositions in addition to two control strategies that were tested to split the feed. Subsequently, the open-loop method was applied to find the optimal location of temperature sensors alongside the column in the steady-state situation. Finally, the disturbances were determined via a close-loop procedure and the minimum possible energy consumption was found by setting the product compositions at the specifications.

Barolo [43] has developed a model-based control procedure using the generic model control structure to improve the automatic startup of a distillation column, which was able to keep the column composition profile to the desired set-points. In the same year, Ganguly et al. [44] studied the startup of a distillation column and proposed nonlinear model predictive control to maintain the startup of the column. However, the computational cost was very high due to the online optimisation that was used in the proposed method. Partial least square regression was used by Mejdell et al. [45] as an estimator for a multicomponent distillation column to predict its product compositions. The estimator used a set of temperate sensors, which were distributed throughout the column, and then, the estimator was tested by close-loop feedback for control purposes. Barolo et al. [46] have implemented a model-based nonlinear controller to keep the startup and operation at the steady state of a pilot-scale binary distillation column. The proposed controller was a single-point configuration, which maintained a one product composition of the column. However, the authors claimed that the proposed controller could be applied to maintain both product compositions with no further tuning needed to switch from the startup to operation conditions.

Macmurray et al. [47] have applied an ANN for a model predictive control system to control a packed distillation column. The ANN-based model showed its superior performance compared with a classical simplified first principle model for the control purpose. A novel multivariable control approach has been presented by Ramchandran et al. [48]. They employed a neural network to model the inverse of the steady-state process, coupled with a simple reference system structure. The proposed controller maintained the dual compositions of the high-purity methanol-water distillation column in two different sizes: lab- and industrial-scale. The presented controller showed more efficient performance compared to the conventional PI control system. FL incorporated with an ANN has been applied by Luo et al. [49] to construct an inferential-based estimator to control a high purity distillation column. The proposed control configuration was compared with a conventional compositions controller, and the superiority of the inferential-based control system was demonstrated.

Halvorsen et al. [50] have designed an optimal control system for controlling the compositions of a fully thermally coupled distillation column, the so-called Petlyuk column. This type of columns is recommended for industrial use due to its saving of energy compared to the traditional cascaded binary columns of multicomponent products. Multicomponent distillation columns specifications and details are presented in Chapter seven. Dutta et al. [51] have developed an ANN for a model-based control system to control the dual compositions of a lab-scale distillation column. The column was used to separate a methanol-water mixture. Two strategies were followed in this study, namely, model-based gain and steady-state inverse prediction, using an ANN for estimating the future horizon of the process. The developed model-based network comparatively overcame other controllers regarding handling process constraints.

Henry et al. [52] have worked on margining the unavoidable disturbance in the feed compositions of a simple binary distillation column. The results showed an improvement to the feedforward control system in terms of dynamic response performance. Frattini et al. [53] have developed an ANN-based model to control a pilot-scale batch distillation column. The network was employed as a self-tuner and a soft computing measurement tool to monitor the product compositions. The results indicated that the designed ANN was feasible and reliable for use when compared with the compositions temperatures inference method for controlling a multicomponent batch distillation process. Ross et al. [54] have investigated the analysis and design of an industrial distillation column, which was implemented to separate iso-propanol, water and normal propanol. The proposed structure of the design dealt well with the sensitivity of a steady-state simulation and eliminated the distributions caused by changing the conditions of the feed.

De Canete et al. [55] have proposed an ANFIS structure as a multivariable control system for a methanol-water distillation column. The backpropagation gradient descent was applied as a learning algorithm to identify the dynamic behaviour of the column to tune the proposed controller. The ANFIS-based controller was examined against inputs variation and external disturbances, with the results reporting an efficient and stable performance of methanol composition control. Abbod et al. [56] have designed an adaptive control strategy that uses a long-range predictive algorithm based on generalised predictive control, by applying Takagi-Sugeno-Kang's (TSK) fuzzy modelling technique. The control design involved a model based on auto-regressive integrated moving average structure, instead of an auto-regressive–moving-average model, with an exogenous inputs model. The performance of the controller was examined by conducting different simulation experiments on a binary distillation column and continuously stirring the tank reactor system as well.

The Wiener model was used by Bloemen et al. [57] for identifying and controlling a high-purity distillation column. The Model Predictive Control (MPC) technique was applied to control the compositions of the column based on Wiener as well as traditional linear methods, for comparison purposes. The proposed Wiener-based MPC outperformed the other ones in terms of handling the nonlinearity and complex relationship of inputs-outputs association. Alpbaz et al. [58] have conducted a modelling and simulation of a binary distillation column, packed type. The simulated model was validated by comparing the outputs with a pilot-scale methanol-water distillation column. The authors investigated a theoretical and experimental analysis of the steady-state and dynamic behaviour of the column, with reflux ratio being chosen as a manipulated input to control the composition of the distillate product of the column. Two control configurations were compared, namely, PID and Dynamic Matrix Control (DMC). The simulation performance showed that that of the DMC-based controller was better than that of PID controller for tracking set-points.

Mahfouf et al. [2] have proposed a long-range predictive control system based on TSK fuzzy modelling that uses an auto-regressive exogenous structure with feedforward configuration. The controller was applied with SISO and MISO configuration separately for a binary distillation process. The simulation results showed that the proposed controller outperformed the comparable predictive control that based on a linear modelling approach.

An ANN was employed by Osorio et al. [59] for modelling a wine distillation column used for a wine purification process. The proposed ANN-based model was compared with a polynomial fitting strategy in terms of efficiency and accuracy. The authors claimed that this novel simulation method could be applied to a complex mixture, such as spirits, juice, perfumes and throughout the food industry. A MPC was developed by Volk et al. [60] to separate chemical oil feed in a multicomponent distillation column. The performance of the proposed controller was tested against feed flow rate disturbances, with the results indicating robustness and feasibility in a wide range of operations. Singh et al. [61] have designed an ANN-based prediction model to estimate the overhead composition of a binary distillation column. The inputs of the network were taken from the temperature profile, which involved 17 temperature entries of 15 trays, a reboiler and a reflux drum. Five liquids constituted the output vector of the estimator and five vapour distillate compositions for the mixture considered. The developed model was validated by conducting a comparison between the simulated and predictive data.

Recently, Fard et al. [62] have proposed a hybrid intelligent fuzzy controller tuned by the Cuckoo optimisation method to control a binary distillation column. The designed hybrid controller maintained both the composition products of the column. The authors found that the performance of the controller was fast with less steady state error when compared with PID and traditional fuzzy controllers. The robustness of the hybrid controller was also tested by operating the column under input variations. Tuan [63] has reduced the variation of the product purity of a binary distillation process that occurs due to operation constraints. The authors simulated the column using Aspen Hysys® and MATLAB® platforms, with all input-output data being collected from Aspen® Hysys®, used to design MPC in a Simulink environment. The robustness test showed that the MPC handled the expected disturbances and obvious process disruptions.

Tututi-Avila et al. [64] have published a study focused on the dynamic control and design of a so-called satellite column; an extended dividing wall column for a multicomponent distillation process. The novel column configuration was compared with a Kaibel column as well as with a direct sequence to separate benzene, toluene, and the three xylene isomer (BTX) mixtures. The conclusion of this study was that the satellite column proved its superiority when compared with other arrangements regarding consumed energy in addition to capital cost. A MIMO PID controller was applied to control all the columns. Bin et al. [65] have proposed an intelligence-based optimisation method to improve the performance of an industrial-scale crude distillation column in a Wuhan refinery in China. The combination of a wavelet-based ANN and a line-up competition optimisation algorithm was used to find the optimal operation process conditions of the column. GA and PSO were also compared with the used optimisation tool for proper validation of the proposed approach.

2.5 Summary

A selection of the relevant recent literature has been reviewed in this chapter regarding introducing and applying intelligence-based control systems. In general, ANN-based controllers could be trained and implemented in a scalable design scheme with reasonably good accuracy. However, ANN-based controllers suffer from reasoning ability in incomplete environments. While, fuzzy logic controllers have a significant curse of the dimensionality problem with an excellent human-like capacity for reasoning and decision making. Therefore, ANFIS benefits from both approaches by combing the advantages of universal approximation and rational reasoning. In addition to several attempts to control distillation columns, and/or model them. Most of the proposed approaches have involved trying to design an efficient method for handling naturally-found behaviour, such as nonlinearities in processes. Also, it has been explained how those controllers need to have remarkable robustness against unavoidable external disturbances. It has been demonstrated that there is rapidly increasing literature on controlling distillation process, especially after the global energy crisis. Such growth indicates that distillation columns are irreplaceable chemical units frequently used for purification and separation with a need to be controlled efficiently to achieve optimal performance for saving energy and attaining high product quality.

Chapter 3

Intelligent Control

3.1 Introduction

Fundamentally, intelligent control developed as alternative approaches to address systematically today's problems of control that cannot be represented by or investigated through mathematical difference or differential equations. Such problems used to be formulated and studied using traditional control theories in the past decades [66].

The term "*intelligent control*" was coined, apparently, by King-Sun Fu, however, up to now there has been no common definition. Antsaklis [13] reported that the apparent struggle in precisely determining what is intended by the intelligent control is because there is no widely agreed definition of intelligent behaviour or human intelligence for that matter. This, in fact, stills a remaining live debate among neuroscientists, educators, psychologists, engineers and computer scientists.

Researchers have given detailed characterisations for intelligent control, some of which are as follows.

"Intelligent control achieves automation via the emulation of biological intelligence. It either seeks to replace a human who performs a control task or it borrows ideas from how biological systems solve problems and applies them to the solution of control problems." Passino [67]

"Intelligent control systems with high degree of automatic should perform well under significant uncertainties in the system and environment for extended periods of time, and they must be able to compensate for certain system failures without external intervention." Antsaklis [68]

"Intelligent control describes a class of control techniques that use various artificial intelligence (AI) techniques such as neural network control, fuzzy logic control, neuro-fuzzy control, expert systems, genetic control, evolutionary algorithms, and intelligent agents. Intelligent control systems are useful when no mathematical model is available a priori and intelligent control itself develops a system to be controlled." Azar and Vaidyanathan [69]

Hence, the main features of intelligent control systems could be summarised as:

- Using artificial intelligence approaches to formulate and solve complicated control problems;
- Achieving automatic acts inspired by biological intelligence;
- Dealing well with high nonlinearities and uncertainties in systems as well as an unforeseen external environment without the need for external intervention.

3.2 A General Framework of Intelligent Control Systems

Many of intelligent system designs have been inspired by the intelligence of human beings. However, up to now, humans are far better than those machines with regard to various features. Such features that are required for achieving control goals are adaptation, reasoning, learning, etc. [70].

3.2.1 Parallel Processing

Clearly, a good decision typically is taken by the interaction between several data sources and knowledge. For an instant, when someone is choosing a dress in a department store, her or his selected decision is taken depending on many criteria, such as colour, fashion, price, material, and users review as previous knowledge, and so on, via parallel processing. Likewise, when a control expert operates a dynamic system, first the system behaviour should be obtained from various affecting parameters. Then, the selected variables should be manipulated by the expert to achieve the desired performance under chosen constraints. As shown in the example above, it is clear that human decisions are taken by processing information in a parallel manner, where it is necessary to keep in mind and deal with at the same time several strands of thought. Accordingly, so-called parallel distributed processing models have been implemented to achieve such human-like responses [71].

In artificial intelligence, the processing of data is carried out by transferring inputs and outputs between units, such as the data processing conducting in ANNs. Often the information obtained by a decision maker is incomplete or imprecise, such as with fuzzy data. Hence, various inference techniques are used to make a proper decision through an approximation, such as fuzzy logic inference methods.

3.2.2 Learning Process

Notably, learning is the most significant feature in natural intelligence; it somehow makes a human smart and even smarter over the time. In general, the learning or training process for artificial intelligence means training an intelligent-based model to perform a pre-described mission, which can be categorised into three branches as follows.

- **Supervised learning:** when a set of training examples is introduced in the form:

$$\begin{bmatrix} u_1^1 & \dots & u_i^1 \\ \vdots & \ddots & \vdots \\ u_1^n & \dots & u_i^n \end{bmatrix} \Rightarrow \begin{bmatrix} y_1^1 & \dots & y_k^1 \\ \vdots & \ddots & \vdots \\ y_1^n & \dots & y_k^n \end{bmatrix}, \tag{3.1}$$

  where, i represents the number of inputs u, k represents the number if outputs y and n represents the number examples.

- **Unsupervised learning:** unlike the supervised learning method, unsupervised learning involves using only the input set without corresponding target outputs. That is, the parameters are modified in response to model inputs only. The main application of the unsupervised learning method is to perform operations, such as clustering and pattern recognition. In terms of industrial application, this learning method can be used in feature extraction and system analysis.

- **Associative reinforcement learning:** this is also called the evaluation-oriented learning method. However, instead of being provided with the actual output for each model input, like supervised learning, the method is only given a score or grade. The score is defined as the level of the model performance over a specified input sequence. This type of learning method is most appropriate in control applications.

3.2.3 Adaptation and Robustness

Another interesting feature in humanesque behaviour is the ability to change according to the environment; an ability known as adaptation. Similarly, intelligent modelling or control requires modification or updating of the system parameters and sometimes the structures, to provide robust or at least satisfactory performance under uncertainty situations [72]. For example, for testing the adaptation of controllers, various tests can be conducted, such as tracking a set of changing desired outputs or subjecting the controlled system to external disturbances, which need to be handled well. Fuzzy controllers tuned by an optimiser, GA or PSO, present an adaptive performance by modifying the FIS's parameters to deal with the process's changing environment. On the other hand, the robustness of the proposed controllers has been assessed by dealing with changing the control objectives and disturbances by altering the process inputs for binary and distillation columns, as will be presented later.

3.3 Artificial Intelligence Techniques

Artificial intelligence techniques have mainly been developed to perform like humans, as mentioned before. It is not intended here to investigate the details of these developing and controversial techniques, which needs many books to be covered and might remain not be complete. The intention here is to draw attention to the most important applied approaches, in particular, the control and modelling applications, with an emphasis on methods such as ANN, FL and ANFIS in addition to optimisation methods, like GA and PSO, which are used in this thesis.

3.4 Artificial Neural Networks

Intelligent systems should efficiently make reasonable decisions in an uncertain environment regarding the ability of various operations, such as machine learning, parallel information processing, generalisation and so on [70]. Given their promising potentiality, ANNs have arisen as a central branch of artificial intelligence. In particular, due to the rapid advances in very-large-scale integration and super-fast computers as well as the growing research on neural system algorithms and architectures, ANNs have been successfully applied to a wide range of applications. One of these attractive applications is intelligent control systems, essentially for the modelling and prediction of incomplete nonlinear and dynamic systems as well as for adaptation and controlling uncertain dynamic systems [73]. The interested reader is advised to refer to the comprehensive literature reviews from using ANNs in modelling and control presented in [74–76]. In the following subsections, a brief description of ANNs fundamentals is provided.

3.4.1 Neuron Model

The basic unit of the biological neural network is a neuron; it is reported that a human has around 10^{11} neurons in the brain. These neurons have three main components, namely, cell body, axon and dendrites, as shown in Figure 3.1.The dendrites are dendroid approachable nets of nerve fibres that transmit signals into the cell body and then, the latter efficiently sums and process those incoming signals. The axon, which is a single long fibre, transmits the signal output from the cell body to other neurons, while the contact point between two neurons, called a synapse, is where the axon of one cell connects with another cell at a dendrite [77].

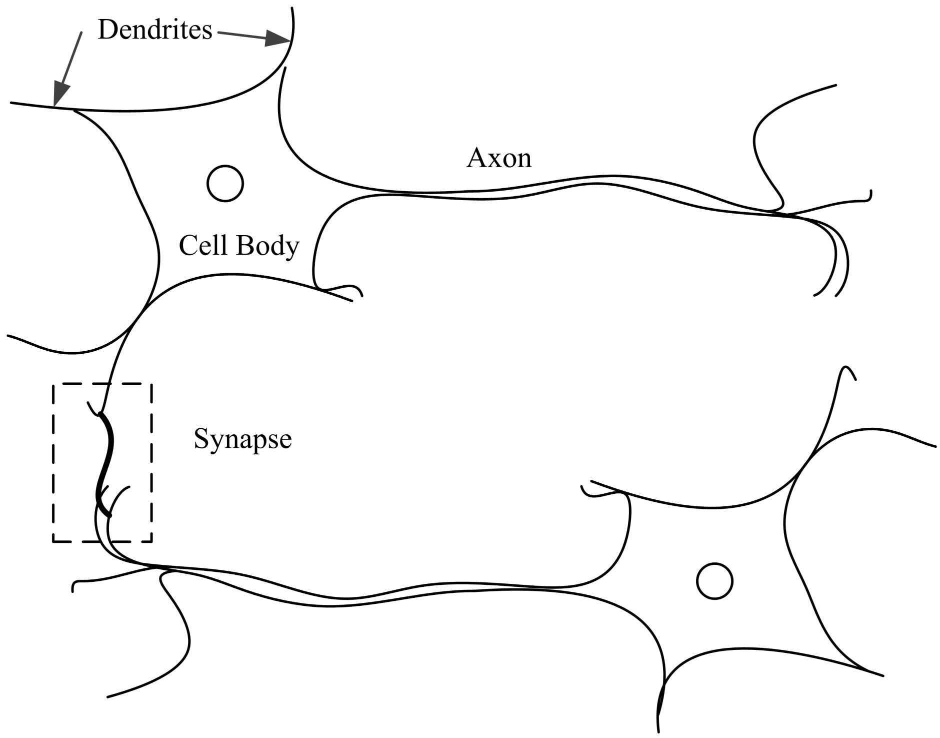

Figure 3.1 Simplified schematic diagram of two connected biological neurons [77]

There are two basic types of artificial neurons; single- and multi-inputs neurons. In a single-input neuron, a scalar input multiplies in a scalar parameter, called weight, to produce a scalar output. On the other hand, a multi-input neuron receives a vector of weighted inputs from the real-world environment or other neurons, subsequently forming a linear combination, as shown in Equation 3.2.

$$\alpha_j = w_{1,j}u_1 + w_{2,j}u_2 + \cdots + w_{i,j}u_i + b_{1,j} = \sum_{i=1}^{n} w_{i,j}u_i + b_{1,j}, \tag{3.2}$$

where, α is activation state of neuron j. From Equation 3.2, it can be seen that the relationship between the input u and activation state α is a linear combination. The activation state is then processed nonlinearly, or linearly by an activation function, as shown in Figure 3.2 and Equation 3.3.

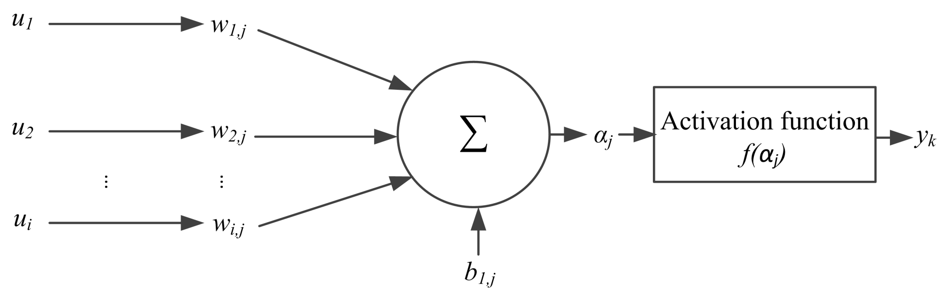

Figure 3.2 Multi-input neuron signal processing [77]

$$y_k = f(\alpha_j). \tag{3.3}$$

There are many activation functions used in ANNs and choosing the type depends on the problem that the neuron needs to solve. All these functions are discussed in detail in Hagan's textbook [77].

3.4.2 Architecture of Neural Networks

Many neurons are employed to perform a parallel operation and a set is called a layer. An ANN's architecture, sometimes called its topology, is commonly constructed by layers. The way the neurons of an ANN are structured is intimately linked with the learning algorithms used to train the network. Generally speaking, there are three fundamentally different classes of network architectures.

A. **Single-Layer Feedforward Networks**: a single layer feedforward network has one layer of connection weights. Often, the unit can be distinguished as an input unit, which receives signals from the real-world and distributes them to other processing elements of the network. For this reason, the first layer is not counted in the layer number, since it is not performing the computation work or producing an output unit, from which the response of the network can be read, as shown in Figure 3.3.

B. **Multi-layer Feedforward Networks**: the second class of feedforward networks distinguishes itself by the presence of more hidden layers, whose computation nodes are correspondingly called hidden neurons or hidden units. The function of hidden neurons is to intervene between the external input and the network output in some useful manner. By adding one or more hidden layers, the network is enabled to extract higher-order statistics [78]; an illustrative schematic of a multi-layer feedforward network is shown in Figure 3.4. A multi-layer feedforward neural network is an important class of neural networks, which has been applied successfully to solve some difficult and diverse problems in many disciplines of science and technology [79].

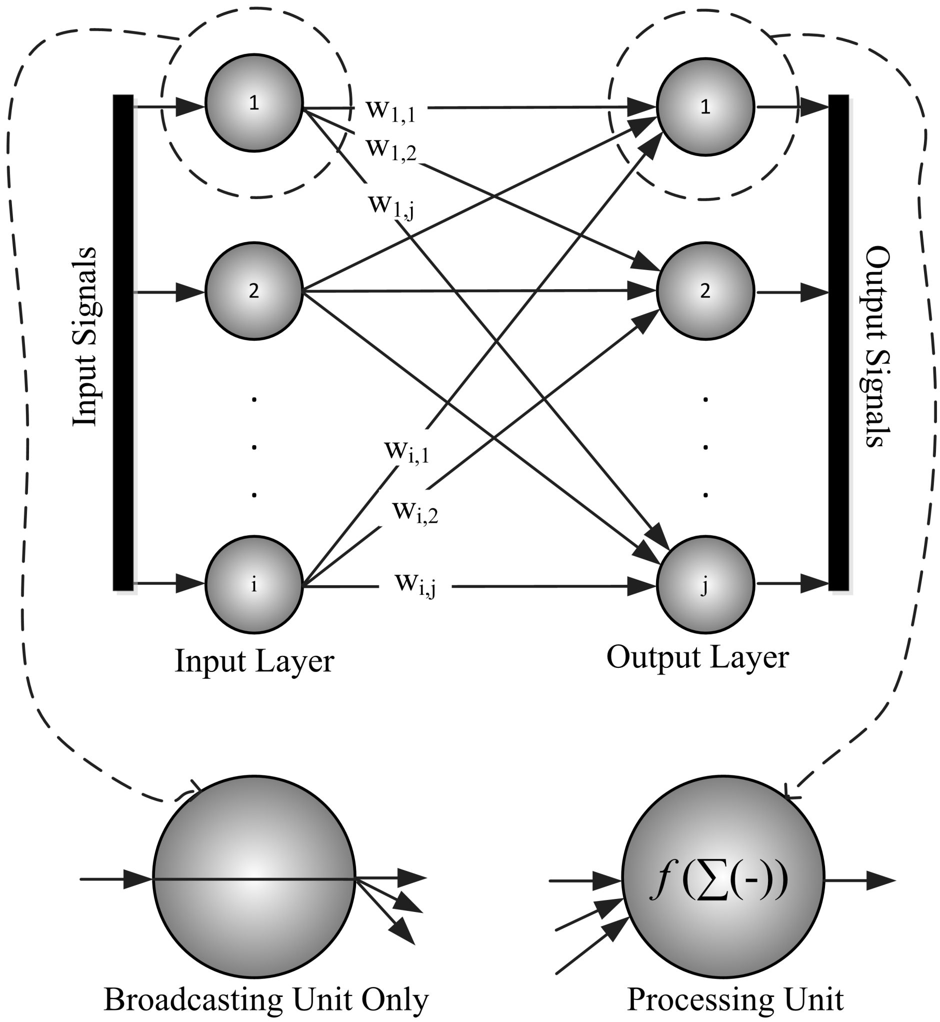

Figure 3.3 Single-layer neural network [79]

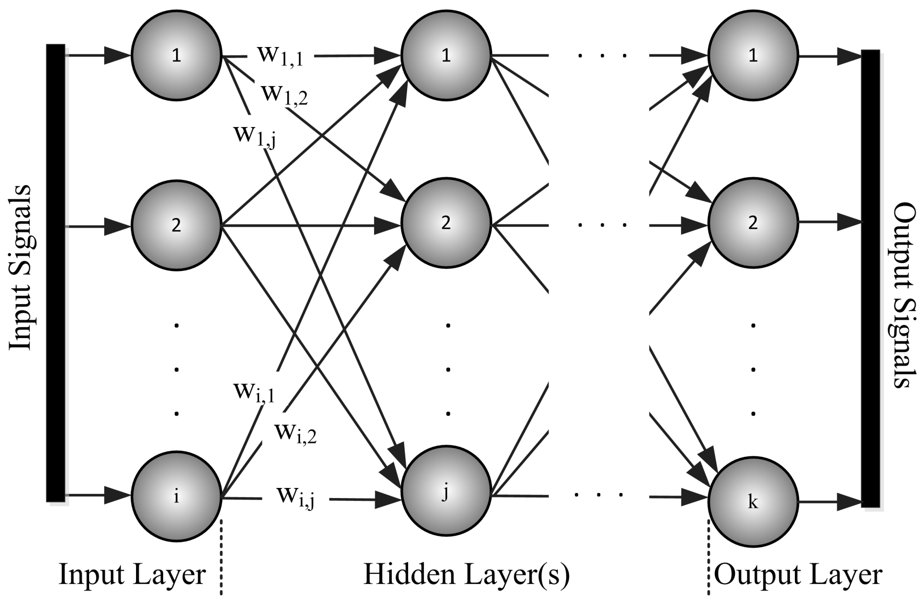

Figure 3.4 Multi-layer neural network [79]

Almost all ANN-based control configurations, which are listed later, use multi-layer feedforward architecture. It is known that ANNs can approximate functions and mathematical operators arbitrarily well. In this regard, Feedforward Artificial Neural Networks (FFANNs) are widely considered as universal approximators, due to their capability of describing the input-output relationship of several types of systems [79]. Accordingly, this architecture has become popular for parameterising nonlinear models and classifiers. It has been extensively applied to pattern recognition, prediction of the output of different processes, nonlinear control, and so on. The main technique of learning used in multi-layer FFANNs is the error Backpropagation (Bp), which was known around 1985, being introduced by several groups of scientists [37]. This learning method is typically employed in conjunction with an optimisation procedure, like gradient descent.

The steps of the error BP are as follows:

(1) **Randomly initialising the network weights**

(2) **Repeat the next steps until the prescribed criterion is reached**

(3) **Summing the weighted input and using an activation function to compute the output of the hidden layer(s)**

$$h_j = f\left(\sum w_{i,j} u_i\right), \tag{3.4}$$

where, h_j is the actual output of hidden neuron j, u_i is the input signal of input neuron i, $w_{i,j}$ is the weight between the input neuron i and the hidden neuron j and f is the activation function.

(4) **Summing the weighted output of the hidden layer and using an activation function to compute the layer output**

$$\hat{y_k} = f\left(\sum h_j w_{j,k}\right), \tag{3.5}$$

where, $\hat{y_k}$ is the output of neuron k.

(5) **Calculating the backpropagation error**

$$\delta_k = \acute{f}\left(\hat{y_j}\right)\left(y_k - \hat{y_k}\right), \tag{3.6}$$

where, $\acute{f}$ is the activation function derivative and y_k is the desired of output (actual output) of the neuron k.

(6) **Calculating the weight correction term**

$$\Delta w_{j,k}(t) = \eta \delta_k h_j + \alpha \Delta w_{j,k}(t-1), \tag{3.7}$$

where, t is a time step, η is an appositive constant called the learning rate coefficient and α is another constant called a momentum factor.

(7) **Summing the delta input for each hidden neuron and computing the error term**

$$\delta_j = \sum_k \delta_k w_{j,k} \acute{f}\left(\sum_i u_i w_{i,j}\right). \tag{3.8}$$

(8) **Calculating the weight correction term**

$$\Delta w_{i,j}(t) = \eta \delta_j u_i + \alpha \Delta w_{i,j}(t-1). \tag{3.9}$$

(9) **Updating the weights**

$$\Delta w_{j,k}(t+1) = \Delta w_{j,k}(t) + \Delta w_{j,k}, \tag{3.10}$$

$$\Delta w_{i,j}(t+1) = \Delta w_{i,j}(t) + \Delta w_{i,j}. \tag{3.11}$$

C. **Recurrent Neural Networks**

Recurrent Neural Networks (RNNs) differentiate themselves from feedforward neural networks in that they have at least one feedback loop. They are configured with internal connections that feedback to another layer or themselves. This configuration allows the network to accommodate unidirectional data flow, as occurs in biological structures, and enables networks to distinguish separate input patterns from the same input sequence and so discern temporal patterns; a function beyond the capability of a feedforward network without pre-processing of the inputs [38]. RNNs have a dynamic memory: their outputs at a given instant reflect the current input as well as previous inputs and outputs. There are four main types of RNNs, which are fully recurrent network, Hopfield network, recursive neural networks and Elman network.

3.4.3 Control Applications of Artificial Neural Networks

The most significant capacity of ANNs, from the viewpoint of control theory, is their ability to cope with nonlinearity in dynamic systems. The great variety of nonlinear systems is the main reason behind no systematic control having so far evolved and hence, there being no unified design theory that is valid for nonlinear control systems [80]. Much classical analysis and synthesis of nonlinear control design for particular forms of nonlinear systems has been undertaken, such as phase plane methods, linearisation methods and approximation functions, but with notable limitations. Hence, owing to ANNs' ability of mapping non-linearity and hence, allowing for the modelling non-linear systems, they are preferred for implementation in control application.

There are basically two phases involved in implementing ANNs in control:

1. **System identification**

   In the identification stage, sometimes called prediction, an ANN is developed to approximate the system that needs to be controlled;

2. **Control design**

   In the control design phase, the developed ANN, which has been trained in the identification phase, is employed to design or configure the control system.

In general, there are two different designs of ANN-based control systems, which are also called neurocontrollers.

1. **Direct Control Design**

   This kind of design considers an ANN as a direct controller which the control parameters directly adjust to reduce some norms of the output error. Frequently, the ANN training (identification phase) is conducted according to an online structure. This class of design includes direct inverse control, internal model control, feedforward with inverse models, feedback linearisation and optimal control structure [81].

2. **Indirect Control Design**

   This is a model-based design, with ANNs being used to approximate the system to be controlled. The ANN-based model is then implemented for traditional control system design. This type of ANN-based control design is flexible due to offline training considerations and the control itself, therefore, depends on the trained ANN model. MATLAB® provides ready to implement neurocontrollers in a Simulink® environment, namely MPC, Model Reference Control and NARMA-based control. An ANN-based NARMA-L2 controller is implemented in this study and the other methods will not be involved in the subsequent investigations and discussions.

3.5 Autoregressive-Moving Average Models

Autoregressive-Moving Average Models (ARMA) fundamentally consist of two parts one for the Auto-Regression (AR) and the second for the Moving Average (MA). Those models provide a powerful prediction ability of dynamic systems in time series form. In addition, there is a non-linear form of these models called NARMA, which describes precisely the input-output behaviour of discrete-time dynamical systems in a neighbourhood of the equilibrium state [82]. This model representation is used in the form of past, current and the future system parameters, as shown in Equation 3.12.

$$y_{(t+d)} = f[y_t, y_{t-1}, \cdots, y_{t-n+1}, u_{t-1}, \cdots, u_{t-m+1}], \tag{3.12}$$

where, y_t and u_t are the input and output of the system, respectively, n and m represent the time delay of input and the output, d is the relative degree, and $f[\cdot]$ is a non-linear approximation function.

In the identification phase, a global approximation can be employed to compute $f[\cdot]$. For control purposes, using Bp to train ANNs for finding a control signal u_t is reported as being quite slow, because of the involvement of dynamic gradient methods. To address this, an efficient method has been proposed by Narendra and Mukhopadhyay, which introduces approximation models to overcome computational difficulties, as shown in Equation 3.13. Two classes of NARMA model have been tested: NARMA-L1 and NARMA-L2. It was found that the second class, involving two sub-function approximators, is more efficient and adequate in the identification and adaptive control contexts [83].

$$\begin{aligned}\hat{y}_{(t+d)} &= f[y_t, y_{t-1}, \cdots, y_{t-n+1}, u_{t-1}, \cdots, u_{t-m+1}] \\ &+ g[y_t, y_{t-1}, \cdots, y_{t-n+1}, u_{t-1}, \cdots, u_{t-m+1}] \times u_t.\end{aligned} \tag{3.13}$$

The schematic configuration of the NARMA-L2 model is shown in Figure 3.5. Once the

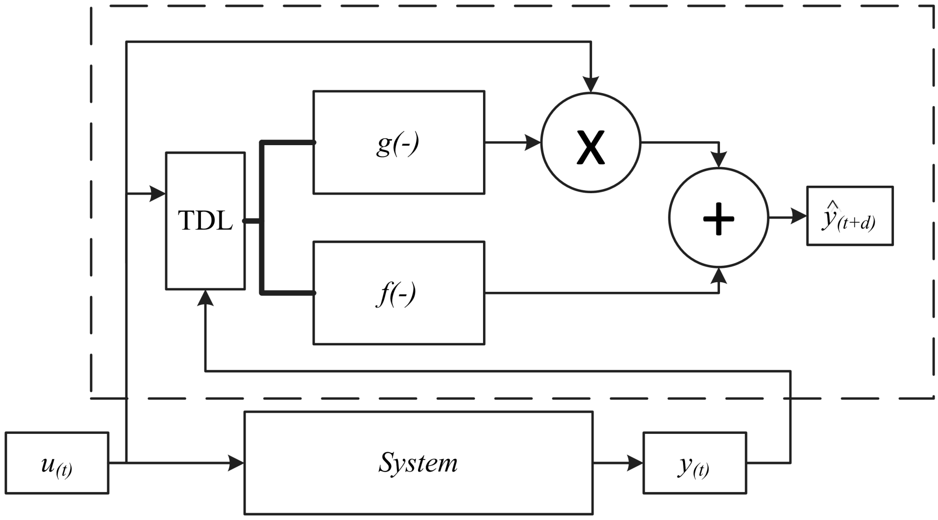

Figure 3.5 NARMA-L2 model representation

NARMA-L2 model identifies the system to be controlled, its controller can be designed by replacing the predicted system output with the desired output (set-point), since the system output is intended to follow the latter. The control output of the NARMA-L2 controller is calculated as follows:

$$u_t = \frac{r_t - \hat{f}(\cdot)}{\hat{g}(\cdot)}, \tag{3.14}$$

where, r_{t+1} is the set-point and $\hat{f}(\cdot)$ and $\hat{g}(\cdot)$ are the approximation submodels found in the identification phase. The schematic block diagram of NARMA-L2 control design is shown in Figure 3.6. The ANN-based NARMA-L2 control design is available in the Simulink® library, and it is ready to be implemented for identification, first, by training the approximation submodels using an ANN. Then, the trained ANN is rearranged to configure the NARMA-L2 controller. However, the ANN-based NARMA-L2 controller provided by MATLAB® could only be designed for SISO dynamical systems [78]. Uçak et al. [84] proposed an online

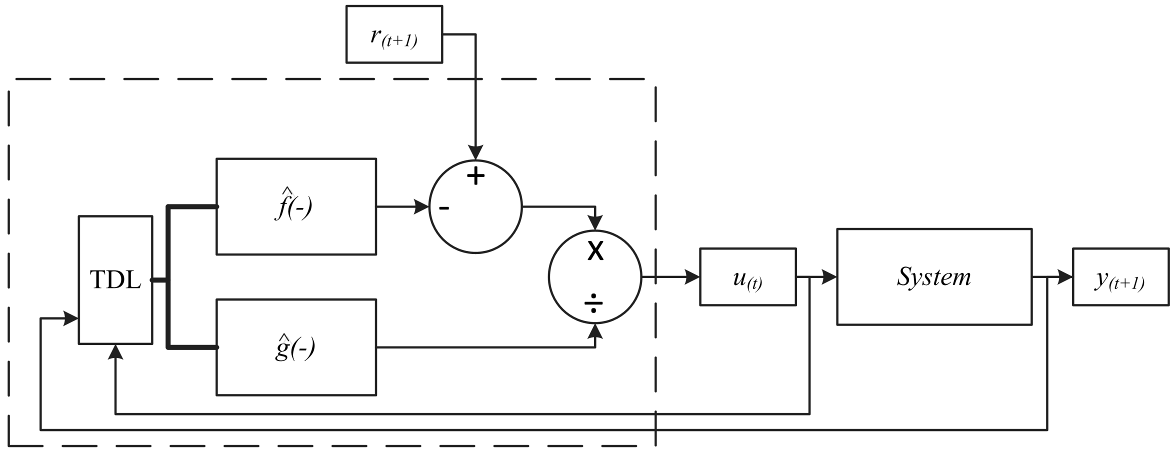

Figure 3.6 NARMA-L2 control system

Support Vector Regression (SVR) to find the approximation submodels instead of using an ANN, also for SISO systems. In this thesis, as it will be discussed later, the ANFIS technique is employed to approximate the submodels of the NARMA-L2 controller to be applied to MIMO dynamical systems.

3.6 Fuzzy Logic

Contrasting with classical logic, FL is targeted at modelling the imprecise manner of reasoning to perform an essential task, as found in the outstanding human capability of making rational decisions in an uncertain and unpredictable environment. Such an ability depends on inferring an approximate solution to a problem based on stored information that is imprecise, incomplete, or not completely dependable [83]. This concept of FL presented by Zadeh, who is widely acknowledged as the father of FL, was first introduced in 1965 as the fuzzy set theory [85]. Since that time, FL has been studied extensively in many fields, from mathematics to intelligent systems. Nowadays, FL is recognised as an essential branch of artificial intelligence. From a control viewpoint, it constitutes a new era of control theory called Fuzzy Logic Control (FLC), which has proven to be an effective control method for several dynamical, complex and nonlinear systems [86]. Recent comprehensive reviews show that there has been successful implementation of FLC in a wide range of applications [87, 88].

3.6.1 Concepts and Definitions

As mentioned previously, FL is principally about dealing with imprecision by emulating reasoning in human thinking with an approximation process. Fuzzy based modelling has been explored widely in the literature and applied extensively in industrial applications, with its biggest advantage being that there is no need for precise quantitative analyses. It mostly depends on the IF-THEN rules, which are linguistic expressions specified by membership functions in the form: **IF X THEN Y** [89].

Most engineering problems deal with several input-output pairs. This contrasts with other problems that look for the relationship between input-output in a set form. Consequently, a pre-processing, called 'fuzzification' and 'defuzzification' should occur before and after the fuzzy inference system, as depicted in Figure 3.7. The four main components of an FL system are a fuzzifier, defuzzifier, rule base, and an inference system. The fuzzifier achieves scale charting, which interprets the range of input values in equivalent universes of discourse and it converts input data into proper linguistic values. The inference system, also known as decision-making logic, mimics human decision-making actions depending on the approximate reasoning principles. The defuzzifier receives a fuzzy output from the inference system and produces a crisp output. Furthermore, the defuzzifier conducts scale charting by converting the range of output values into the matching application domain.

3.6.2 Fuzzy Set

A fuzzy set concept is represented as an extension of a classical set, in which all the elements have degrees of Membership Function (MF) ranging from 0 to 1. Accordingly, in a universe of discourse $U = \{u_i\}$, where $i = 1, \cdots, n$, a fuzzy set F is described by its MF:

$$\mu_f : U \to [0,1]. \tag{3.15}$$

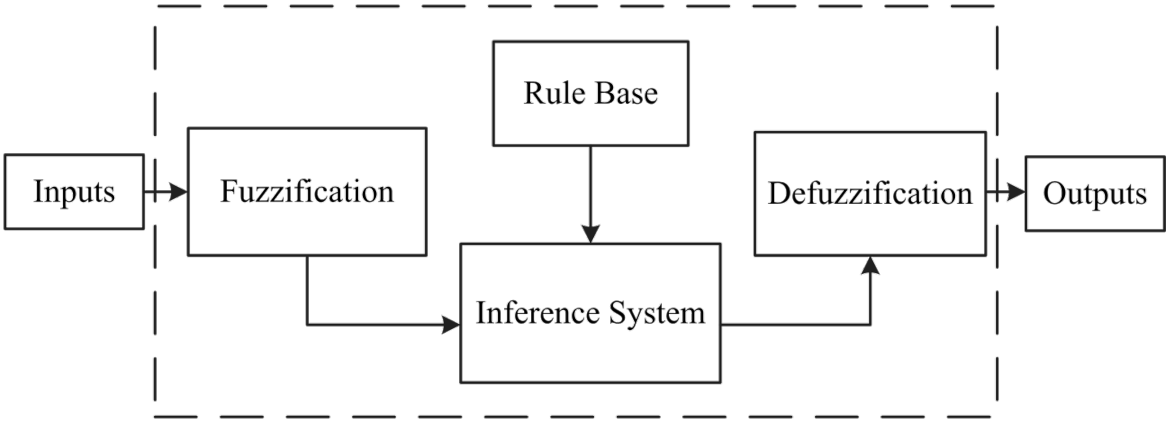

Figure 3.7 Basic block diagram of a fuzzy system [89]

There are various types of MFs; the simplest ones are shaped by straight lines. Of these, the simplest is the triangular-shaped MF, which is a collection of three-points creating a triangle, while the trapezoid-shaped MF has a plane top and is just a trimmed triangle curve. These straight-line MFs have been applied extensively due to their simplicity. There are also two MFs based on the Gaussian distribution curve, one being a simple and the second is a two-sided compound of two different Gaussian curves. Three points define the generalised bell MF, which has one more point than the Gaussian MF. Attributable to their compact notation and smoothness, Gaussian and bell MFs are common approaches for defining fuzzy sets. Both these MFs have the benefit of being nonzero and smooth at all points. Even if the Gaussian and bell MFs realise smoothness, they are incapable of specifying asymmetric MFs, which are significant in specific applications. Moreover, there are other shapes of MFs, such as sigmoidal and polynomial-based, with more details about them being available in FL textbooks [90].

3.6.3 Linguistic Variable

A linguistic variable can be defined in linguistic terms or expressed as fuzzy numbers. For instance, if a temperature is understood as a linguistic variable, so the linguistic values of it might be expressed in five degrees (or MFs):

$$f(temp.) = \{\textit{very cold, cold, moderate, hot, very hot}\}. \tag{3.16}$$

In a particular framework, a temperature may be interpreted as follows:

"very cold", below 10 °C

"cold", about 10 °C

"moderate", about 20 °C

"hot", about 30 °C

"very hot", up 30 °C

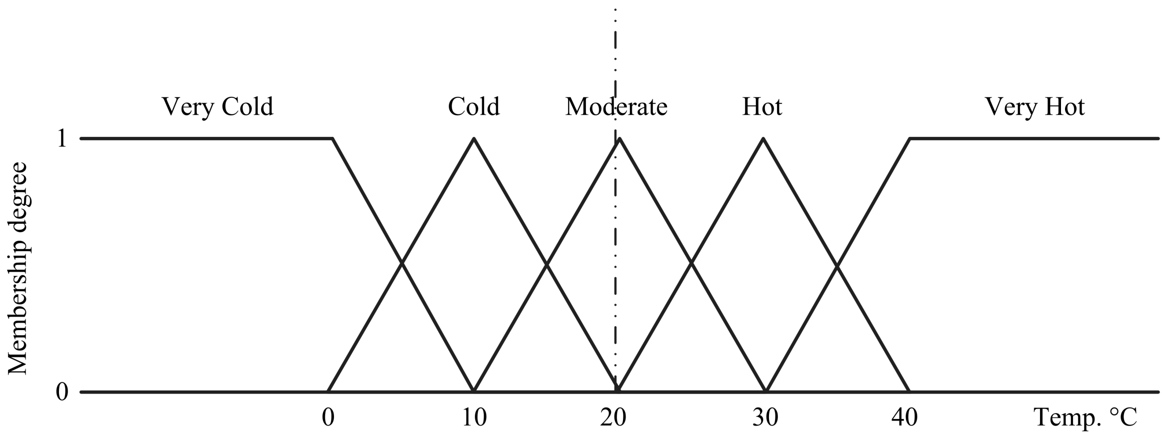

Figure 3.8 Schematic representation of a fuzzy set employed to describe a temperature

3.6.4 Operations on Fuzzy Sets

The operations on fuzzy sets are expressed by their MFs. For example, let x and y be two fuzzy sets in T, with MFs, μx and μy, respectively. The operations could be as follows:

- **Union:** the membership function $\mu_{x \cup y}$ of the union $x \cup y$ is expressed pointwise for all $t \in T$, which is also called the maximum criterion, as shown schematically in Figure

3.9 and mathematically by:

$$\mu_{x\cup y}(t) = max\{\mu_x(t), \mu_y(t)\}. \tag{3.17}$$

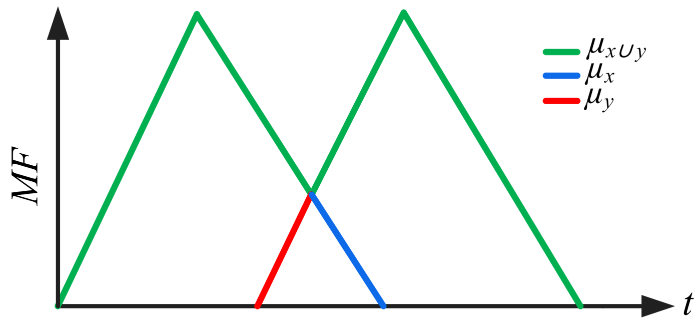

Figure 3.9 Union operation in fuzzy sets

- **Intersection:** the membership function $\mu_{x\cap y}$ of the intersection $x \cap y$ is expressed pointwise for all $t \in T$, which is also called the minimum criterion, as shown schematically in Figure 3.10 and mathematically by:

$$\mu_{x\cap y}(t) = min\{\mu_x(t), \mu_y(t)\}. \tag{3.18}$$

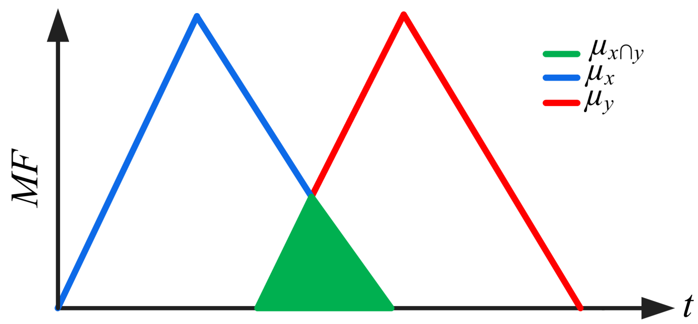

Figure 3.10 Intersection operation in fuzzy sets

- **Complement:** the membership function $\mu_{\bar{x}}$ of the complement x is expressed pointwise for all $t \in T$, which is also called the negation criterion, as shown schematically in

Figure 3.11 and mathematically by:

$$\mu_{\bar{x}} = 1 - \mu_x. \tag{3.19}$$

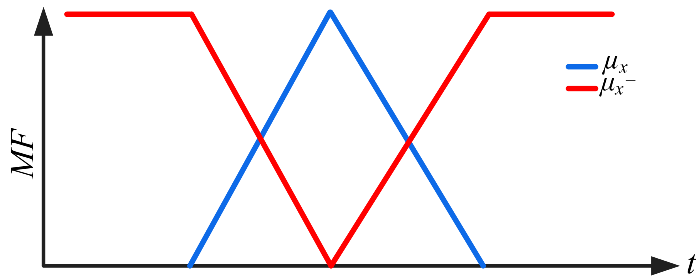

Figure 3.11 Compliment operation in a fuzzy set

There are also common rules that are applied to classical sets, which can also be used with fuzzy sets, such as De Morgan's law, commutativity, associativity and the distributive property.

3.6.5 Fuzzy Rule Base

As mentioned earlier, the fuzzy rule base comprises a group of IF-THEN rules, as expressed by:

$$IF\ x_1\ is\ A_1^k\ ,and\ ,\cdots\ x_n\ is\ A_n^k \quad THEN\ y\ is\ B^k, \tag{3.20}$$

where, $(x_1, \cdots, x_n) \in X$, and $y \in Y$ are the real inputs and outputs of the fuzzy logic system, A_i^k and B^k are labels of the fuzzy sets in X and Y, respectively, and $k = 1, \cdots, M$ is the number of MFs. Each IF-THEN rule expressed in Equation 3.20 describes a fuzzy implication as:

$$A_1^k \times \cdots \times A_n^k \rightarrow B^k, \tag{3.21}$$

which is a fuzzy set expressed in the product space $X \times Y$. There are many widely deployed fuzzy implication rules that have been used in the literature, based on the generalisation implications of multi-value logic, some of which are:

- Product operation;
- Minimum operation;
- Arithmetic operation;
- Max-min operation.

3.6.6 Fuzzy Inference System

A Fuzzy Inference System (FIS), as shown in Figure 3.7, does a mapping from fuzzy sets X coming out of fuzzification to fuzzy sets Y, going to defuzzification, depending on the compositional rule of inference and the IF-THEN rules in the fuzzy rule base. There are basically two FISs that can be implemented in fuzzy systems and they differ, to some extent, in the way in which mode outputs are calculated, these being as follows.

- **Mamdani:** in 1975, Mamdani proposed [91] an FIS as a challenge to control a steam engine by creating a set of linguistic control rules attained from expert operators. This inference approach was among the earliest control systems implemented using fuzzy set theory. Mamdani's fuzzy inference is reported as the most popularly realised fuzzy procedure.

- **Sugeno:** in 1985, the Sugeno-type, or sometimes called the Takagi-Sugeno-Kang (TSK), FIS was introduced [92]. In general, it can be employed to model any system in which the MFs of the output can be either constant or linear, and this is main difference with Mamdani type.

When it comes to comparison of the above types of inference systems, it is reported that Sugeno's FIS is a computationally efficient representation and more compact than Mamdani's FIS. Moreover, the former offers a good ability regarding the implementation of adaptive methods for building fuzzy systems, which can be employed to modify the MFs. Consequently, the FIS well represents the data.

3.6.7 Fuzzy Controllers

FLC is well known as one of the most effective intelligence-based control designs for nonlinear industrial processes. The main motivation for using the fuzzy concept in control systems development is basically to cope with difficulty facing the control designer in relation to the modelling and simulation of complex real-world processes. Albeit a comparatively accurate model of a dynamic system can be obtained, it is occasionally too complex to implement for control design purposes, particularly with any traditional control methods that necessitate limiting assumptions for the process, such as linearity [93].

The most significant benefits of FLC can be summarised as follows:

- A universal approximation or so-called nonlinear-associative memory can be provided by FLC from its input signals to output, control actions, and the nonlinearity can be designed by picking the MF type and tuning the associated parameters [94];
- FLC does not need mathematical modelling to construct the control design, and hence, this, which is considered as the most problematic task, can be side-stepped [70];
- Using a fuzzy approach with another intelligence-based method to update the MFs and associative parameters automatically makes it relatively easier to design an adaptive FLC;
- Lastly, FLC is considered easier to implement by either hardware or software, in comparison with maths model based control.

There are different configurations for designing FLC to control a process, with the three most widely applied having been investigated by Qiao et al. [95], as shown in Figure 3.12, all of which are applied in this thesis. where, $K_{1,2,3,4}$ are scaling factors or gains, u is the process input (control action) and e is the difference between the desired output (set-point) r and process output y, or error and $\dot{e}$ is the change in error over the time.

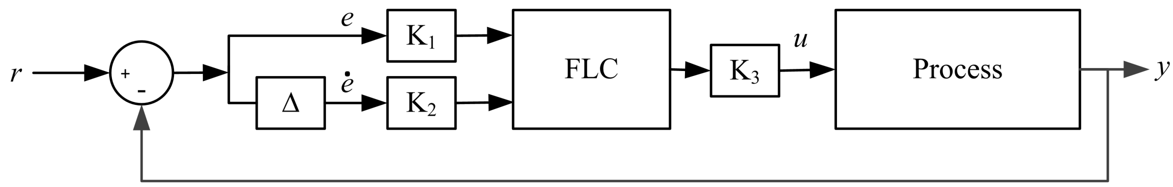

(a) PD-like Fuzzy logic controller block diagram

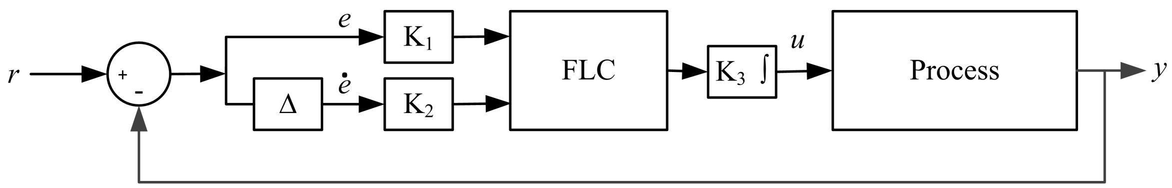

(b) PI-like Fuzzy logic controller block diagram

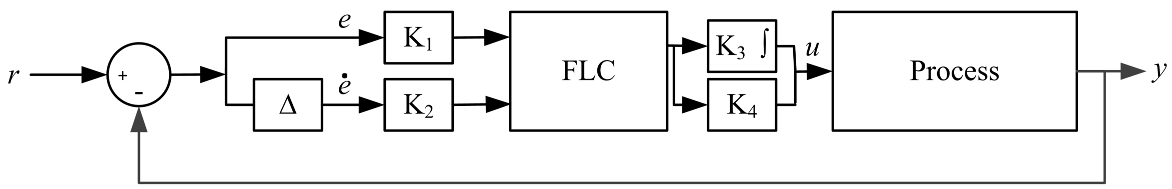

(c) PID-like Fuzzy logic controller block diagram

Figure 3.12 Block diagrams of different FLCs

3.7 Adaptive Neuro-fuzzy Inference Systems

ANFIS, is a combination between an ANN and TSK fuzzy inference system, with this method being introduced at the beginning of the 1990s [96]. Subsequently, by integrating both ANN and FL fundamentals, it has given a powerful ability to capture the advantages of both approaches in a single structure. That is, ANFIS is considered to be an effective universal approximator [97]. Basically, the implementation of ANFIS offers an automatic adjustment of MFs and related parameters of FIS. The main motivational aims of using ANFIS are the features that present the learning capabilities of both ANN and FL. The learning algorithm adjusts the MFs of a Sugeno fuzzy model using the training input-output dataset. Figure 3.13 shows an example of the simplified ANFIS architecture, which contains two MFs (A, B) for both inputs (x_1, x_2) and four rules as well as four MFs of output Y. Where, w_1 to w_4, which are the weights of correctness for the rules, are calculated through T-norm. Additionally, these weights are used to compute y_1, y_2, y_3 and y_4 respectively. The

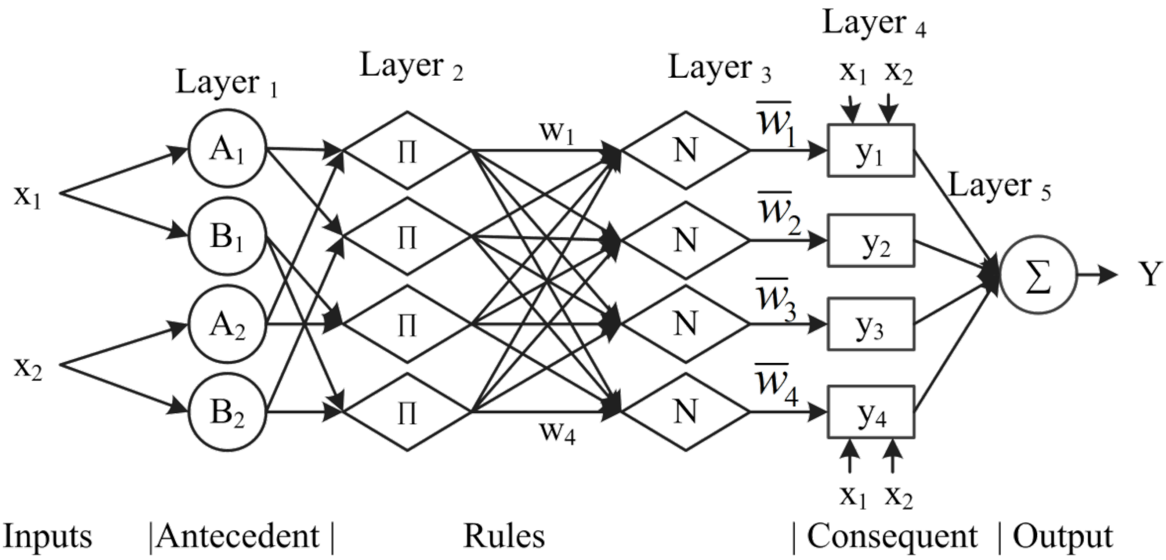

Figure 3.13 ANFIS architecture of two inputs, four rules and the first order Sugeno model [97]

final output Y is expressed as:

$$Y = \frac{w_1 y_1 + w_2 y_2 + w_3 y_3 + w_4 y_4}{w_1 + w_2 + w_3 + w_4}. \tag{3.22}$$

After normalising the weights, the output is written as:

$$Y = \bar{w_1} y_1 + \bar{w_2} y_2 + \bar{w_3} y_3 + \bar{w_4} y_4. \tag{3.23}$$

There are two methods used in the ANFIS approach for training the network to find the optimal weights, which are:

- Backpropagation;
- Hybrid learning, which is a combination of backpropagation and least square error.

The obvious limitation of using ANFIS as process modelling and control is that it contains only a single output, which is inadequate for applying to multivariable processes.

3.8 Evolutionary-based Optimisation Methods

Optimisation is a significant tool in modelling and control, which refers to finding the optimal, or near-optimal solution to a specified problem, according to a predetermined criterion, which is called an objective function or fitness. Evolutionary-based optimisation methods, or Evolutionary Computation (EC), are a set of algorithms mimicking the evolution process in biology and natural selection theory. In other words, they are a group of generation-based optimisation tools that use trial and error to solve stochastic problems with a metaheuristic feature [98, 99]. In general, evolutionary-based optimisation methods have been developed over the past 40 years. Firstly, the original group of EC comprised three archetypes: GAs [100], evolutionary programming [101] and evolution strategies [102]. These evolutionary-based methods were established to solve different problems. The next generation of EC methods involved several new and correspondingly remarkable archetypes. The most distinguished of the second generation were methods that evolved generations of data structures instead of string representations [103], as well as GAs that advanced populations of programs, recognised as genetic programming.

In the last decade, a new generation of evolutionary-based optimisation methods has been developed in addition to the so-called cultural algorithms, PSO [104], Ant Colony Optimisation (ACO) [105] etc. All generations of ECs optimisation tools have been implemented widely in a broad range of applications, especially with other intelligent based approaches to construct hybrid intelligent systems that are used in advanced modelling and control. It is unfeasible to investigate all these optimisation methods in this thesis, but the most popular methods of ECs, GA and PSO are implemented in this thesis and thus, are discussed in the next subsections.

3.8.1 Genetic Algorithms

Introduced first in 1975 by Holland [100], GAs can be defined as self-adjusting global optimisation search algorithms. Fundamentally, they based on the concept of the Darwinian theory of biological evolution and natural selection. GAs work by mimicking the biological developments that are detected in nature as driving the phenomena of genetic and evolutionary mechanisms. Due to the natural selection connotation, GAs offer solutions to complex problems by using code procedure and reproduction methods [106]. Those bio-inspired operators include mutation and crossover in addition to a selection mechanism. Each individual, which represents a candidate solution of a problem, is characterised by a data structure and involves two parts: a chromosome and an objective function. The chromosome of an individual is formed by genes and the values that are given to a gene of a chromosome are denoted as the alleles of that gene. A set of individuals together shapes what is identified as a generation or population. In most of the GAs, the size of the generation remains fixed for the search time. Individuals nominated from the current generation, termed parents, are carefully chosen based on their objective function and are eligible for generating offspring. Typically, individuals with above average objective function have an above average potential of being nominated. When the selection procedure has been undertaken, crossover and mutation, as a reproduction process, are applied to the surviving individuals, or parents. In the crossover operation, parents generate replicas of their genes to produce a chromosome for an offspring. On the other hand, mutation necessitates one parent. The offspring which is made up by mutation typically bear a resemblance to its parent apart from a few reformed genes. After creating the offspring or children, the potential solutions are assessed based on an objective function, whereby every child has a fitness function. The passed-away individuals should be removed in the current generation to make space for the newborn children. Habitually, individuals are uninvolved depending on their fitness function with low average individuals having a high average potential of being chosen to die. This mechanism of deciding which individuals must die based on their objective function is known as natural selection. An interesting feature of GAs, and generally all ECs, is that the initial generation of individuals' necessity is not perfect. In fact, at first generation, each individual normally represents an arbitrarily produced potential solution. The repetitive selection and reproduction processes of GAs are described in the flowchart shown in Figure 3.14. GAs have been employed extensively with other intelligent-based approaches to building hybrid intelligent systems, which have been applied to a wide range of applications in modelling, estimation and control

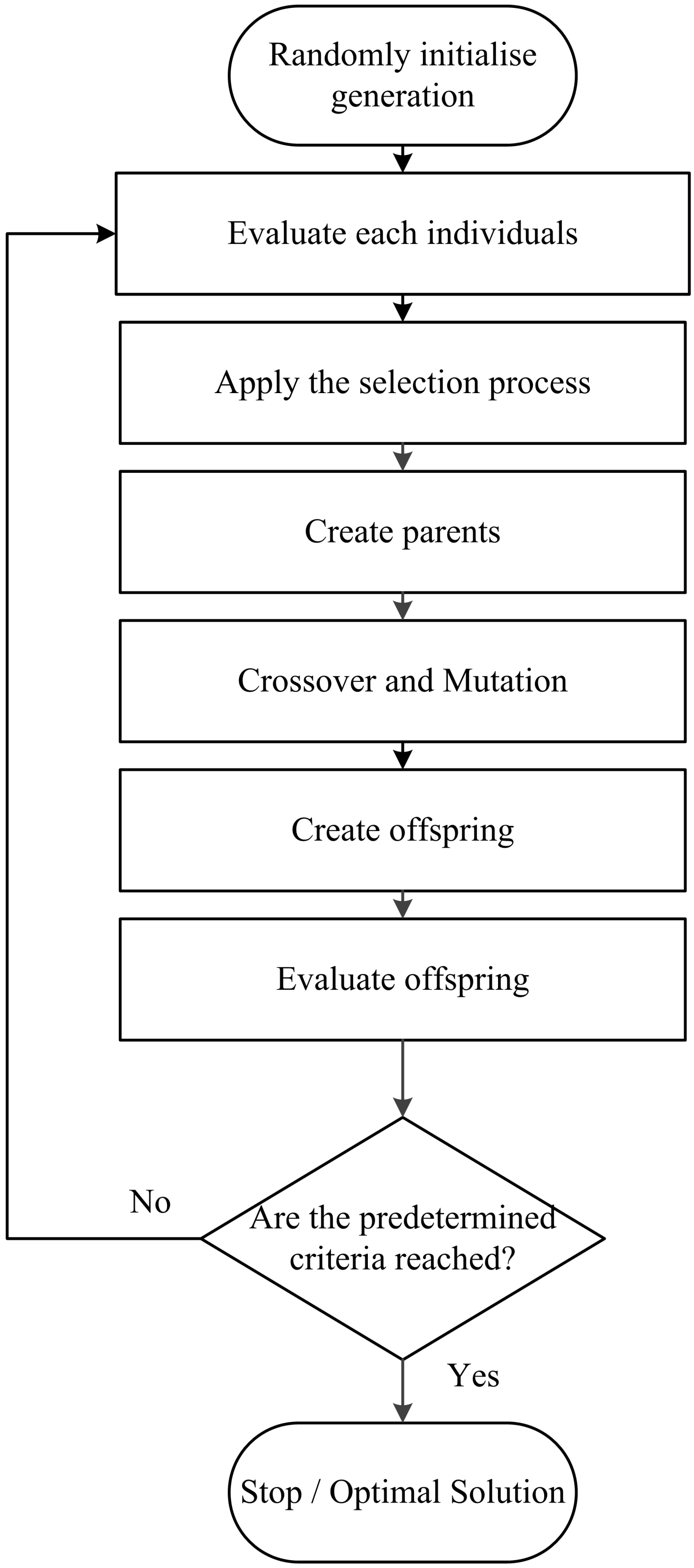

Figure 3.14 Search mechanism of GAs

[107, 108]. Many researchers have applied GAs to tune different controllers using several applications, such as conventional PID controllers [109], FLCs [110, 111], PID-like FLCs [112], ANFIS controllers [113], etc.

3.8.2 Particle Swarm Optimisation

PSO was proposed as a heuristic optimisation approach in 1995 [114] and updated in 2001 [115]. Hence, it is comparatively new and vastly successful, being a subfield of EC. Swarm Intelligence (SI) investigates the collective activities of decentralised and self-organised natural or artificial systems. Typically, SI approaches comprise a population of individuals or particles interacting in the vicinity to one another in addition to others in the domain. The stimulation habitually comes from nature, particularly biological systems [116]. Widely known cases of SI consist of ant colonies, animal herding, bird flocking, fish schooling, and bacterial growth. One of the most interesting features of PSO, and in general SI-based algorithms,is self-organisation, which is a procedure, whereby global order arises out of the local interactions between the individuals of an initially stochastic system. This procedure is unprompted, i.e. it is not managed by any agent within or outside of the system.

Many authors have proposed a modification of the standard PSO to build an improved version of the algorithm by integrating it with other approaches and/or taking advantage of other concepts. Jan et al. [117] proposed a modified version that befits from quantum mechanics theory, which they called Quantum-behaved PSO. Also, Kennedy proposed a modification of the standard algorithm by changing some operators and called it Bare Bones PSO [118]. There is also a modified version called Chaos-based PSO, in which PSO is integrated with chaos theory to improve the search performance [119]. The proposals of modifying the standard PSO are ongoing for improving the performance or application the algorithm in a complex environment. However, the standard PSO is still applied widely in a wide range of engineering problems [120], especially in modelling and control application. Consequently, the standard PSO is implemented in this thesis in modelling and control, as will be discussed later.

The realising of PSO is detailed as follows: all particles or candidates are placed at a random location and are theoretically considered to travel randomly within the search space. The direction of each particle then changes gradually to move more assuredly along the direction of its best previous position, to determine an even better one, per predefined criteria or an objective function. The preliminary velocity and location of the particles are nominated randomly and the subsequent velocity can be updated by the following equation:

$$V_{i+1} = \omega V_i + C_1 R_1 (LB_i - x_i) + C_2 R_2 (GB - x_i). \tag{3.24}$$

The position of the new particle is computed by adding the previous position to the obtained velocity, as shown in the following equation:

$$x_{i+1} = x_i + V_{i+1}, \tag{3.25}$$

where, V is the particle's velocity, x is the particle's position, $R1$; $R2$ are independent random factors uniformly distributed from 0 to 1, $C1$; $C2$ are acceleration coefficients and ω is the inertia weight. Equation 3.24 is used to compute the new velocity of the particle, per its previous value and the distance of its current position from its own local best position (LB) and the global best position (GB). Then, the particle travels to a new position in the search space, per Equation 3.25. The mechanism search of the standard PSO is presented in the flowchart shown in Figure 3.15.

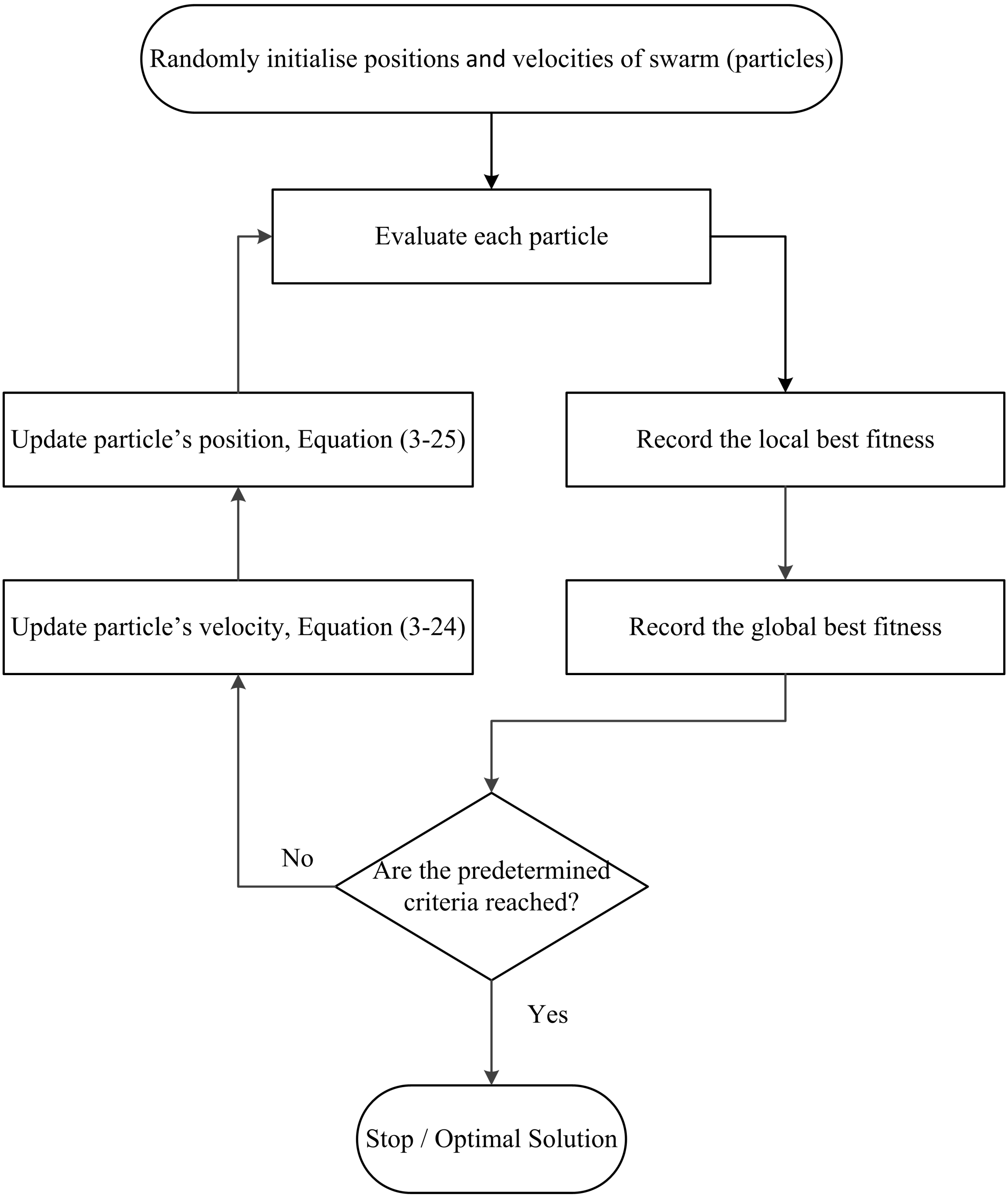

Figure 3.15 Search mechanism of the standard PSO

3.9 Summary

In this chapter, a general introduction to intelligent control has been provided and approaches have been presented, such as ANNs and FL as well as hybrid intelligent-based systems like ANFIS and the ANN-based NARMA model. The chapter demonstrated the importance of AI techniques with an emphasis on modelling and control application for dealing with complex and hard-to-control environments like nonlinearities and uncertainties. These techniques are implemented in this thesis in addition to optimisation methods, namely, GA and PSO, which also been introduced with a brief presentation about their principles, classification and search mechanisms. In the next chapter, the distillation process will be introduced as a vital MIMO industrial process that needs to be efficiently controlled.

Chapter 4

Modelling and Control of a Binary Distillation Column

4.1 Introduction

Distillation is undoubtedly the most extensively employed process method for separating mixtures, in the liquid phase, into their chemicals. Usually, a vertical column is used to achieve the process called a distillation column. These columns are reported as being the most widely implemented unit in the petroleum, chemical, liquid and natural gas industries [121]. Despite the wide use of these columns, it is generally agreed that they have the disadvantage of being the most wasteful energy consuming entity in chemical the industry. Regarding which, in the USA, the Department of Energy issued a report stating that distillation columns are the largest consumers of energy in that industry. Typically, they account for 40% of the energy consumed by all petrochemical plants. Even with this high energy consumption, distillation is still commonly operated for the purification as well as separation methods [122]. Consequently, resourcefully operating these types of columns requires a high degree of automatic control [121]. There are several types of distillation process and columns depending on the mixture to be separated and the degree of purity required for the output of the column. However, in general, the process can be classified as binary distillation when the feed mixture needs to be separated into two components and multicomponent distillation, when the output of the column is more than two separated products. In this chapter, a binary distillation column is investigated in relation to modelling and control, while a multicomponent distillation column is discussed and implemented in Chapter six.

4.1.1 Historical Background of Distillation

Originally, distillation was known as a purification process carried out by Greek alchemists in the first century AD. The first application of distillation was probably the distillate water obtained from the purification of seawater during a process conducted in simple equipment known as an alembic. The alembic used the basic principles of distillation to split the salt from the seawater, as shown in Figure 4.1. In around 800 C.E., the Arabic alchemist Jabir ibn Hayyan developed distillation into its contemporary formula, with the origination of the alembic. He is also attributed with the development of several other chemical units and processes that are still in use today [123].

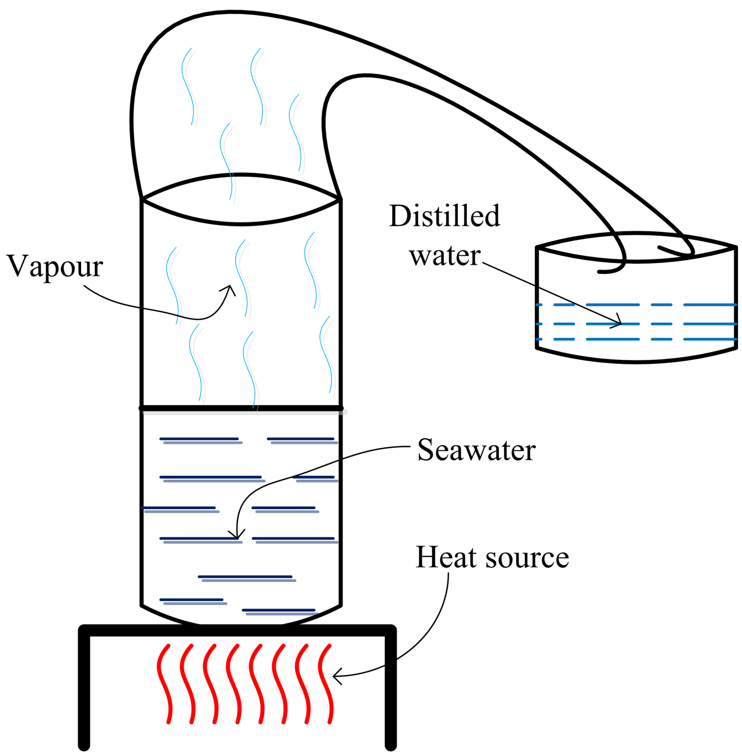

Figure 4.1 Schematic diagram of an alembic used in medieval times for seawater distillation

The alembic design served as the foundation for some of the subsequent microscale distillation units. Alchemy contributed to the advance of chemical science, with its widely used alembic, also called a retort, being used for distillations. Retorts or alembics are made of glassware with extended necks linking to the side at a downhill angle, which work as a condenser; using air to cool the vapour, to condense the distillate and finally, producing the distillate water for collection. The distillation process was evolved for many different applications. At the end of the nineteen-century, with the rise of chemical engineering as a scientific field, scientists became increasingly more interested in design than experimental approaches. The emerging petroleum industry at the beginning of the twenty-century provided the motivation for the development of powerful design procedures, like the Fenske equation and the McCabe–Thiele scheme. The distillation columns were becoming relatively trouble-free for simulation and were investigated theoretically to save time and cost.

4.2 Binary Distillation

A binary distillation process is implemented when the mixture comprises only two products to be separated, which can be piped into the column in various ways. For instance, it is merely fed into the column if the source pressure of the mixture higher than the column pressure. If not, then the mixture is compressed or pumped into the column. The mixture may be a saturated vapour, a superheated vapour, a partially vapourised liquid-vapour mixture, a sub-cooled liquid or a saturated liquid, which is a liquid that at its boiling point has the same pressure as inside the column. If the mixture has a much higher pressure than the column pressure and streams through a pressure let-down regulator just ahead of the column, it will instantly expand and undertake a partial flash vaporisation, producing a liquid-vapour combination as it passes through the column.

The binary distillation process can be briefly described as follows: the feed mixture is separated into two products, one being a distillate or overhead, and the other is the bottoms product. Heat is supplied to the column via a reboiler, in order to vapourise the liquid in the base of the column. The vapour goes up through trays inside the column to reach the top, which then liquefies in the condenser and the liquid from the condenser drops into the reflux drum. Finally, some of the distillate product is removed from this drum as a pure product. The rest of the liquid is fed back near the top of the column as reflux, while another product is produced at the bottoms.

A schematic diagram of a binary distillation column is shown Figure 4.2. There are different vapour-liquid contacting approaches inside the distillation columns to offer the essential quantity of equilibrium stages. As aforementioned, these instruments are known as trays or plates [124]. The temperature, and sometimes pressure of each stage vary, depending on their positions inside the column. At the bottoms of the column, the stage has the highest temperature and similarly, sometimes pressure, due to its close location to the reboiler.

Continuing upwards in the column the conditions, temperature and pressure, keep declining for each next stage. That is, the equilibrium state of vapour and liquid for each component in the mixture distinctively responds to the changed conditions, temperature and pressure, at each stage of the column. This indicates that each element creates a different composition at each of the stages for the vapour and liquid states, which lead to the component separation. The Vapour–Liquid Equilibrium (VLE) is defined as the distribution of a chemical component between the vapour and a liquid state at all stages across the column. Figure 4.3 shows a schematic diagram of a theoretical stage in a continuous distillation column.

4.2.1 Modelling and Simulation of a Binary Distillation Column

When modelling a binary distillation column via representing all the mathematical relationships, several assumptions need to be considered. Such considerations will facilitate the modelling of a binary distillation process. Luyben [125] has listed all the assumptions for a 20-stage binary distillation column, which have also been taken into account in this thesis, as:

1. No chemical reactions occur inside the column;
2. There is constant pressure;
3. Binary mixture;

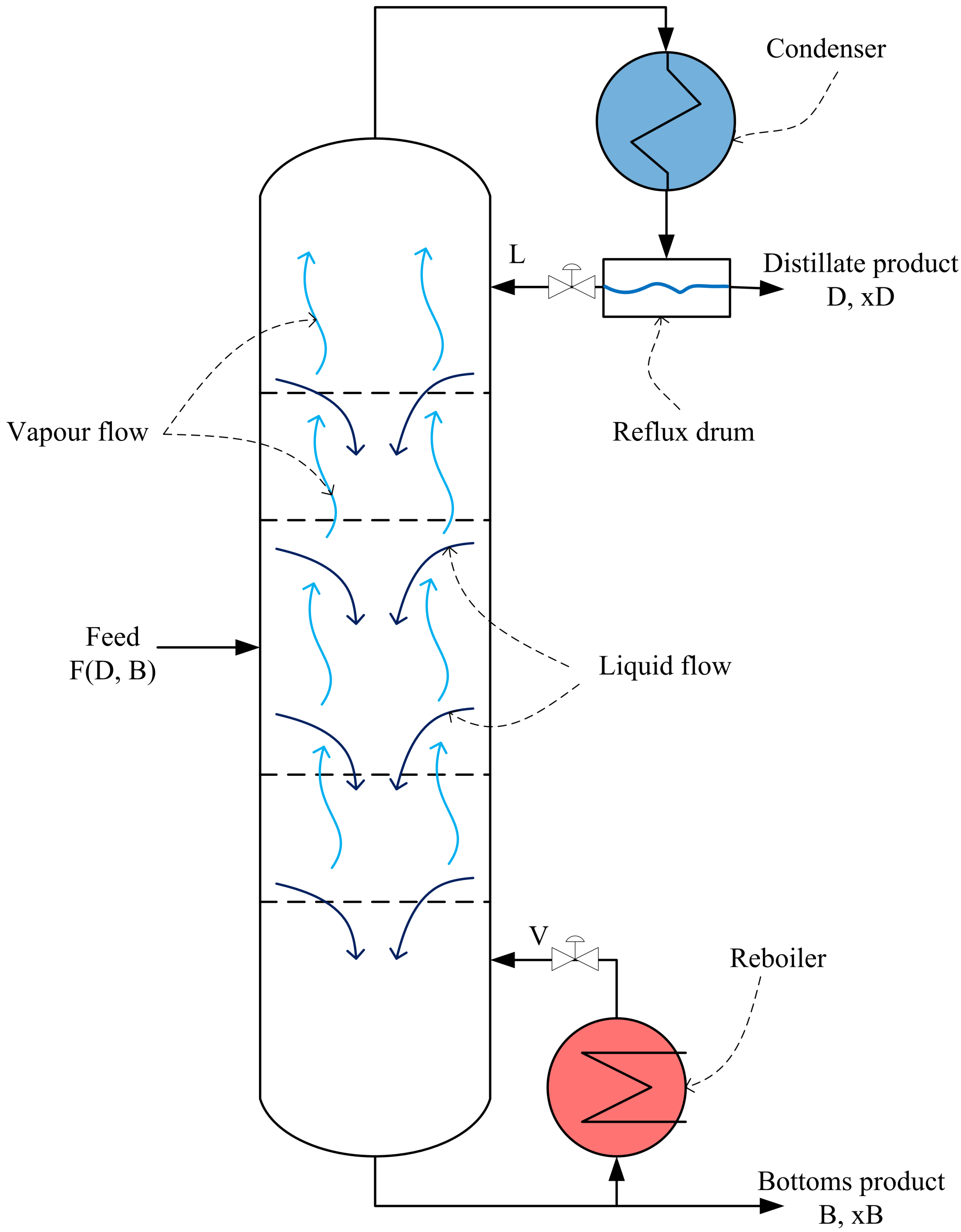

Figure 4.2 Schematic diagram of a typical binary distillation column

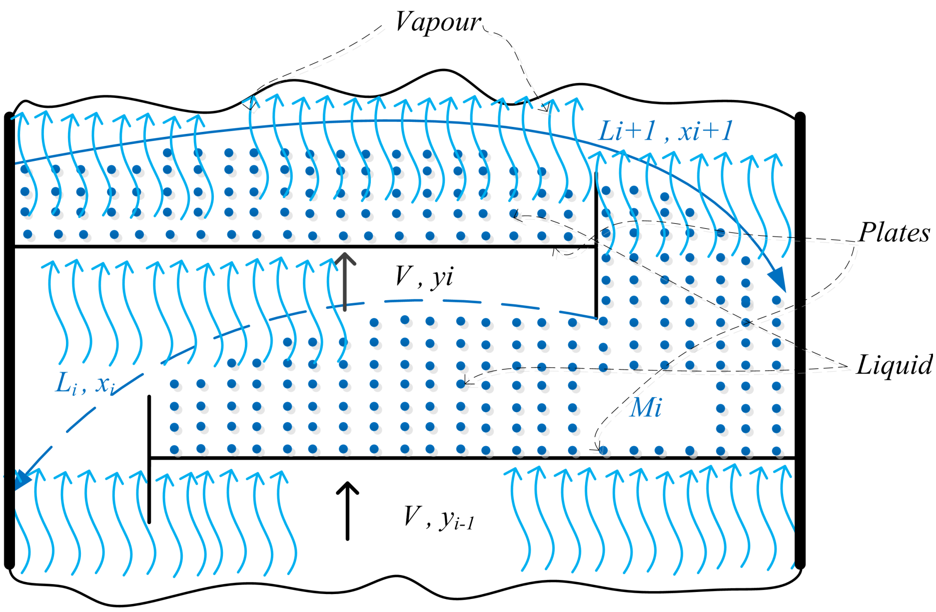

Figure 4.3 Theoretical stage in continuous distillation column

4. Constant relative volatility;
5. No vapour hold-up takes place in any stages;
6. Constant hold-up of liquid in all trays;
7. Perfect mixing and equilibrium for the vapour-liquid at all stages.

Hereafter, the mathematical equations of the model can be written per stage as follows [125].

- At each stage (excluding the reboiler, feed and condenser stages):

$$M_i \frac{dx_i}{dt} = L_{i+1}x_{i+1} + V_{i-1}y_{i-1} - L_i x_i - V_i y_i. \tag{4.1}$$

- Above the feed stage, $i > NF$:

$$M_i \frac{dx_i}{dt} = L_{i+1}x_{i+1} + V_{i-1}y_{i-1} - L_i x_i - V_i y_i + F_V y_F. \tag{4.2}$$

- Below the feed stage, $i <= NF$:

$$M_i \frac{dx_i}{dt} = L_{i+1}x_{i+1} + V_{i-1}y_{i-1} - L_i x_i - V_i y_i + F_L x_F. \tag{4.3}$$

- At the reboiler and column base, $i = 1$, $x_i = x_B$:

$$M_B \frac{dx_i}{dt} = L_{i+1}x_{i+1} - V_i y_i + Bx_B. \tag{4.4}$$

- At the condenser, $i = N+1$, $x_D = x_{N+1}$:

$$M_D \frac{dx_i}{dt} = V_{i-1}y_{i-1} - L_i x_D - Dx_D. \tag{4.5}$$

- Vapour-liquid equilibrium relationship of each tray:

$$y_i = \frac{\alpha x_i}{1 + (\alpha - 1)x_i}. \tag{4.6}$$

The flow rate of constant molar flow:

- Above the feed stage:

$$L_i = L, \quad Vi = V + F_V. \tag{4.7}$$

- At or below the feed stage:

$$L_i = L + F_L, \quad V_i = V. \tag{4.8}$$

  since

$$F_L = Fq_F, \tag{4.9}$$

$$F_v = F + F_L. \tag{4.10}$$

The constant hold-up for both the condenser and the reboiler is as follows.

- Reboiler:

$$B = L + F_L - V. \tag{4.11}$$

- Condenser:

$$D = V + F_V - L. \tag{4.12}$$

The feed compositions x_F and y_F are calculated from the flash equation as:

$$F_{zF} = F_L x_F - F_V y_F. \tag{4.13}$$

Equation 4.1 to 4.6 represent the nonlinear behaviour of the binary distillation column since they at least involve multiplication of two time-dependent variables. The abbreviations, operation conditions and steady state of the column are shown in Table 4.1, and the nominal values of liquid composition at every stage of the simulated binary column is presented in Table A.1.

The simulation of a binary distillation column is straightforward and relatively easy. Many of researcher have used a special platform called Aspen HYSYS®, which is also widely used in industry for design, optimisation and operation. Such a platform involves ready-to-use libraries that enable the designer to use drag and drop to build different chemical plants including distillation columns. Nevertheless, the Aspen HYSYS® environment does not support a lot of useful tools that are used extensively in data analysis, control design, powerful visualisations and so on. Such advantages are offered by Simulink® platform, from MathWorks, which is well known as a featured simulator due to its strong combination with MATLAB®, the de facto standard for engineering and scientific analysis as well as data

Table 4.1 Steady state values of the binary distillation column used in the modelling and simulation

Symbol	Description	Value	Unit
N	Number of stages (trays)	20	-
NF	Feed stage location	11	-
F	Typical inlet flow rate to the column	1	kmol/min
D	Typical distillate flow rate	0.5	kmol/min
B	Typical bottoms flow rate	0.5	kmol/min
q_F	Light component in the feed (mole fraction)	0.5	-
x_F	Mole fraction of the liquid in the feed	0.5	-
L	Typical reflux flow rate	1.28	kmol/min
V	Typical boilup flow rate	1.78	kmol/min
α	Relative volatility	2	-
x_D	Distillate composition (mole fraction)	0.98	-
x_B	Bottoms composition (mole fraction)	0.02	-
i	Stage number during distillation	-	-
x	Mole fraction of light component in the liquid	-	-
y	Mole fraction of light component in the vapour	-	-
M	Tray hold-up liquid	0.5	kmol
M_D	Condenser hold-up liquid	0.5	kmol
M_B	Reboiler hold-up liquid	0.5	kmol

visualisation software [126]. Hence, due to these facilities, MATLAB® and Simulink® were used to build the distillation columns and all the control design used in this thesis.

As aforementioned, the simulation of a binary distillation column is straightforward. The main complexity is a significant number of algebraic equations, and Ordinary Differential Equations (ODE's) that must be solved. There are two ODE's per stage, one for total continuity and the second for component continuity, as well as two algebraic equations per stage: one for the vapour-liquid equilibrium and the second for hold-up quantity, as expressed by equations 4.1 to 4.13.

The simulation of a binary distillation column is based on building a stage by stage model using Simulink® starting from bottoms to the distillate. The Simulink® block diagram of the reboiler stage is shown in Figure 4.4, while Figure 4.5 shows the Simulink® block structure of each stage of the stripping section, that is, stages 1 to 9.

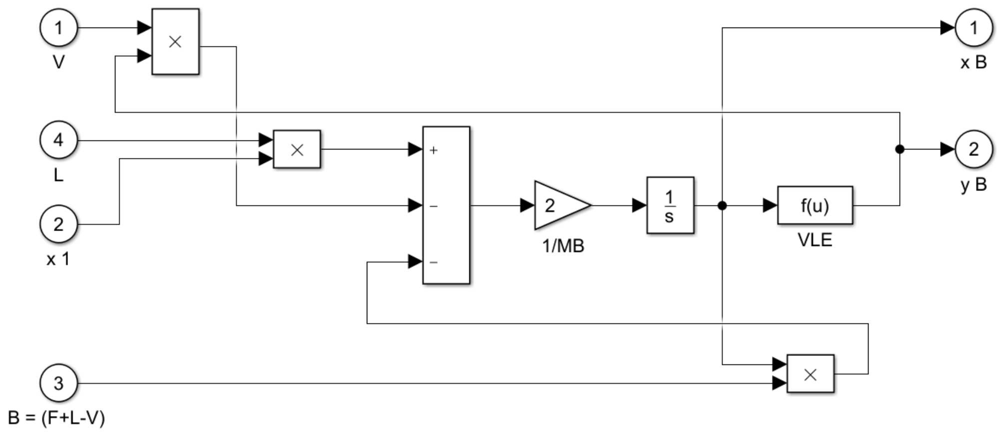

Figure 4.4 Simulink block diagram of the reboiler stage

The feed stage is represented in Figure 4.6, which is located at stage number 10. Figure 4.7 shows the Simulink block structure of each stage of the rectifying section, i.e. stages 11 to 19. At the distillate of the column, the total condenser stage, when the distillate composition is produced, is depicted in Figure 4.8. The Simulink model of the binary distillation column involving 20 stages in addition to the reboiler and condenser is shown in Figure 4.9.

In order to collect a dataset that represents the dynamic behaviour of the modelled column, the first step is to determine the input-output pairs of the column. One of the most common control loops of the binary column is the so-called (L-V) configuration [127], where the

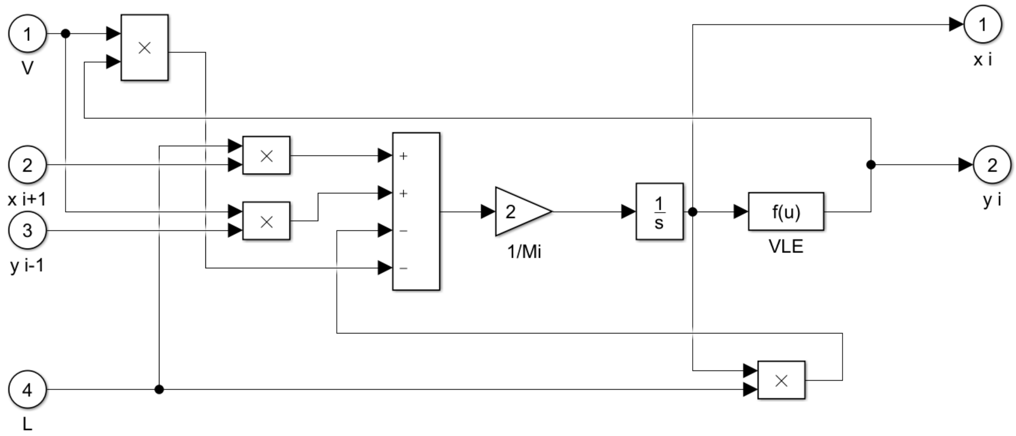

Figure 4.5 Simulink block diagram of a stage in the stripper section

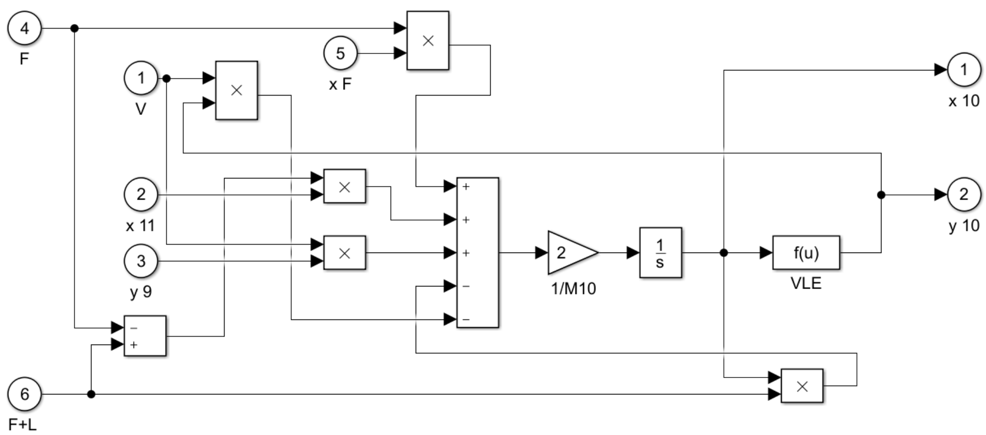

Figure 4.6 Simulink block diagram of the feed stage

reflux flow rate L is designated to control the mole fraction of the distillate product x_D, while the reboiler steam flow rate V is selected to control the composition of the bottoms product x_B, as expressed by the following equation:

$$\begin{bmatrix} xD \\ xB \end{bmatrix} = G^{LV} \begin{bmatrix} L \\ V \end{bmatrix}, \tag{4.14}$$

where, G^{LV} is a representation of the transfer function of the binary distillation column.

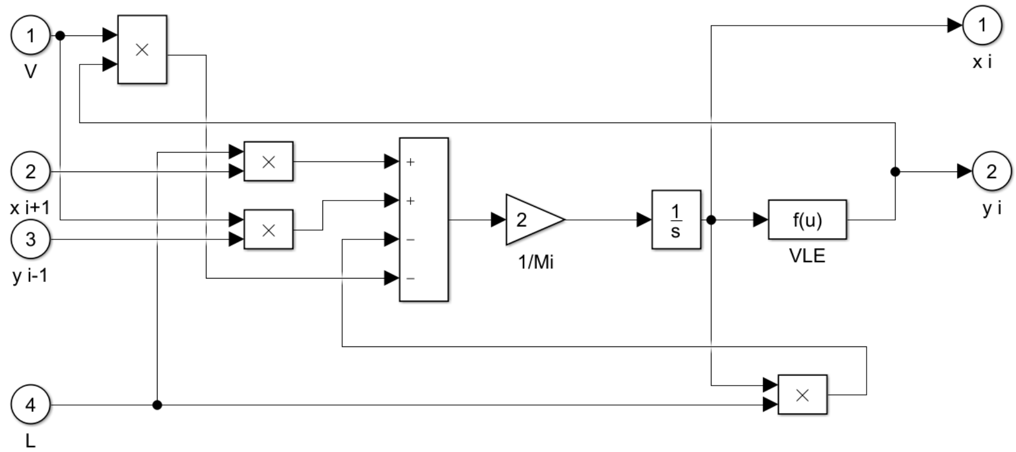

Figure 4.7 Simulink block diagram of a stage in the rectifying section

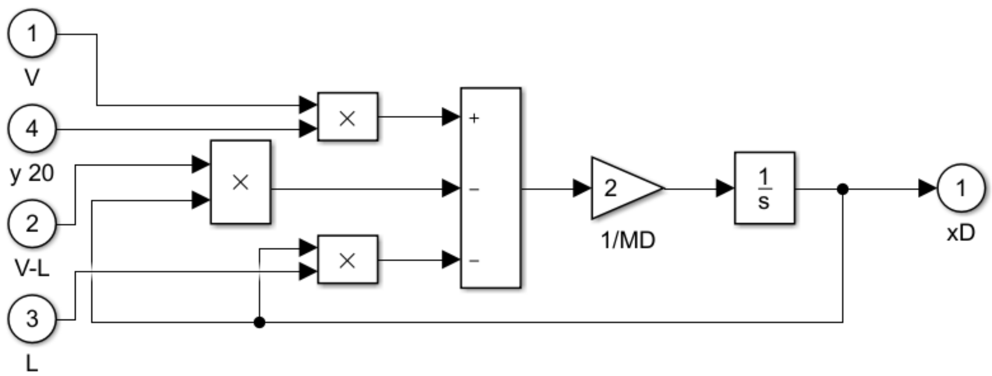

Figure 4.8 Simulink block diagram of the condenser stage

Obtaining as accurately as possible the model of the system to be controlled is the second step, which is achieved by mapping input-output pairs. In order to collect sufficient information to design a good model that represents the system's behaviour, the inputs are selected as a Pseudo-Random Binary Sequence (PRBS) within the operating range, each lasting 50 sampling times for L and V to collect the product compositions, x_D and x_B, at different situations. The distillate composition is approximately between 0.95 and 1 (mole fraction), while the bottoms composition is around 0.005 to 0.12 (mole fraction). A total of 2,000 records were collected for the identification stage. Figure 4.10 shows the reflux and

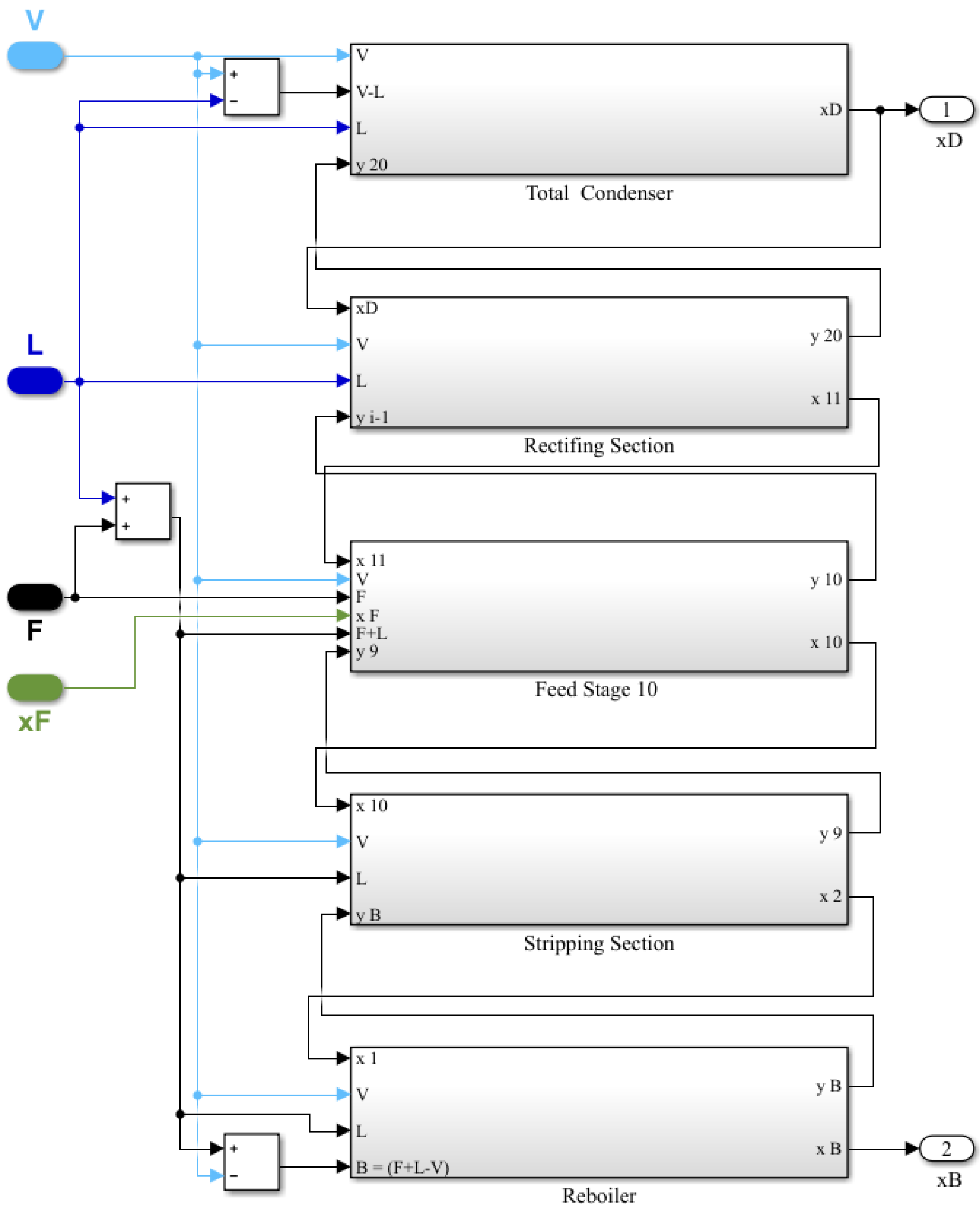

Figure 4.9 Simulink block model of a binary distillation column

vapour flow rate as inputs for the simulated model, while the output products composition is provided in Figure 4.11.

The collected dataset will be employed to obtain a NARMA-L2 model to design the proposed controller, which uses NARMA structure, in the next chapter. However, this chapter is devoted to modelling and simulating a binary distillation column, in addition to implementing the conventional PID controller for comparison purposes. Before applying any control design to the simulated model, an essential validation assessment of the simulated model should be undertaken. Such a test can be carried out either by a practical comparison with real data taken from a real industrial distillation column, which is obviously inaccessible or by comparing the simulated model behaviour with published data in the literature for the same specifications of a binary distillation column. Fortunately, a binary distillation column is a well-applied dynamic system in the literature, as presented in Chapter two. So, an evaluation of the applicability of the simulated model was conducted by comparing the behaviour of the model with the model used by Luyben [125].

In order to make a fair evaluation, the inputs of the simulated column were taken exactly as applied in Luyben's model. After conducting the simulation for 9.5 minutes, the same time chosen in Luyben's model, the distillate and bottoms compositions response to the inputs were entered, as shown in Figure 4.12. The graphical comparison shows very close behaviour of the simulated column with Luyben's model [125], which indicates an acceptable outcome and hence, the applicability of the model to be implemented in the proposed simulation control experiments.

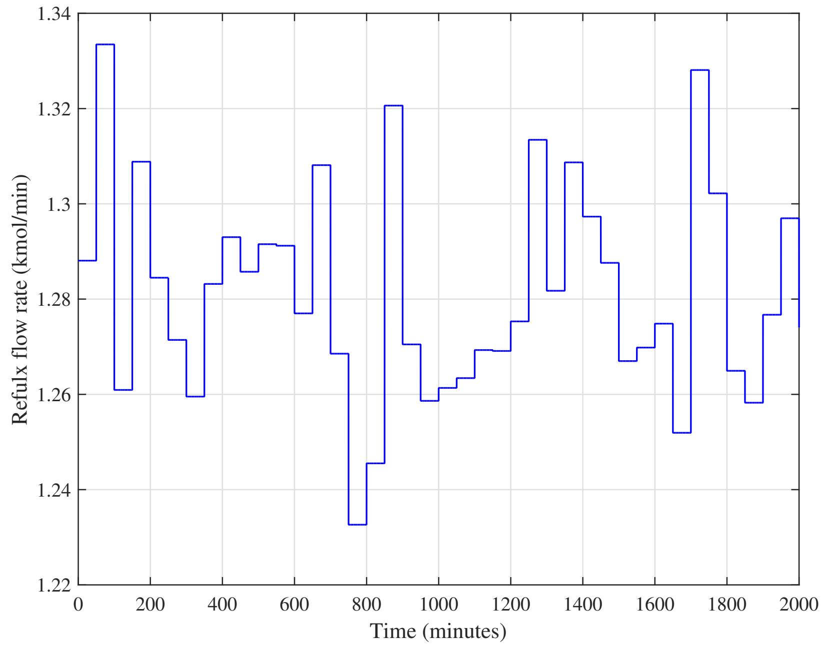

(a) Reflux flow rate

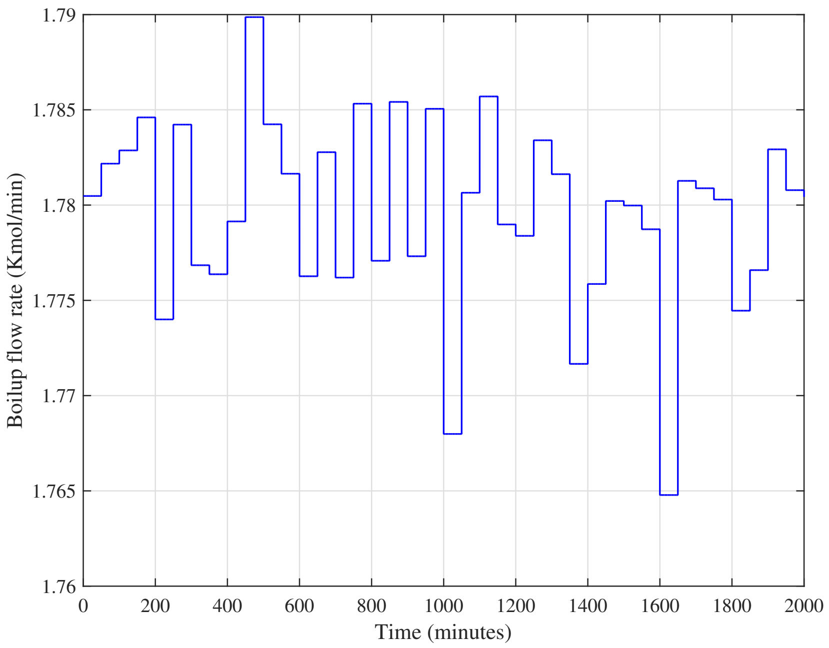

(b) Boilup flow rate

Figure 4.10 Reflux and vapour flow rate as inputs for the simulated binary distillation column

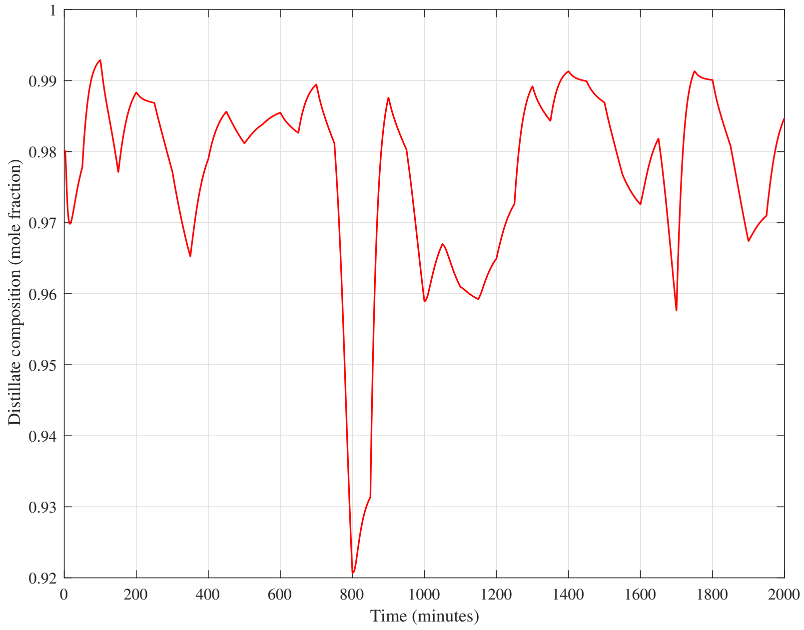

(a) Distillate product

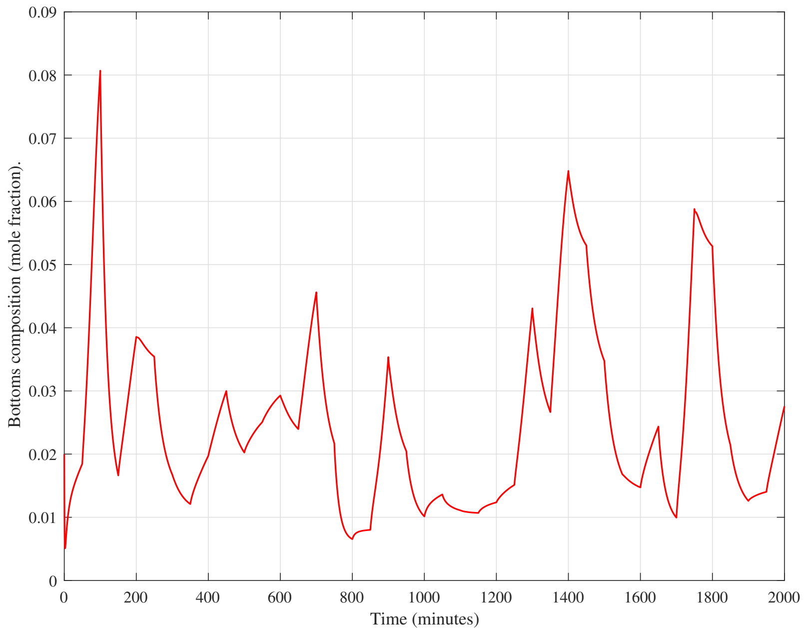

(b) Bottoms product

Figure 4.11 Distillate and bottoms product compositions as outputs of the simulated binary distillation column

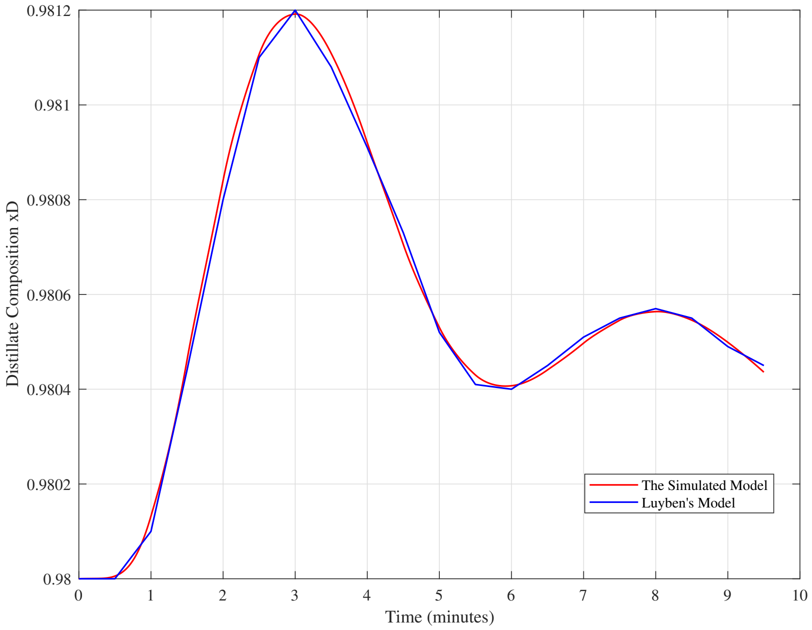

(a) Distillate product

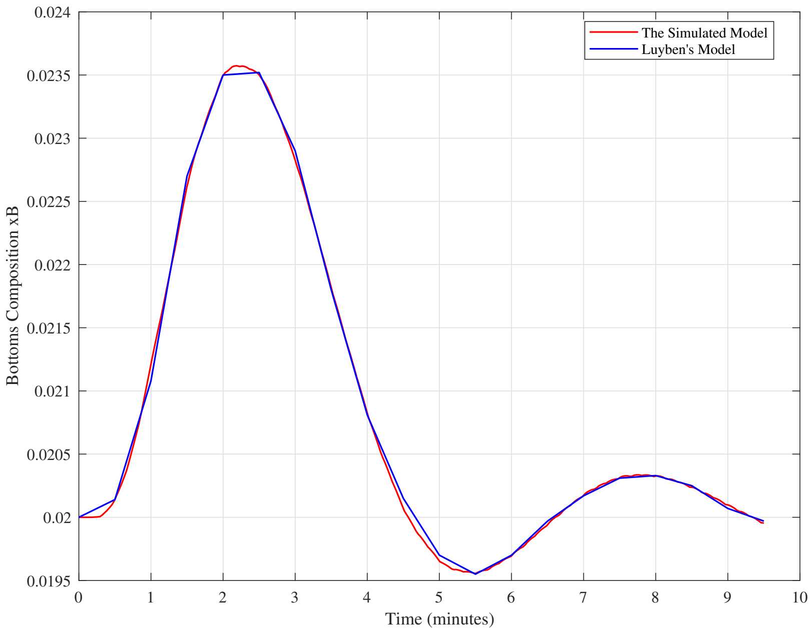

(b) Bottoms product

Figure 4.12 Graphical comparison of the product compositions of the simulated model with Luyben's model

4.3 Control of the Binary Distillation Column

Distillation is well recognised as a difficult process to control due to the following reasons [37]:

1. Nonlinearity, which characterises the behaviour of distillation columns, especially when separating high-purity compositions;

2. Considerable disturbances are expected in the feed flow rate and mixture composition;

3. There is significant coupling for two-product composition control.

These challenges are most significant for two-product composition control. When single-product control is required, the coupling is disregarded, and the follow-on control problem is critically shortened.

Satisfactory operation of a binary distillation column typically necessitates specific control objectives, such as:

- Control of both compositions of the distillate and bottoms products;

- Control of the liquid level in the reflux drum and at the column base.

The two-products' flow rates are characterised by the first control objective, while controlling the levels at the reflux drum, and the column base is essential for operational practicability in order to prevent overflowing and dryness of the reflux drum and the column base. The dynamic responses of controlling the liquid levels are habitually much quicker than those of compositions control. In the development of the simulated column, the dynamics introduced by level control have consequently been ignored, and the liquid levels have been assumed as being constant. Figure 4.13 shows the composition control loops of the simulated binary distillation column, in which the distillate composition is controlled by manipulating the reflux flow rate, while the boilup flow rate is controlling the bottoms composition. In the next section, a decentralised PID controller is implemented in an attempt to control the binary distillation column by a conventional controller. Its performance will be compared with different intelligent controllers, as investigated in the next chapter.

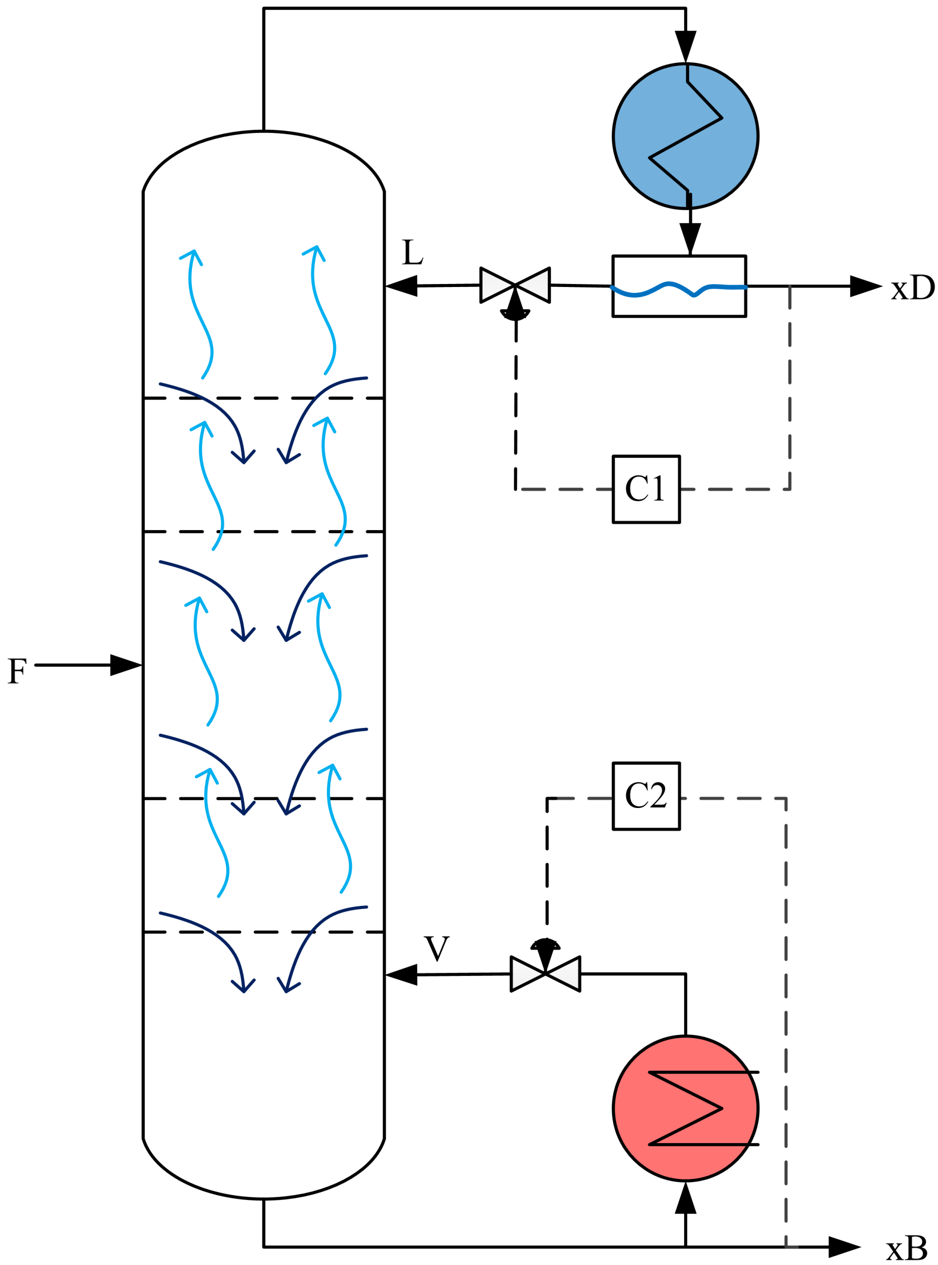

Figure 4.13 Control loops of a binary distillation column

4.3.1 Proportional–Integral–Derivative Controller

PID is a feedback loop control design widely implemented in industrial control applications. Fundamentally, a PID controller computes the difference between a measured process variable and the desired set-point and produces a control signal $u(t)$ as an amendment based on proportional, integral, and derivative actions. PID control design has been investigated extensively in the literature with successful applications in several domains. Its simplicity is considered the main advantage and weakness at the same time; it bounds the range of the processes that it can control efficiently [72]. A block diagram of a PID controller is presented in Figure 4.14.The PID control structure is termed after its three amending aspects, whose sum produces the control signal which is the Manipulated Variable (MV) of the process. The proportional, integral, and derivative actions are summed to compute the PID controller output. The final algorithm expression of the PID controller is:

$$u(t) = K_p e(t) + K_i \int_0^t e(\tau) d\tau + K_d \frac{e(t)}{dt}, \tag{4.15}$$

where;
K_p: the proportional coefficient
K_i: the integral coefficient
K_d: the derivative coefficient
e: the difference between the desired output r (also known as the set-point) and the process output y, which is calculated as:

$$e(t) = r(t) - y(t), \tag{4.16}$$

where, t is the instantaneous time and τ is the integration time.

Correspondingly, the PID controller algorithm form in the Laplace domain can be expressed as:

$$L(s) = K_p + \frac{K_i}{s} + K_d s. \tag{4.17}$$

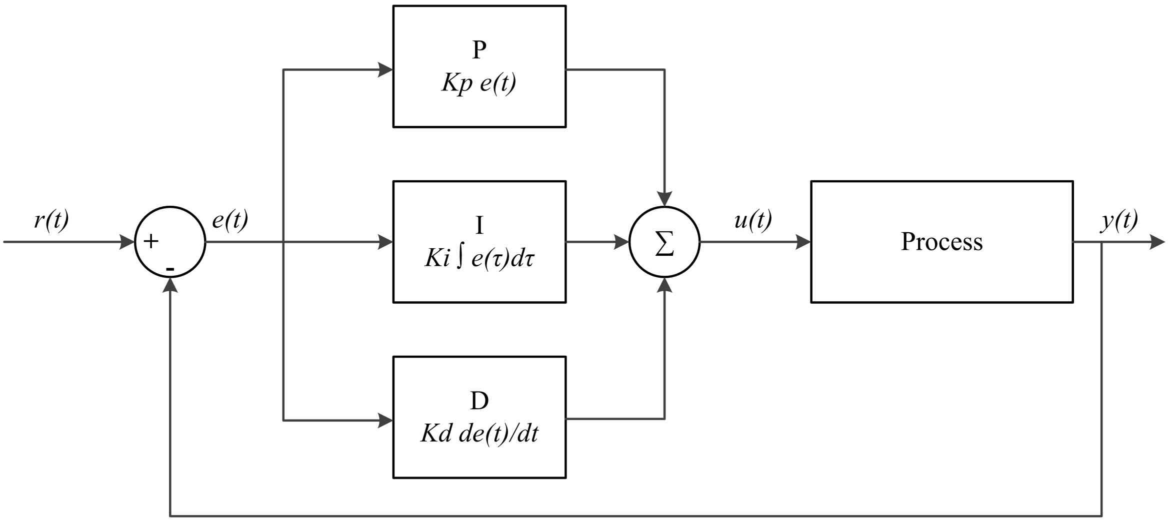

Figure 4.14 Block diagram of a PID controller

The PID controller has been investigated as a group of sub-controllers, such as PI, PD and PID. The best selection of one these controllers is the requirement and the degree of simplicity for application (process), for example, the response speed, the steady state error, oscillation behaviour and so on. Generally, the PID configuration that contains delivers the optimum dynamic response. In addition, PID can be implemented as a controller for high-order processes [128].

In addition to the parallel form of PID controller presented in Figure 4.14, there is another type in which all parts are arranged in a serial manner, as shown in Figure 4.15 and expressed mathematically as:

$$u(t) = \left(K_p e(t) + K_i \int_0^t e(\tau) d\tau\right)\left(1 + K_d \frac{e(t)}{dt}\right). \tag{4.18}$$

The coefficients of the PID controller are often called tuning parameters. The performance of the controller depends primarily on fitting those parameters so as to reduce the difference between the set-point and the process output. In the literature, there are many traditional methods for tuning PID control parameters, such as Ziegler-Nichols, Cohen-Coon, Tyreus-Luyben and Åström-Hägglund [129, 130]. All these approaches are employed to find the optimal PID gains and also are considered as manual tuning efforts, which basically depend on previous experience and/or trial and error attempts. Recently, software-based tuners have

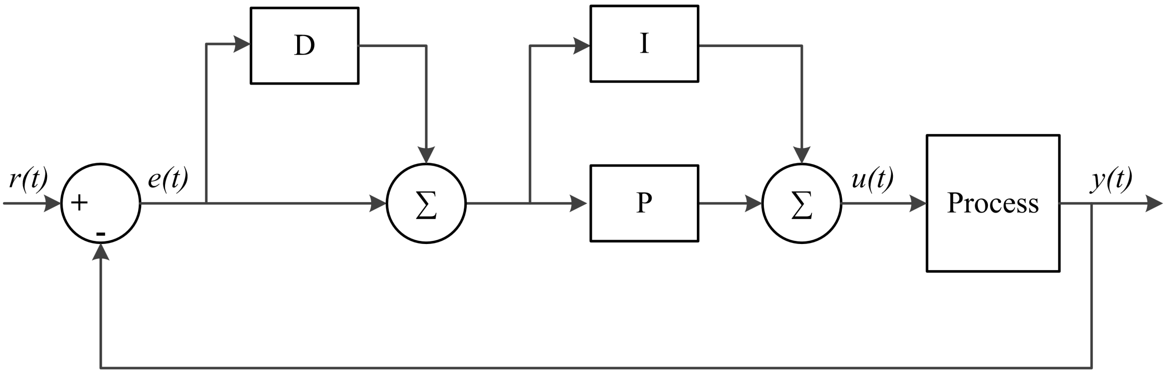

Figure 4.15 Parallel form of a PID controller

been used widely in order to tune various types of PID controllers, which are so-called auto-tuning methods. There are also methods used for optimisation approaches to tuning PID controllers, such as GA and PSO and so on. In this regard, auto-tuning is used to tune two separate PIDs to control the simulated binary distillation column, as this is available as a ready-to-use technique in MATLAB® and on a Simulink® platform,Table 4.2 shows the tuned gains for both PID controllers.

Table 4.2 Gains of the PID controllers

To control	K_p	K_i	K_d
Distillate composition	226.68	0.0268	39542.63
Bottoms composition	38.53	70.36	2.11

A simulation block diagram of the binary distillation column controlled by PID controllers is shown in Figure B.6 in Appendix B, where the subsystem "Distillation Column" shown in the figure contains a 20-stage distillation column, as represented in Figure 4.9. There are also saturations blocks, which have been attached to the control signals and the simulated column to ensure that the inputs of the column are within the operation limits.

To evaluate the PID controllers, simulations experiments were conducted by setting the desired product compositions to 0.99 and 0.08 (mole fraction) for the distillate and bottoms product, respectively. The model has been simulated for 100 minutes, a time long enough for the response to settle, Figure 4.16 shows the controller's performance in tracking the set-points. This performance suffers, in terms of reaching the set-point for both product compositions with large oscillations and steady state errors. However, after 80 minutes both controllers managed to reach the set-points, and the steady state errors were reduced, as can be seen in Figure 4.16.

To check the robustness of the PID controllers, the desired compositions of the column were set to change asynchronously for examining the controller performance regarding the inputs variance that brings undesirable loop interactions, which must be handled well. Figure 4.17 shows the behaviour of the column controlled by PID when the set-points were being changed asynchronously. It is clear that the controlled column is unable to handle the input variation efficiently and unwanted oscillations are present when the desired compositions update its value. The same procedure will be followed to test several intelligent controllers in the next chapter.

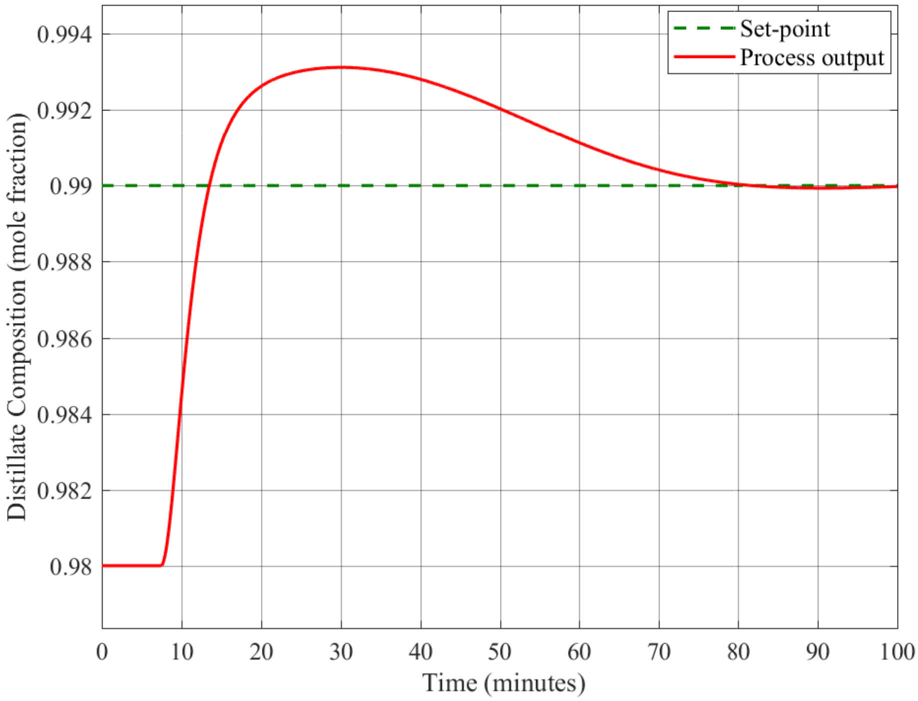

(a) Distillate product

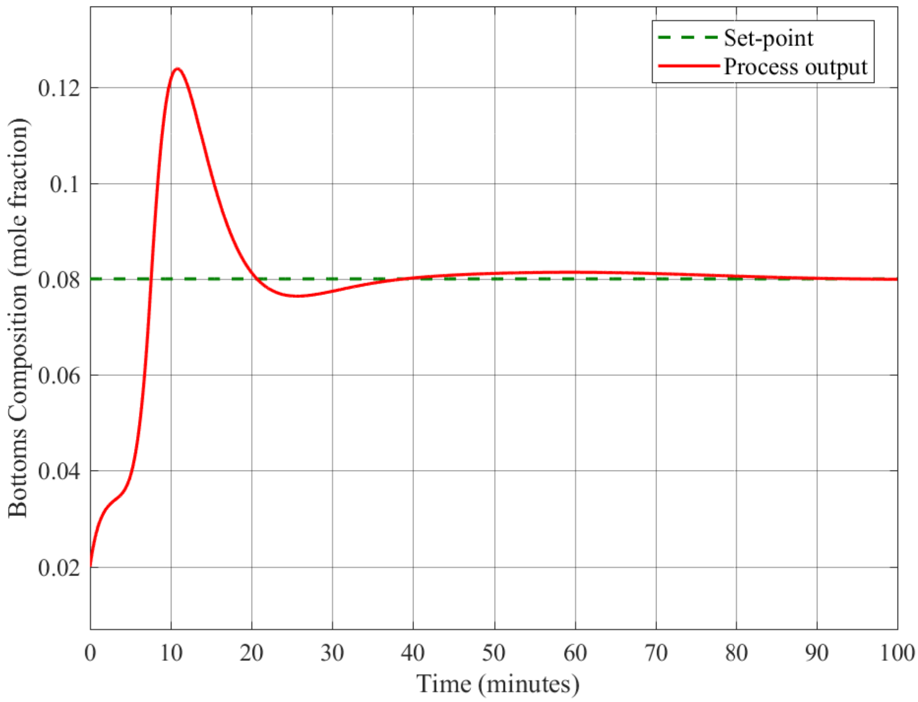

(b) Bottoms product

Figure 4.16 Step response of the PID controller of the binary distillation column

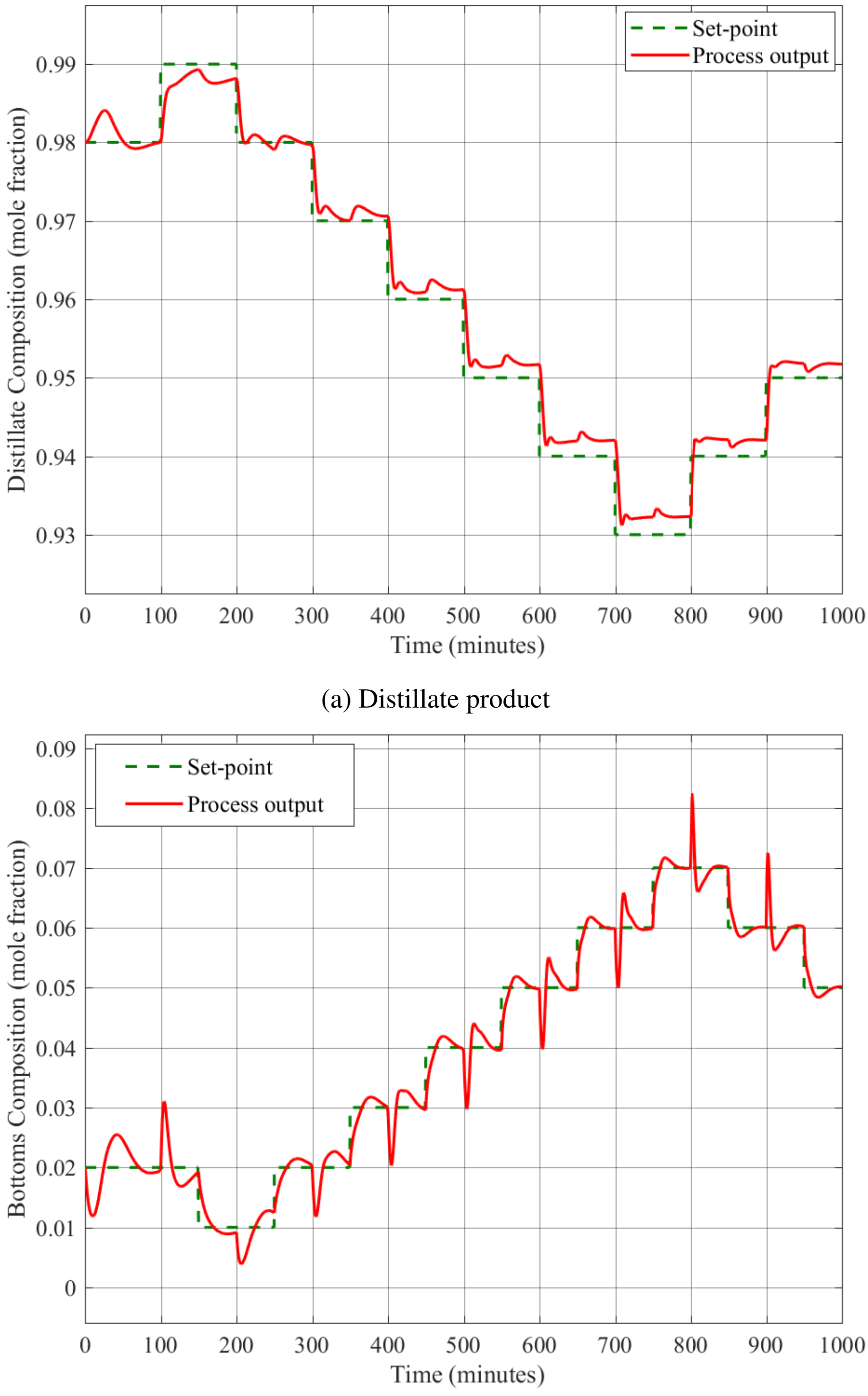

(a) Distillate product

(b) Bottoms product

Figure 4.17 PID controller's response to track changing steps as the desired composition of both products

4.4 Summary

In this chapter, the distillation process has been explained in detail and its importance in vital separation processes, as used widely in chemical industries, has been stressed. Despite the complexity and high energy levels consumed by distillation columns, they are still used as separate units requiring powerful and efficient control design. The properties of a binary distillation column have also been demonstrated with modelling and simulation application to prepare a suitable environment for conducting several control experiments. The simulated binary distillation column, which is simulated using MATLAB® and a Simulink® environment, has been verified by comparing the column behaviour with a published model. That is, the graphical comparison showed that the simulated column is close enough to the model used by Luyben. Finally, a brief outline of PID control theory has been introduced as a classical control system that is still being used nowadays in a wide range of industrial applications. The controller has been tested in two ways: one by setting the desired compositions separately to a step change and the second, by choosing changing set-points updated every 100 minutes to test the robustness of the controller. Poor performance has been recorded when the set-points were changed asynchronously. The purpose of implementing PID control is to compare its performance with the several intelligent controls, as will be executed in Chapter five.

Chapter 5

Intelligent Control of the Binary Distillation Column

5.1 Introduction

The main approaches to intelligent control, as highlighted in Chapter two, have been aimed at investigating optimal performance among various configurations. Such configurations include FL, ANNs and evolutionary-based optimisation tools in addition to predictive mathematical approaches. The proposed intelligent controllers are being applied to the simulated binary distillation column, which was modelled and simulated in the previous chapter. Performance evaluation of the applied controllers has been conducted through visual comparisons of the column response as well as performance indexes, including Integral of Squared Error (ISE), and Integral Time-weighted Absolute Error (ITAE). GA and PSO have been chosen for tuning the various controllers separately, is discussed in this chapter.

5.2 Fuzzy Controllers

The design of an FLC fundamentally comprises three key steps, as follows:

1. Design of fuzzy rules;

2. Design of the membership functions;

3. Tuning of the control parameters.

In order to achieve optimal performance with FLCs, the MFs and controller parameters have been widely tuned in the literature, with the employment of general fuzzy rules. Tuning MFs has been applied to improve the performance of FLCs in [131, 132], and adjusting scaling factors as control tuning parameters has been deployed in [133, 134]. Woo et al. [135] have claimed that only through the adjustment of the control parameters (scaling factors) can optimal performance of real-time control be attained. Thus, tuning the scaling factors of FLCs, which is considered as an independent adjustment, is an essential prerequisite. To this end, a general rule base is used in the FLCs design implemented in this thesis, as shown in Table 5.1, with scaling factors tuning the different types of FLCs. Figure 5.1 represents the output surface of the FIS containing two inputs, error e and the change rate of error ce, with one output which is the control signal u. The actual values of error, change in error and control signals for both compositions is presented in Table 5.2.

Table 5.1 General fuzzy rules base used in the design of FLCs

Output		**Error**						
		NB	**NM**	**NS**	**SS**	**PS**	**PM**	**PB**
Change in Error	**NB**	SS	NS	NM	NM	NB	NB	NB
	NM	PS	SS	NS	NM	NM	NB	NB
	NS	PM	PS	SS	NS	NM	NM	NB
	SS	PM	PM	PS	SS	NS	NM	NM
	PS	PB	PM	PM	PS	SS	NS	NM
	PM	PB	PB	PM	PM	PS	SS	NS
	PB	PB	PB	PB	PM	PM	PS	SS

The linguistic expressions that described the inputs and output of the FLC are demonstrated via fuzzy sets as follows:

PB: Positive Big

PM: Positive Medium

PS: Positive Small

SS: Steady State

NS: Negative Small

NM: Negative Medium

NB: Negative Big

The rules are applied in **IF-Then** form as follows:

IF Error is NB **AND** Change in Error is NB **THEN** Output is SS

IF Error is NM **AND** Change in Error is NB **THEN** Output is NS

⋮

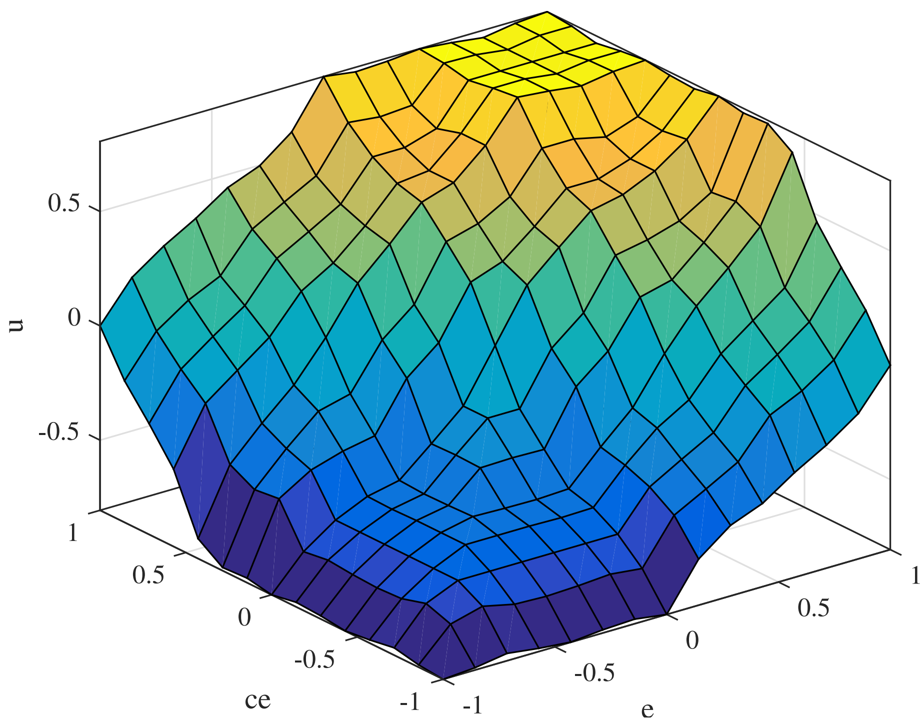

Figure 5.1 General FLC control surface representation

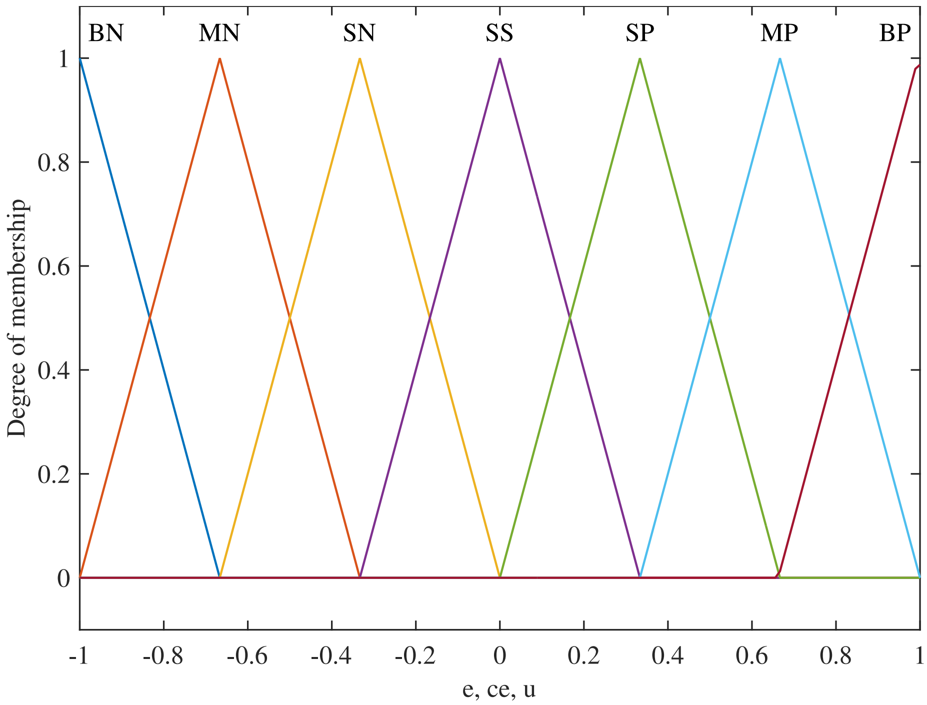

Figure 5.2 Degree of MFs of FLC inputs and output

Table 5.2 The actual values of error, change in error and control signals for both compositions.

	e		***ce***		***u***	
	min	**max**	**min**	**max**	**min**	**max**
Distillate composition	1×10^{-3}	0.98	1×10^{-5}	0.86	1.232	1.35
Bottoms composition	1×10^{-7}	0.02	1×10^{-8}	0.0024	1.77	1.853

5.2.1 PI, PD and PID-like Fuzzy Controllers

As mentioned earlier, there are three types of configurations for designing FLC, PD, PI and PID-like, all of which have been implemented with scaling factors tuning using GA and PSO separately.

In order to make a fair comparison, there some share standard specifications of all the applied FLCs have been implemented, which are:

1. Seven triangular membership functions for the FLC inputs and output, from -1 to 1, as presented in Figure 5.2;

2. AND logical operation with a unit weight;

3. 49 fuzzy rule-base, as shown in Table 5.1;

4. 20 runs of implementation GA and PSO, due to the random initialisation stage;

5. The simulation experiments haven been conducted for 100 minutes to track the desired output as a constant value for both compositions of the column, and for 1,000 minutes to track the desired output as asynchronous changes for both compositions;

6. All the FLC controllers' responses have been evaluated via the performance indexes ISE and ITAE, as shown in equations 5.1 and 5.2, respectively. Basically, ITAE is used to measure the ability to adjust the transient response indications like percentage overshoot, rise time and settling time. While, ISE is employed to measure the steady-state errors, and these performance indexes is also applied as objective functions to the optimisation tools, as will be presented later.

$$ITAE = \int_0^t t \times |e(t)| dt, \tag{5.1}$$

$$ISE = \int_0^t e(t)^2 dt. \tag{5.2}$$

As mentioned earlier, the controllers have been implemented to maintain both composition products of the column. So, four indexes evaluate the controller's performance, ISE and ITAE for the controller of the distillate composition product, and the same for the bottoms composition product. Since the range of the controllers' performance indexes varies widely, objective functions will not work properly without a preprocessing, such as normalisation. A normalisation process has been used to rescale the range of the four indexes into a scale range between 0 and 1, which is also called feature scaling [136], as presented in the following formula:

$$\acute{x} = \frac{x - min(x)}{min(x) - max(x)}, \tag{5.3}$$

where, x are the original data and $\acute{x}$ are the normalised data. So, the objective function used in GA and PSO to tune the controllers implemented in this thesis can be expressed as:

$$OF = \frac{1}{4}\left(IT\acute{A}E_{xD} + IS\acute{E}_{xD} + IT\acute{A}E_{xB} + IS\acute{E}_{xB}\right). \tag{5.4}$$

The PD-, PI- and PID-like FLCs of the simulated binary distillation column are shown in Figures 5.3, 5.4 and 5.5, respectively, and all FLCs have been implemented in a MIMO form to control both compositions. Hence, there are four FLC Simulink blocks in each type.

5.2.2 Optimisation and Tuning of FLCs

In order to find the best set of the scaling factors of the FLCs, real-coded GA and PSO have been applied separately. The metadata of both optimisers have been selected in a similar manner, as far as possible, in order to make a fair comparison. These metadata include the number of generations or particles and the number of iterations and so on. The metadata of the GA are shown in Table 5.3, while those for PSO are provided in Table 5.4. $C1$, $C2$ and ω have been chosen after conducting extensive simulation experiments. PSO has been programmed from the scratch to work as an optimiser tool in MATLAB® and a Simulink® environment. While the default of the GA metadata has been implemented as provided by

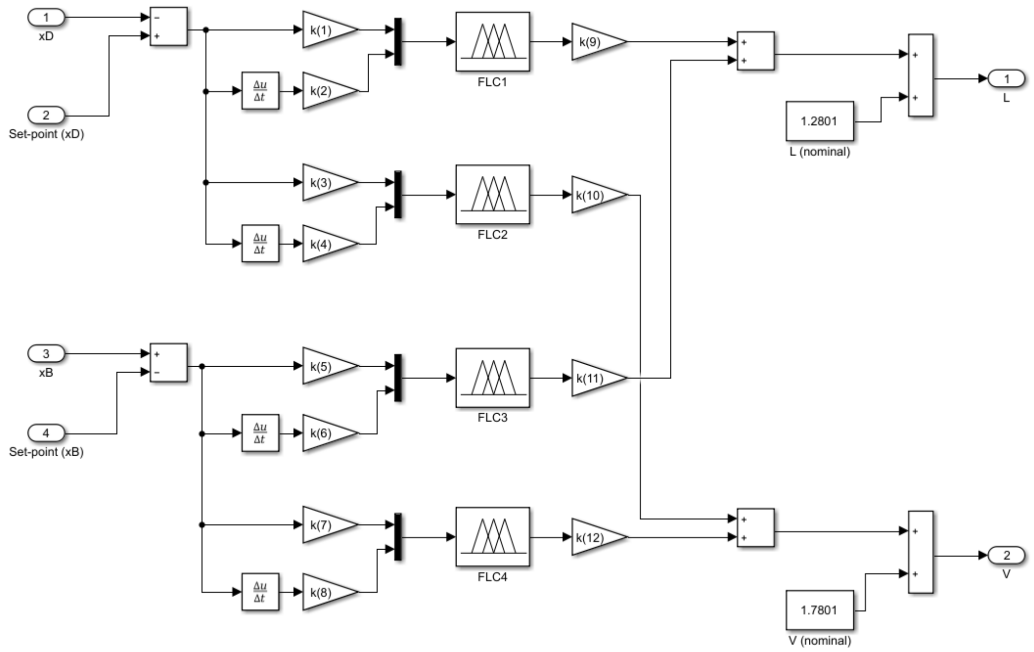

Figure 5.3 Simulink block diagram of a MIMO PD-like FLC with 12 scaling factors

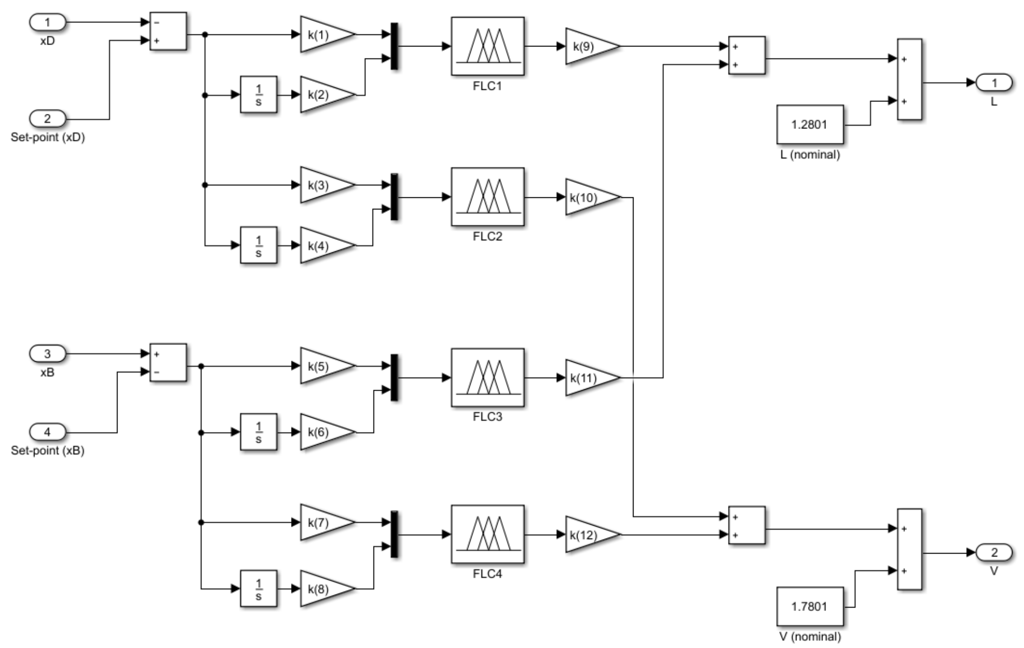

Figure 5.4 Simulink block diagram of a MIMO PI-like FLC with 12 scaling factors

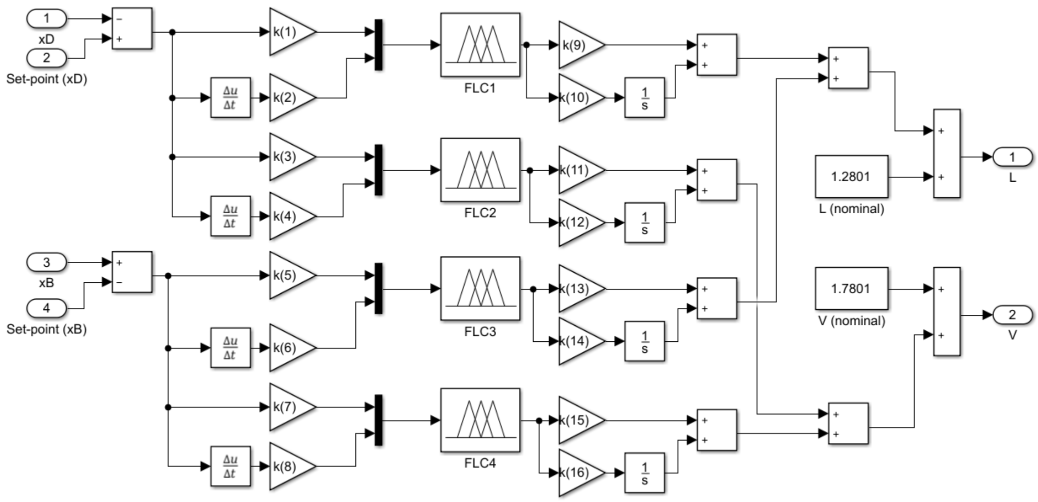

Figure 5.5 Simulink block diagram of a MIMO PID-like FLC with 16 scaling factors

the Optimisation Toolbox in MATLAB® platform.

Table 5.3 Metadata of PSO used in the tuning of the FLC scaling factors

Parameter	**Value**
Number of particles (size of the swarm)	100
Maximum number of iterations	100
Cognitive acceleration ($C1$)	1.2
Social acceleration ($C2$)	0.12
Momentum or inertia (ω)	0.9

Table 5.5 shows a comparison of the performance indexes of different types of fuzzy controllers tuned separately by PSO and GA, for two test scenarios, as follows.

1. The desired output for the distillate product is set to be a constant at a value 0.99 (mole fraction), and the bottoms composition is selected as 0.08 (mole fraction) and the simulation time is 100 minutes. Figure 5.6 shows the controllers' efforts to track the desired compositions for the distillate and bottoms products, respectively.

Table 5.4 Metadata of GA used in the tuning of the FLC scaling factors

Parameter	**Value**
Population Size	100
Maximum number of iterations	100
Function tolerance	0.0001
Crossover fraction	0.8
Migration fraction	0.2

2. The desired outputs are set to change asynchronously every 100 minutes, with the distillate product composition starting to change at 100 minutes, while the bottoms one does so at 150 minutes, checking the control loop interaction and the efforts to eliminate it by the fuzzy controllers. In addition, the simulation time is set to 1,000 minutes. The controllers' response to track the changing desired compositions for the distillate and bottoms products is shown in Figure 5.7.

As stated earlier, because of the randomisation of the candidate solution at the initial stage, both optimisers, GA and PSO, have been run 20 times to tune the different fuzzy controllers. As shown in Table 5.5, the PID-like fuzzy controllers outperformed the other configurations tuned by both GA and PSO, with less ISE and ITAE. In addition, it showed the superiority regarding the transient response properties, including the rise time, overshoot, settling time and steady state errors for both test scenarios, as presented in Figure 5.6 and Figure 5.7.

GA and PSO have been run 20 times separately to tune the scaling factors of PID-like fuzzy controllers against the objective function and their performance is compared as a bar chart, as shown in Figure 5.8. It is clear that PSO performed better than GA in 18 out of 20 runs, with the second run of PSO showing the best objective function at 0.179. Whilst GA performed better in just 2 out of the 20 runs and its best objective function is 0.244 in the run number 17, as shown on the bar chart. Also, the average run of PSO took about 4.6

(hours), while GA took approximately 6.8 (hours) to find the optimal set of scaling factors of the PID-like fuzzy controllers.

The convergence comparison of the best run of PSO was plotted alongside the best run of GA to tune the PID-like fuzzy controllers, as shown in Figure 5.9. Due to the above advantages, including the best convergence and computational time efficacy, PSO has been implemented henceforward, whenever an optimiser is required in this thesis. In addition, the PID-like fuzzy controller performance will be considered in comparison with other controllers, at the end of this chapter, owing to its performance superiority.

Table 5.5 Comparison of performance indexes of different types of fuzzy controllers tuned by PSO and GA

Test scenario	**Tuning / Configuration**		**Performance Index**	
			ISE	**ITAE**
Step set-points	**PSO**	**PD-like**	0.0053	0.7832
		PI-like	0.0026	0.4476
		PID-like	0.0013	0.0747
	GA	**PD-like**	0.0027	0.1342
		PI-like	0.0024	0.631
		PID-like	0.0019	0.2170
Asynchronies set-points	**PSO**	**PD-like**	0.0018	26.6249
		PI-like	0.0047	37.2752
		PID-like	0.0011	10.0091
	GA	**PD-like**	0.0092	57.1706
		PI-like	0.0042	33.2897
		PID-like	0.0014	11.4034

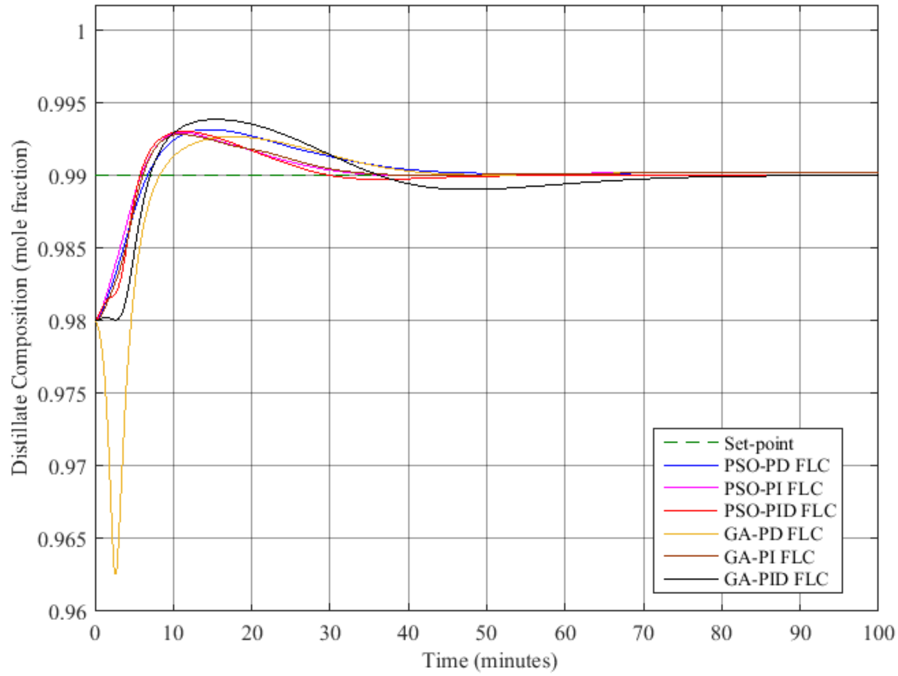

(a) Distillate product

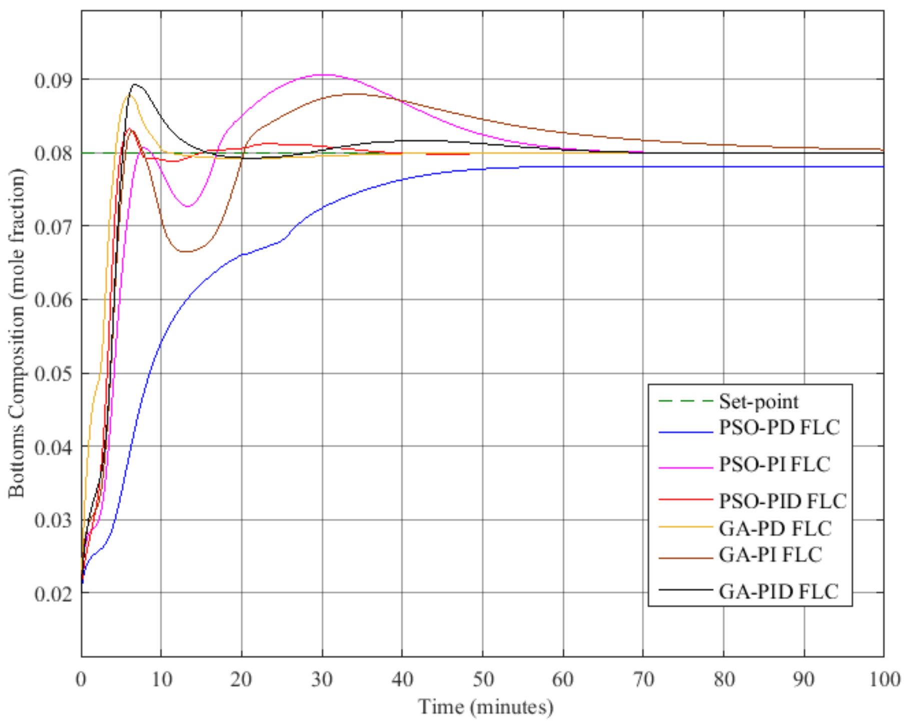

(b) Bottoms product

Figure 5.6 Step response of the different fuzzy controllers of the binary distillation column tuned by PSO and GA separately; (a) distillate composition and (b) bottoms composition

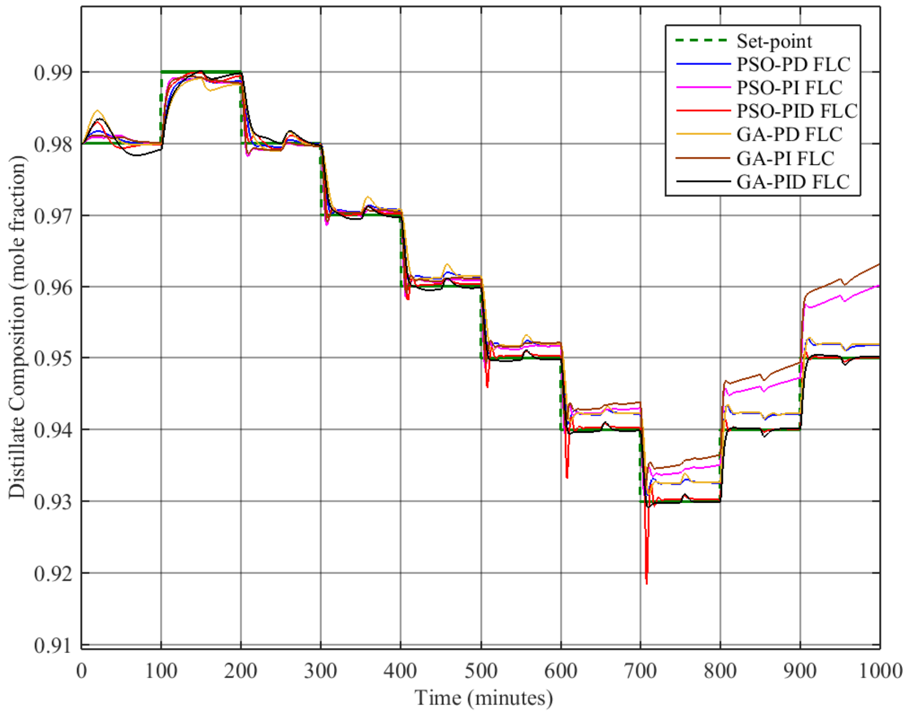

(a) Distillate product

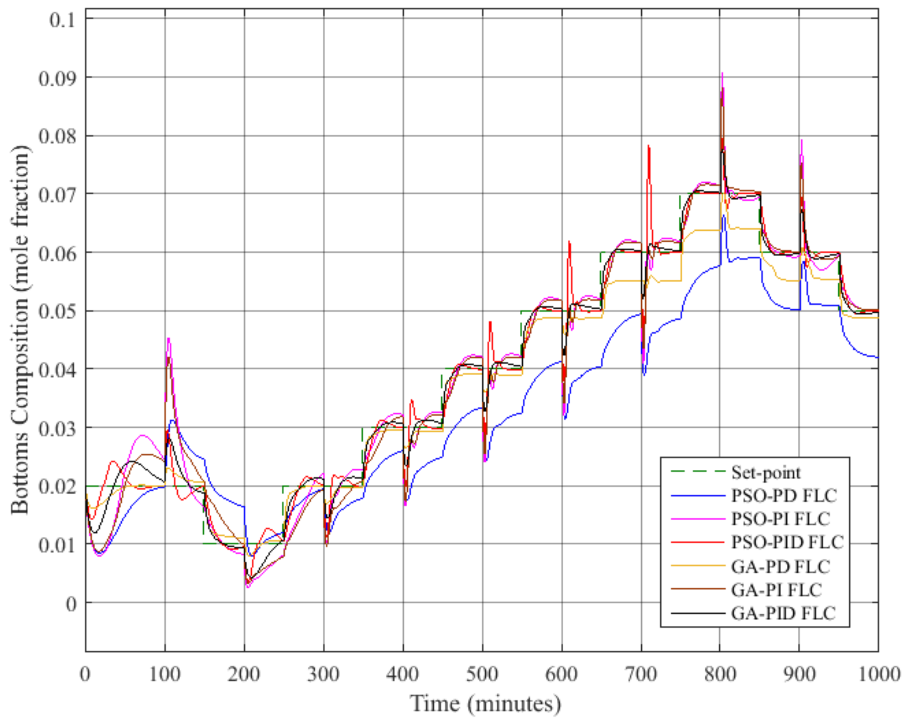

(b) Bottoms product

Figure 5.7 Changing-step response of the various fuzzy controllers of the binary distillation column tuned by PSO and GA separately; (a) distillate composition and (b) bottoms composition

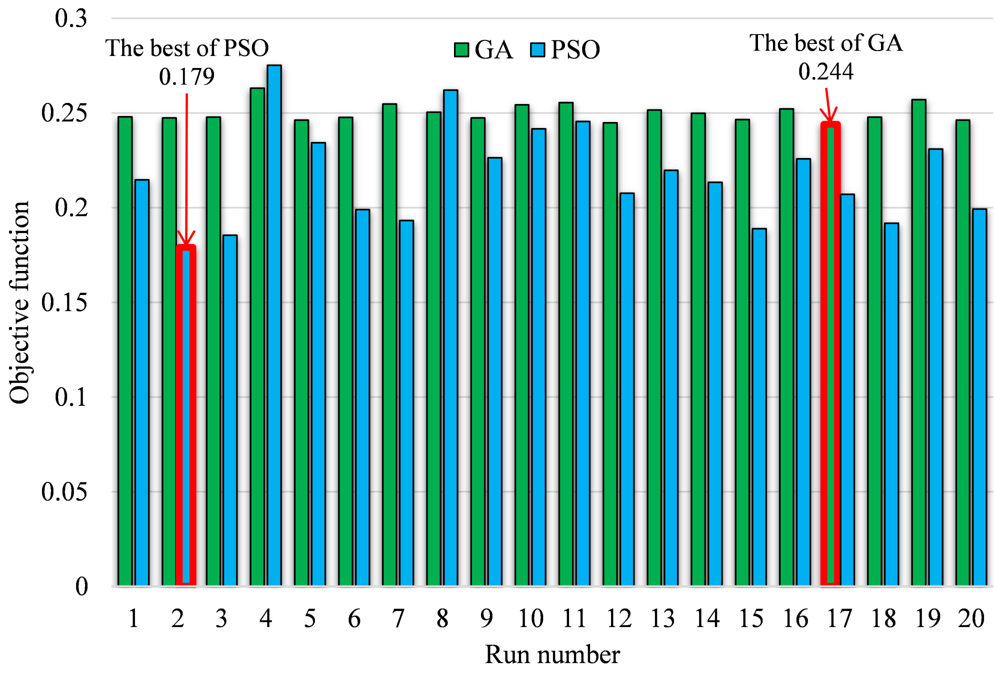

Figure 5.8 Different number of runs of GA and PSO to tune the PID-like fuzzy controllers vs. the objective function

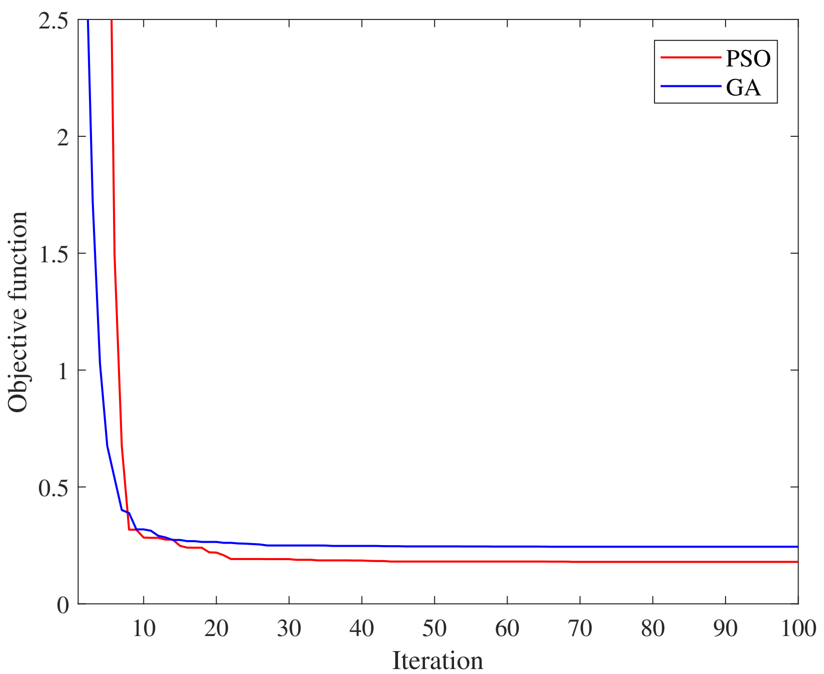

Figure 5.9 Convergence of the best runs of PSO and GA

5.3 NARMA-L2 Controller

As highlighted in the previous chapters, the NARMA-L2 controller has been recently implemented in various applications. One of the most powerful facilities enabling the control designer to apply this controller is its availability as a built-in block in the Simulink® environment. However, only SISO control design can be implemented to control dynamic systems by this ready-to-use block controller. Also, the NARMA-L2 block controller employs only ANNs to approximate the system to be controlled. So, no flexibility is given to designer to try another approximation method, like ANFIS.

In this section, the NARMA-L2 controller is implemented to control compositions of the simulated binary column using two ANNs as approximators. The first step of implementing NARMA-L2 control design is to train the approximation submodels (f, g), as shown previously in Equation 3.13 and presented in Figure 3.5. In the simulation of the binary distillation column, a dataset including 2,000 points has been collected to represent the dynamic behaviour of the column, as presented in Figure 4.10 and Figure 4.11. This dataset is used for the offline training of submodels of NARMA-L2 controllers. There are initial parameters that should be set before identifying the column by the ANN model. These parameters have been selected arbitrarily for both ANNs as follows:

1. The collected dataset is divided randomly into three subsets: 70% for training, 15% for testing and 15% for validation;
2. The size of the hidden layer is 12 nodes;
3. The number of delayed column inputs is 1;
4. The number of delayed column outputs is 1;
5. The maximum training iterations (epochs) is 400;
6. The ANN training method is the Levenberg-Marquardt algorithm (the default method).

The submodels of both SISO NARMA-L2 are approximated unconnectedly and the training performance of ANN models are shown in Figure 5.10 and Figure 5.11 of the distillate and bottoms compositions, respectively. It can be seen that, in general, the error reduces after more iterations of training, but it might start to rise on the validation sub-dataset when the ANN starts overfitting the training sub-dataset. In the default circumstance, the training breaks after six successive rises in validation error and the best performance is indicated at the iteration when the lowest validation error is recorded.

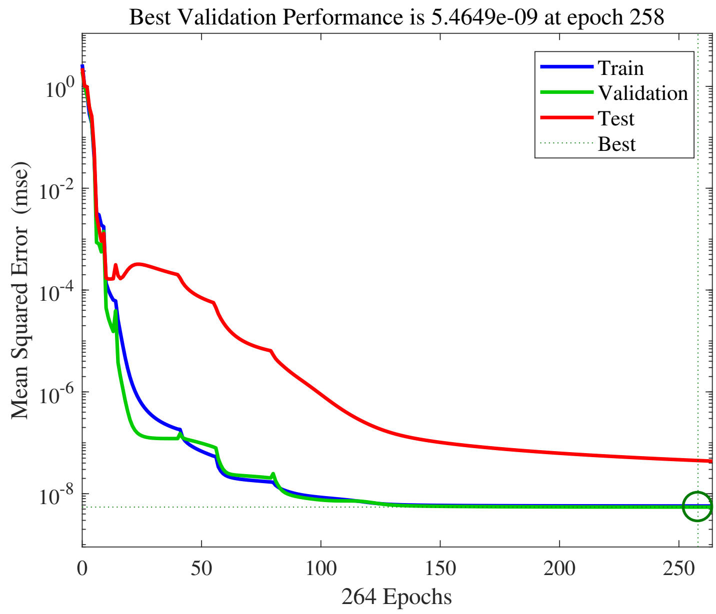

Figure 5.10 Training performance of ANN submodels to model the distillate composition of the simulated binary distillation column

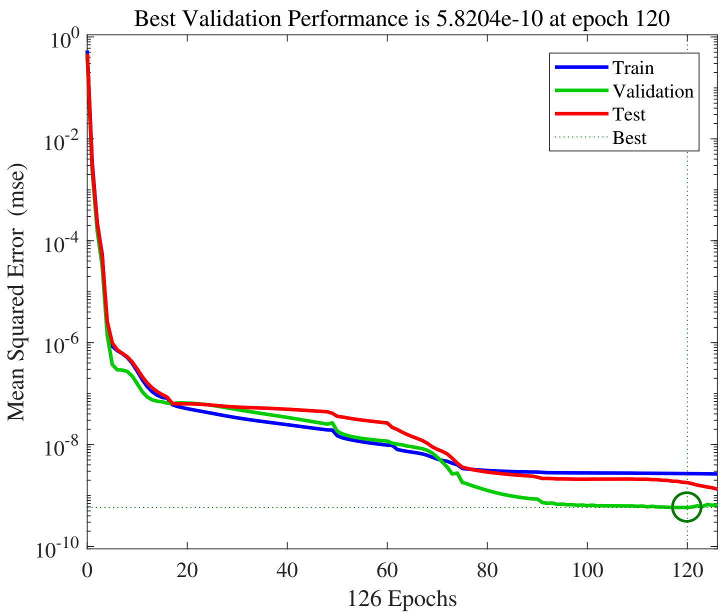

Figure 5.11 Training performance of ANN submodels to model the bottoms composition of the simulated binary distillation column

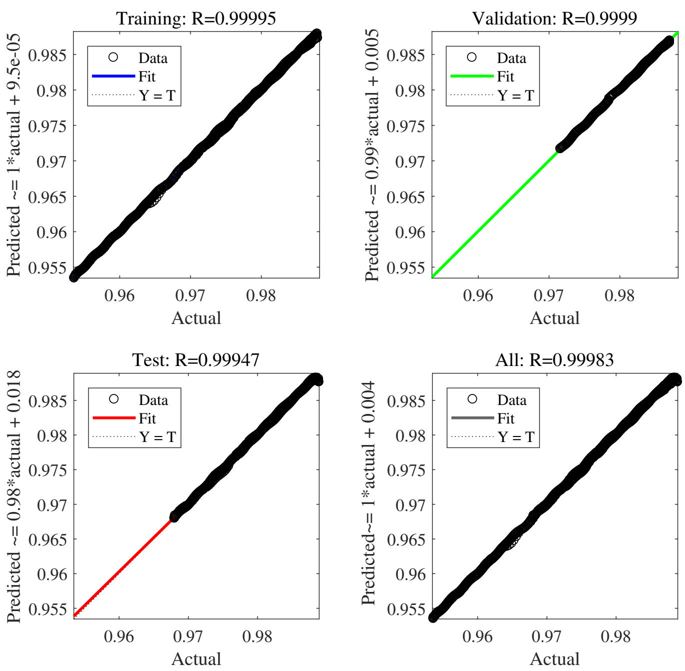

Figure 5.12 Relationship between the predicted and the actual output (x_D)

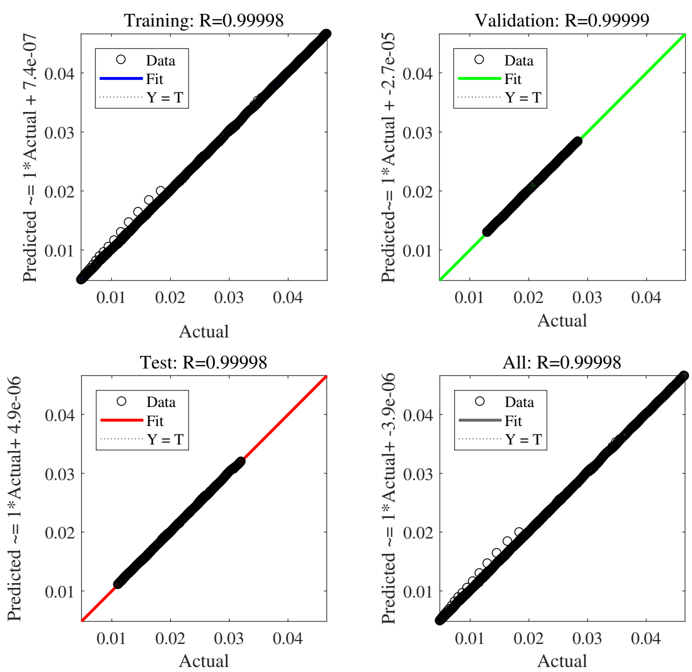

Figure 5.13 Relationship between the predicted and the actual output (x_B)

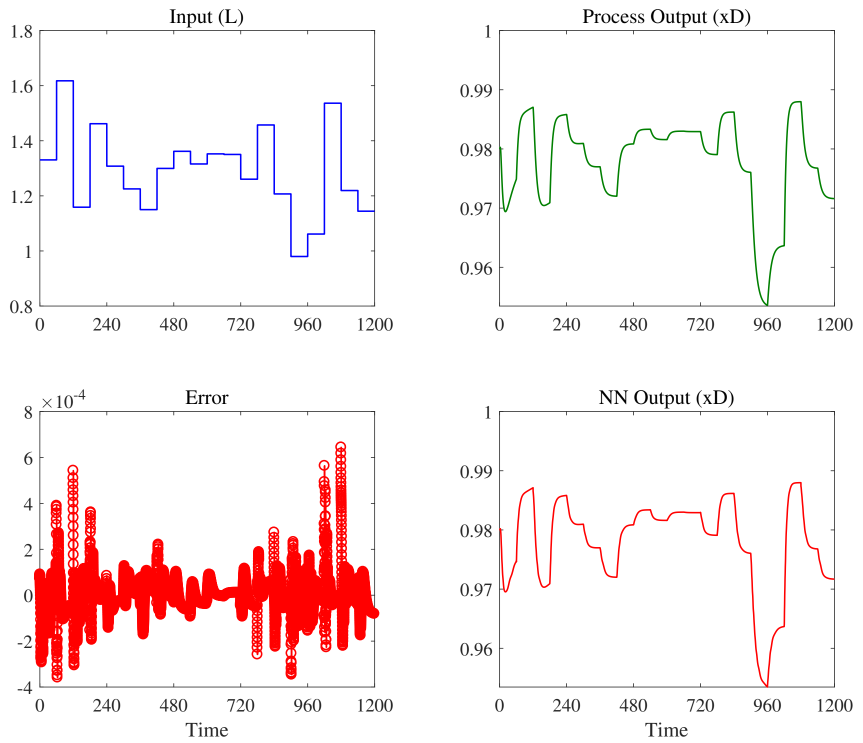

(a) Training subset

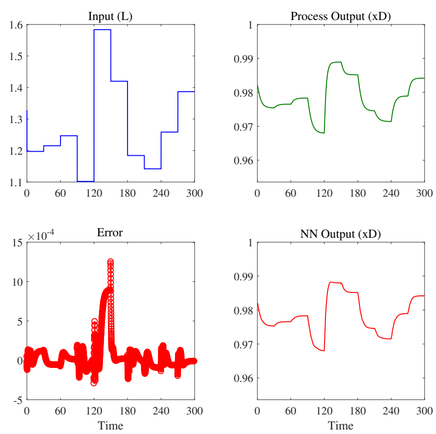

(b) Testing subset

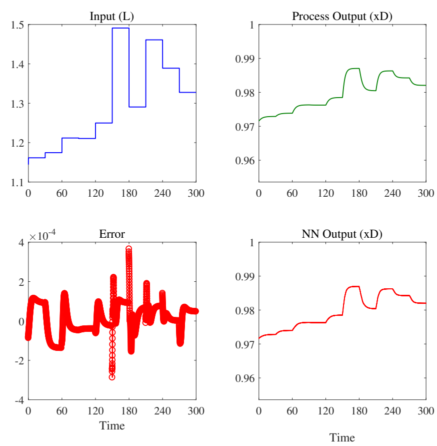

(c) Validation subset

Figure 5.14 Training, validation and testing of an ANN model to identify the distillate composition

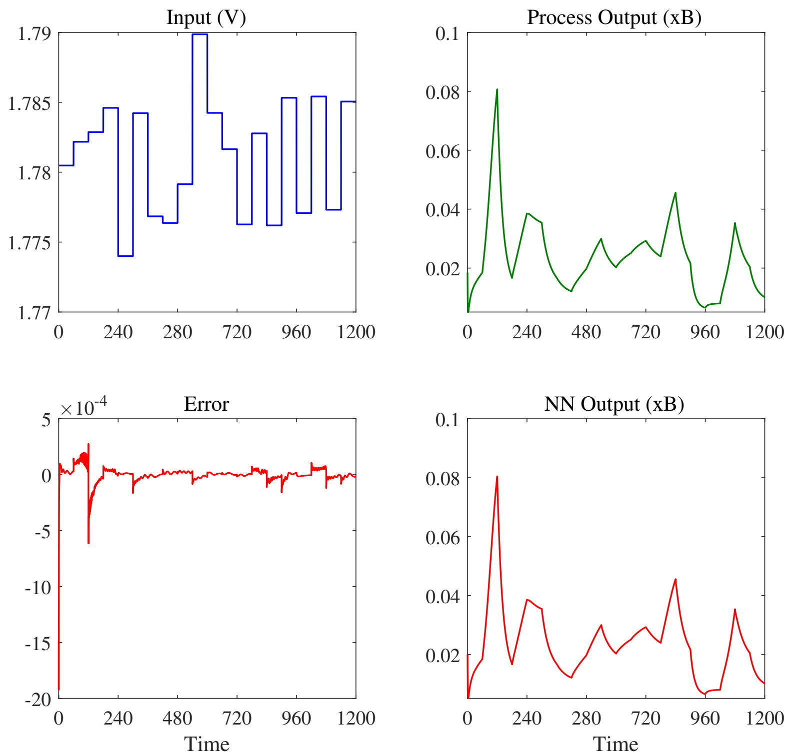

(a) Training subsets

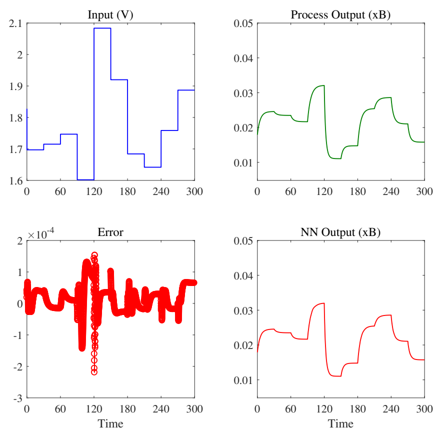

(b) Testing subsets

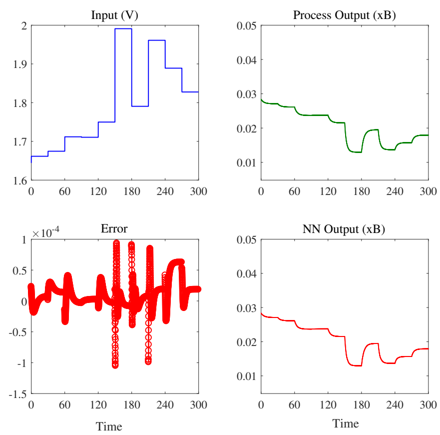

(c) Validation subset

Figure 5.15 Training, validation and testing of an ANN model to identify the bottoms composition

5.4 ANFIS-based NARMA-L2 Controller

In this section, a new MIMO controller is proposed based on the NARMA-L2 configuration that uses an ANFIS approach as approximation method for the submodels which is presented

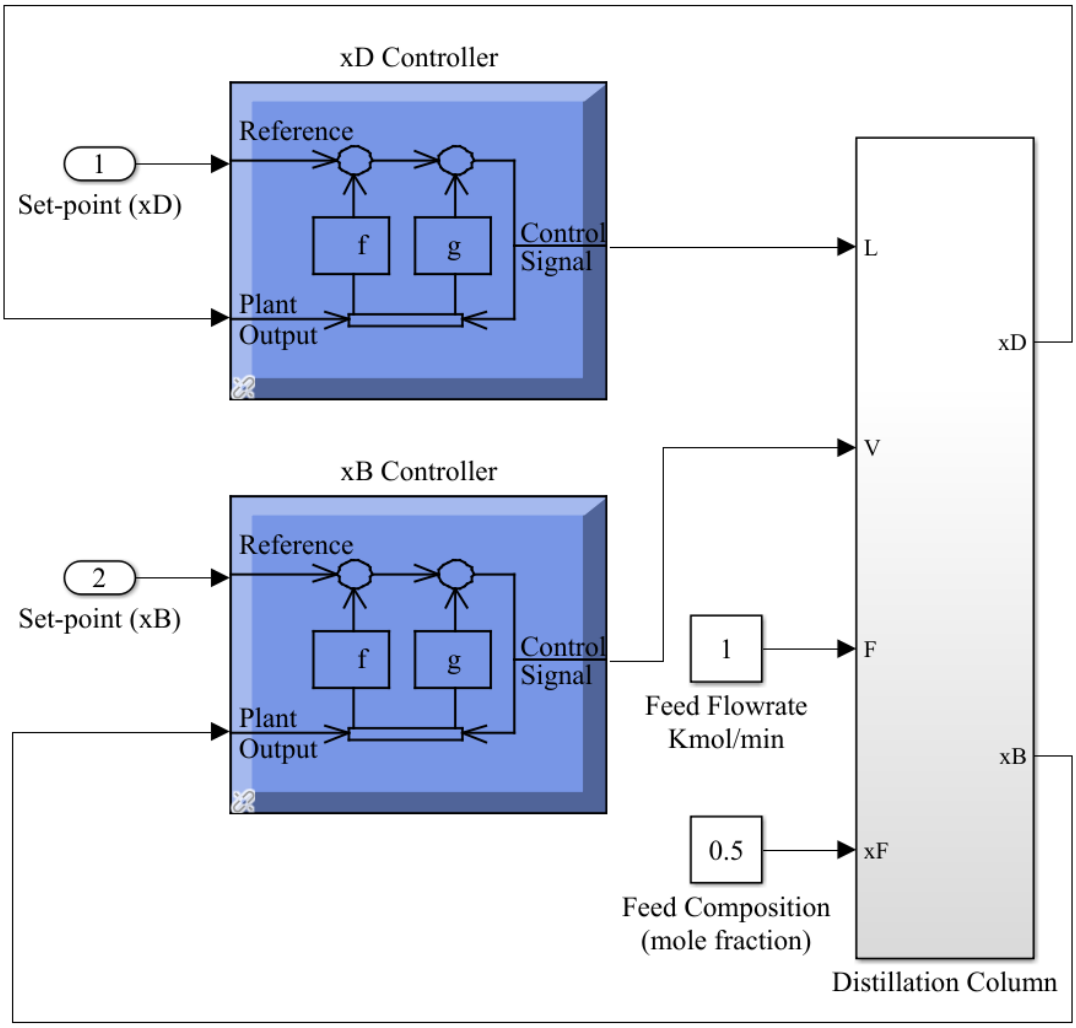

Figure 5.16 Simulink block diagram of the simulated column controlled by two separated NARMA-L2s

in Equation 3.13 and depicted in Figure 3.5. As far as this researcher is aware, no SISO or MIMO controller based on NARMA-L2 that uses ANFIS has been implemented in the literature. The key advantage of ANFIS compared to backpropagation-based identification approaches is that reasoning and learning in the uncertain and vague situations are guaranteed [137].

5.4.1 ANFIS-based NARMA-L2 Identification Model

To implement an ANFIS-based NARMA-L2 controller, the first step is to identify the model by mapping the input-output relationship. Equation 3.13 can be rewritten for identifying MIMO (2-inputs and 2-outputs) systems as:

$$\begin{bmatrix} y_1(t+1) \\ \\ y_2(t+1) \end{bmatrix} = \begin{bmatrix} f_1(\cdot) \\ \\ f_2(\cdot) \end{bmatrix} + \begin{bmatrix} g_1(\cdot) \\ \\ g_2(\cdot) \end{bmatrix} \times u_1(t) + \begin{bmatrix} g_3(\cdot) \\ \\ g_4(\cdot) \end{bmatrix} \times u_2(t), \tag{5.5}$$

where, the f and g functions represent submodels that contain the time series of the inputs and outputs of the process to be identified, i.e.:
$\Big(y_1(t), y_1(t-1), \cdots, y_1(t-n+1), y_2(t), y_2(t-1), \cdots, y_2(t-m+1), u_1(t-1), \cdots, u_1(t-j+1), u_2(t-1), \cdots, u_2(t-k+1)\Big)$,
where, n, m, j and k are the time delays of the inputs u and the outputs y of the process, while the 1 and 2 subscripts define the inputs and output numbers.

For the ANFIS-based NARMA-L2 identification model, the $f_{1,2}$ and $g_{1,2,3,4}$ functions should be approximated by ANFIS, while PSO is employed as a tuner to find the optimal parameters of the FISs as shown in Figure 5.17. The identification performance index is usually measured using the statistical criteria such as Root Mean Squared Errors (RMSE), which is the difference between the predicted and actual outputs, as expressed by the following equation:

$$RMSE = \sqrt{\frac{1}{N}\sum_{i=1}^{N}(\hat{Y}_i - y_i)^2}, \tag{5.6}$$

where, $\hat{Y}$ is a vector of N predictions and y represents the vector of actual values corresponding to the inputs.

Selecting the time delayed signals, n, m, j and k, which represent the regressors for inputs and outputs, is not straightforward. The optimal selection of these factors, which are also called the lag space, has an essential impact on the performance of the identification process.

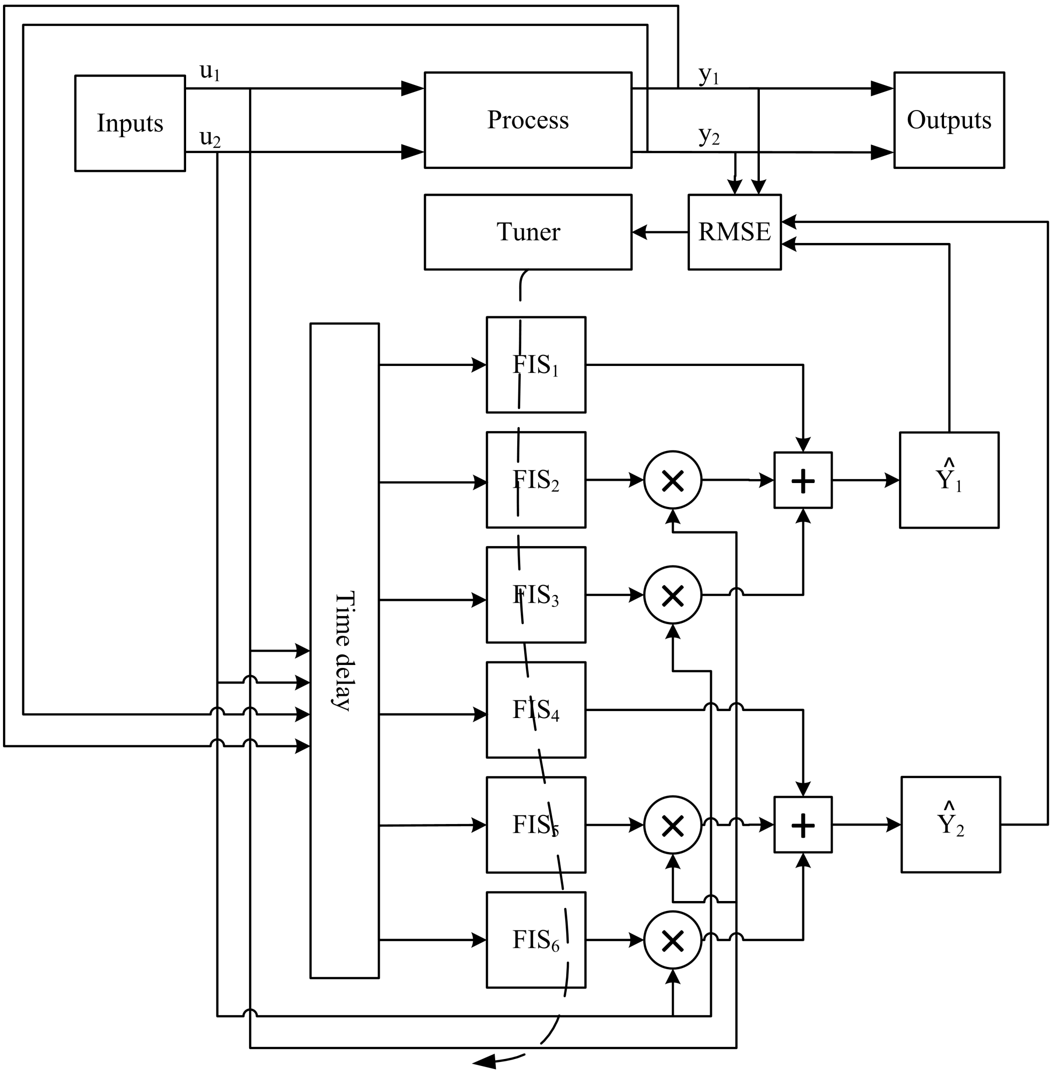

Figure 5.17 Schematic diagram of ANFIS-based NARMA-L2 controller for MIMO systems

Too small delayed signals may imply that the significant dynamic of the identified process will not be captured. On the other hand, if they are too large, this can be a problem due to high dimensionality [81]. In the literature, there have been many attempts to find the optimal model structure of the time series models. Basically, most of them have been based on trial and error, such pruning algorithms, which take an overlarge number of regressors of the inputs and outputs model and reduce this steadily until the optimal performance is achieved. However, this selection process is time-consuming in addition to being computational inefficient. Hence, PSO is proposed for finding the optimal combination structure of the regressors of the ANFIS-based NARMA-L2 model. For simplicity, the range of inputs and outputs delay, *m*, *n*,

j and k is between 1 to 3, to form the inputs candidates for the proposed model, as follows:

$$\begin{aligned} M(t) = \Big(&u_1(t-1), u_1(t-2), u_1(t-3), u_2(t-1), u_2(t-2), u_2(t-3), \\ &y_1(t-1), y_1(t-2), y_1(t-3), y_2(t-1), y_2(t-2), y_2(t-3)\Big). \end{aligned} \tag{5.7}$$

For an ANFIS-based NARMA-L2 identification model, two overlapping PSOs have been implemented to find the best combination of the input candidates as well as to tune the submodels that are represented by ANFIS. The flowchart in relation to using the optimisation method to find the optimal lag space to the proposed model is presented in Figure 5.18. an exhaustive search has been used to determine the best number combination of input candidates by running a loop from 1 to 12 to cover all the proposed candidates presented in Equation 5.7. The best number of inputs versus the RMSE is shown in bar chart form in Figure 5.19 for the predicted first and second output, respectively. The best combination of the input candidates is selected based on a training subset of the collected dataset, which represents 70% of the total. To evaluate the trained model regarding the generalisation, the identification model is tested by a test subset, which is unseen during the training process, comprising 30% of the whole dataset. Table 5.6 shows the ANFIS-based NARMA-L2 model inputs versus RMSE in the training and testing subsets.

An example of the modified MFs and the relationship between the inputs and output of the PSO-tuned $FISs$, MFs of the FIS_1 inputs and the PSO-modified surf of the inputs and output of FIS_1 is illustrated in Figure 5.20, whereas the tuned MFs and surfs of FIS_2 to FIS_6 are presented in the Appendix B.

Table 5.6 RMSE of different NARMA-L2 model structures

Predicted output	**The best number of inputs**	**The best combination**	**RMSE**	
			Training	**Testing**
$\hat{Y}_1$	3	$\big(y_1(t-1), y_1(t-2), y_2(t-1)\big)$	0.000076	0.00063
$\hat{Y}_2$	3	$\big(u_2(t-1), y_1(t-1), y_2(t-1)\big)$	0.000132	0.00846

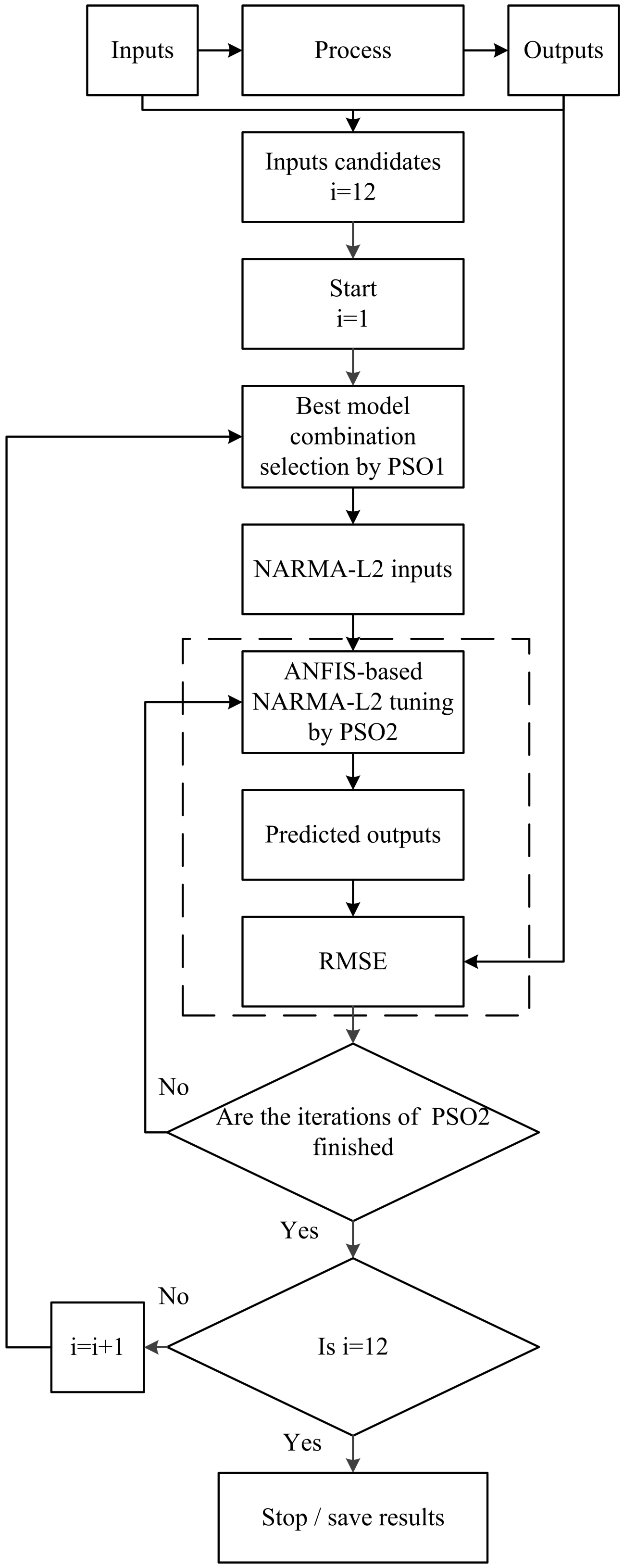

Figure 5.18 Flowchart of the proposed identification model

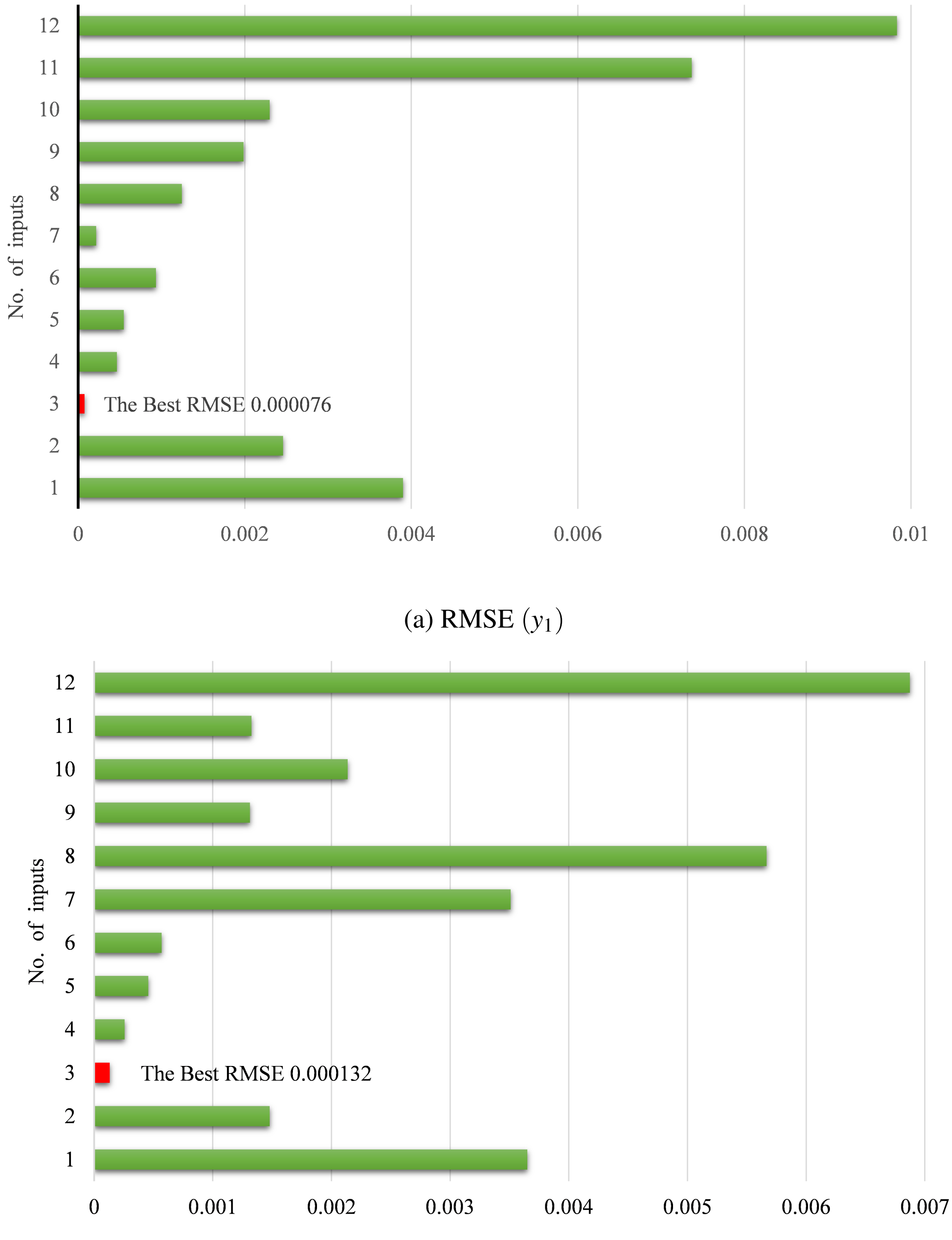

(a) RMSE (y_1)

(b) RMSE (y_2)

Figure 5.19 RMSE of the ANFIS-based NARMA-L2 model versus different numbers of input candidates

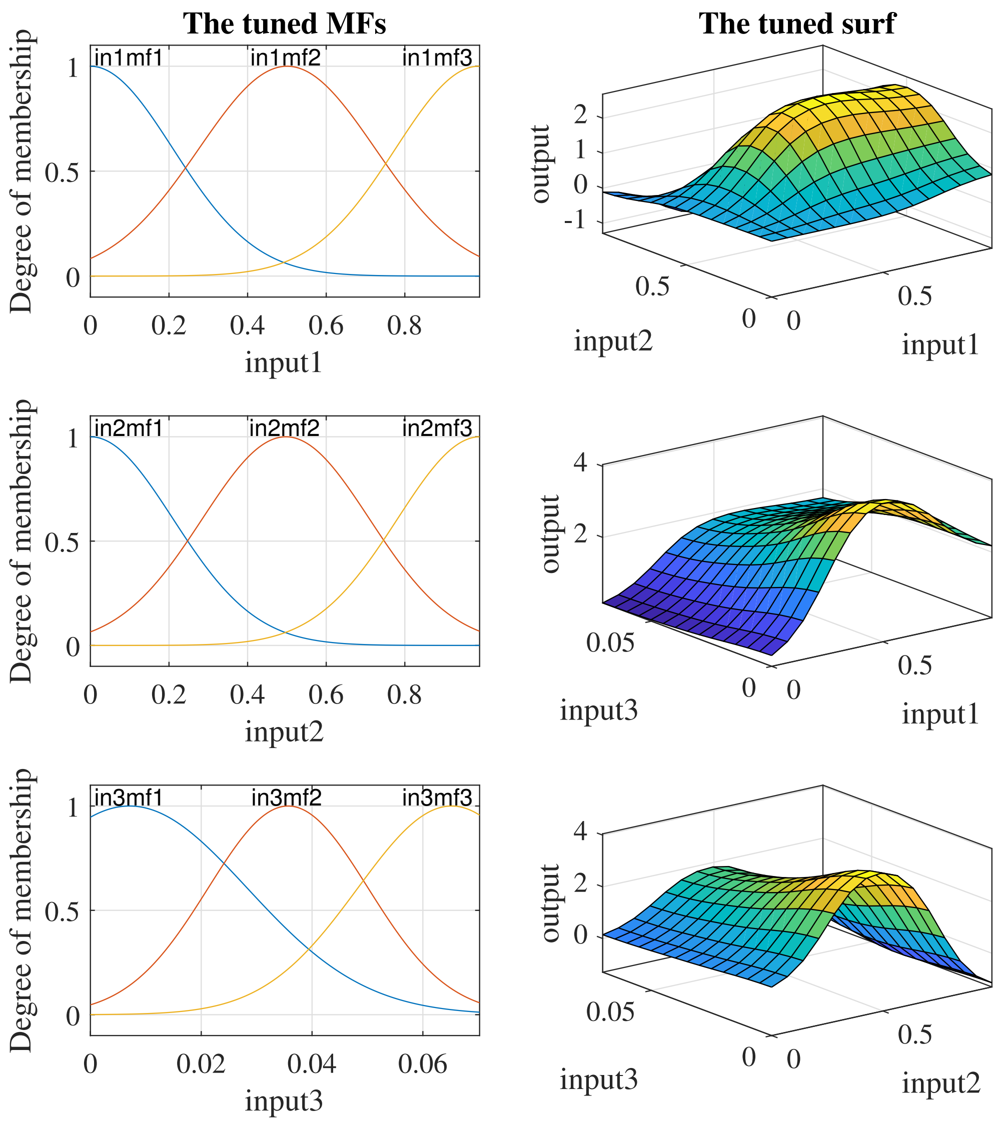

Figure 5.20 PSO-tuned MFs and surf of FIS_1

5.4.2 ANFIS-based NARMA-L2 Control Design

Similar to that of ANN-based NARMA-L2, ANFIS-based NARMA-L2 control is designed by rearranging the approximated submodels, which were obtained in the previous identification stage. The generalisation of the model is evaluated by testing with unseen data, which is a test subset and a graphical block diagram of the proposed control design is shown in Figure 5.21.

The control signal can be calculated as:

$$\begin{bmatrix} r_1 \\ \\ r_2 \end{bmatrix} = \begin{bmatrix} F\hat{I}S_1 \\ \\ F\hat{I}S_4 \end{bmatrix} + \begin{bmatrix} F\hat{I}S_2 \\ \\ F\hat{I}S_5 \end{bmatrix} \times u_1 + \begin{bmatrix} F\hat{I}S_3 \\ \\ F\hat{I}S_6 \end{bmatrix} \times u_2, \tag{5.8}$$

$$\begin{bmatrix} r_1 \\ \\ r_2 \end{bmatrix} - \begin{bmatrix} F\hat{I}S_1 \\ \\ F\hat{I}S_4 \end{bmatrix} = \begin{bmatrix} F\hat{I}S_2 \\ \\ F\hat{I}S_5 \end{bmatrix} \times u_1 + \begin{bmatrix} F\hat{I}S_3 \\ \\ F\hat{I}S_6 \end{bmatrix} \times u_2, \tag{5.9}$$

$$\begin{bmatrix} r_1 \\ \\ r_2 \end{bmatrix} - \begin{bmatrix} F\hat{I}S_1 \\ \\ F\hat{I}S_4 \end{bmatrix} = \begin{bmatrix} F\hat{I}S_2 & F\hat{I}S_3 \\ \\ F\hat{I}S_5 & F\hat{I}S_6 \end{bmatrix} \begin{bmatrix} u_1 \\ \\ u_2 \end{bmatrix}, \tag{5.10}$$

$$\begin{bmatrix} u_1 \\ \\ u_2 \end{bmatrix} = \begin{bmatrix} F\hat{I}S_2 & F\hat{I}S_3 \\ \\ F\hat{I}S_5 & F\hat{I}S_6 \end{bmatrix}^{-1} \times \left(\begin{bmatrix} r_1 \\ \\ r_2 \end{bmatrix} - \begin{bmatrix} F\hat{I}S_1 \\ \\ F\hat{I}S_4 \end{bmatrix} \right). \tag{5.11}$$

$\hat{FIS}_{123456}$ represent the approximation submodels identified by ANFIS in the identification stage and r_1 and r_2 are the desired outputs (set-points).

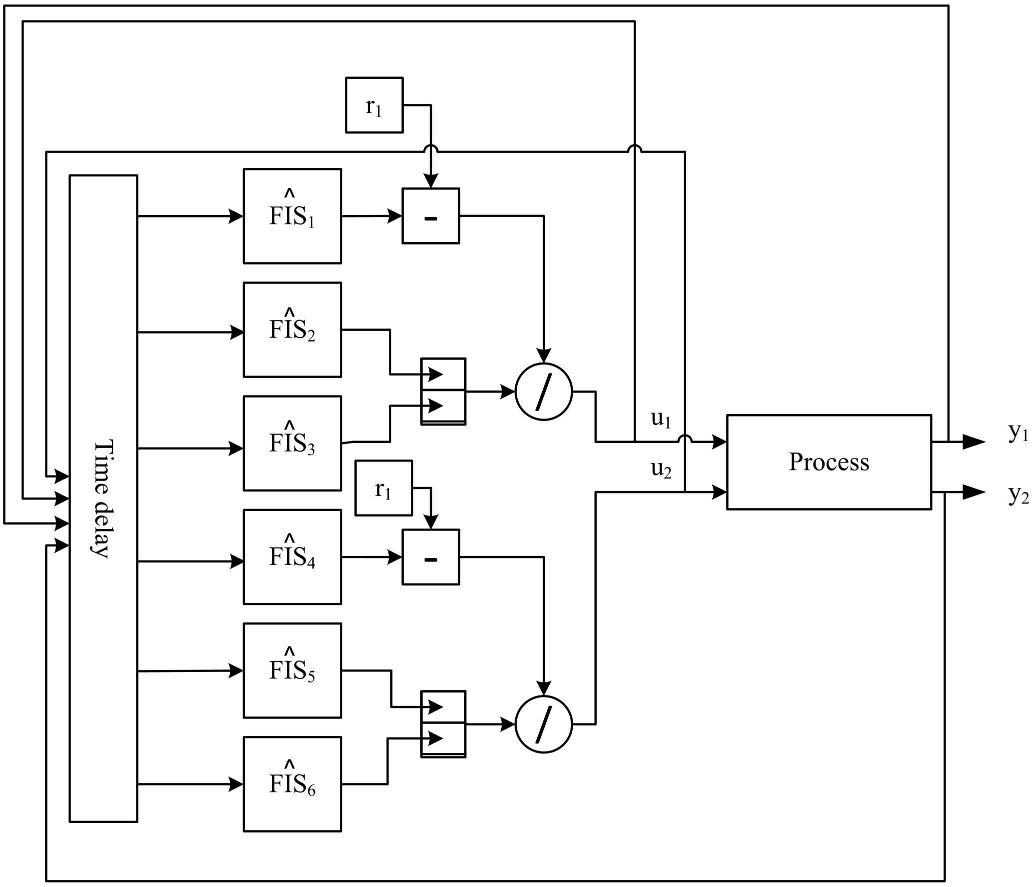

Figure 5.21 MIMO ANFIS-based NARMA-L2 control design

5.4.3 Performance Evaluation of Various Controllers

When evaluating the controllers that are implemented to control the binary distillation column, the following are included:

1. Traditional PID controller;
2. PSO-tuned PID-like fuzzy controller, due to its best performance among PI- PD- and PID-like configurations;
3. The ANN-based NARMA-L2 controller;

4. The new proposed ANFIS-based NARMA-L2 controller.

Table 5.7 shows the parameters types which are tuned for design different controllers. There different scenarios have been applied to check the performance of the above controllers, as follows.

1. The desired output for the distillate product is set to be a constant value of 0.99 (mole fraction), and the bottoms composition is selected as 0.08 (mole fraction), with a simulation time of 100 minutes. Figure 5.22 shows the controllers' efforts to track the desired compositions for the distillate and bottoms compositions.

2. The desired outputs are set to change asynchronously every 100 minutes, with the distillate product composition starting to change at 100 minutes, while the bottoms one does so at 150 minutes, to check the control loop interaction and the efforts to eliminate it by the controllers. The simulation time is set to 1,000 minutes. The controllers' response to track the changing desired compositions for the distillate and bottom compositions is shown in Figure 5.23.

3. The robustness of the controllers has been tested by exposing the simulated column to disturbance situations, for the feed flow rate and the feed composition, separately. The response of changing the feed flow rate by +50% at 50 minutes is shown in Figure 5.24 for both composition products. On the other hand, Figure 5.25 shows the response of the controllers when the column is subjected to a change of liquid composition in the feed mixture by +50% at 50 minutes. It is very improbable that the feed and its composition are constant all the time. Consequently, it is important that the controlled column can handle those changes where the column is in operation.

The performance indexes, including ISE and ITAE of controlling both compositions of the simulated binary distillation column, are presented in Table 5.8. Various controllers have been assessed at different scenarios to check the ability to track the desired set-points as well as examining the robustness and stability by subjecting the column to disturbances. As shown in Figures 5-27 to 5-30 and Table 5.8, in general, it can be seen that all the designed controllers that use diverse configurations passed the transient response requirements. Nonetheless, the performance of the ANFIS-based NARMA-L2 shows better attainment regarding the performance indexes, as well as better transit responses in terms of presenting less steady state error. It is also clear that the ANFIS-based NARMA-L2 controller provides a powerful response regarding the input variance and eliminating the undesired loop control interaction. In addition, it demonstrates its superiority regarding disturbances rejection when compared with the other controllers.

Table 5.7 The tuned parameters of each controller.

Controller	Tuning parameters
PID	gains
PID-like FLC	scaling factors
ANN-based NARMA-L2	weights and biases
ANFIS-based NARMA-L2	membership functions

Table 5.8 Comparison of various controllers' performance for different test scenarios

Test scenario	Controller	Tuning	Performance Index	
			ISE	ITAE
Step set-points	PID	Auto-tuning	0.0025	0.1363
	PID-like FLC	PSO	0.0017	0.0689
	ANN-based NARMA-L2	···	0.0017	0.0402
	ANFIS-based NARMA-L2	PSO	0.0007	0.0145
Asynchrony set-points	PID	Auto-tuning	0.0015	18.5396
	PID-like FLC	PSO	0.0014	11.4034
	ANN-based NARMA-L2	···	0.0006	4.0751
	ANFIS-based NARMA-L2	PSO	0.00021	3.289
Changing the feed flow rate (+50%)	PID	Auto-tuning	0.00423	4.1919
	PID-like FLC	PSO	0.00141	2.6912
	ANN-based NARMA-L2	···	0.00828	6.2601
	ANFIS-based NARMA-L2	PSO	0.00047	1.349
Changing the liquid composition in the feed mixture (+50%)	PID	Auto-tuning	0.00265	2.956
	PID-like FLC	PSO	0.00095	1.8417
	ANN-based NARMA-L2	···	0.00006	1.3721
	ANFIS-based NARMA-L2	PSO	0.00004	1.341

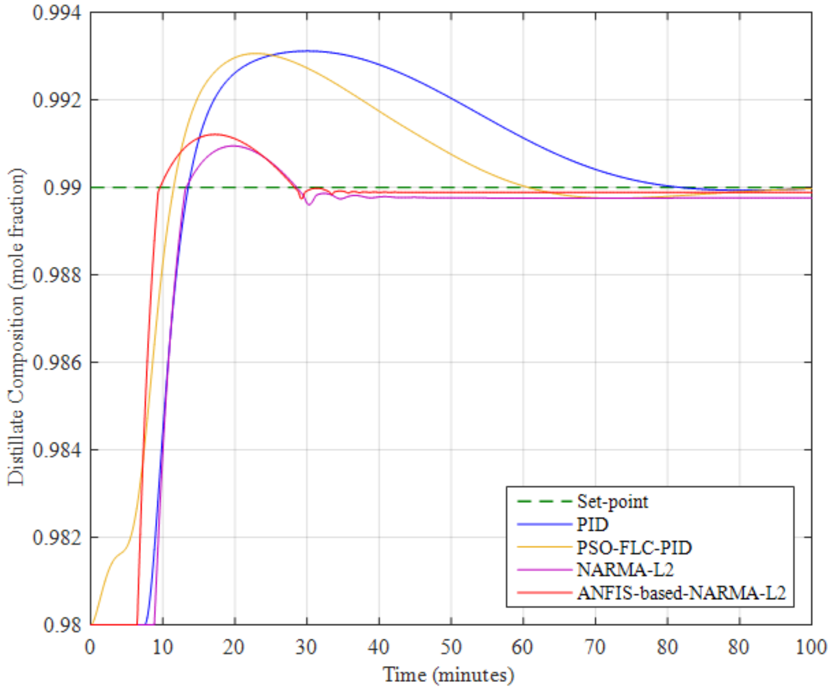

(a) Distillate product

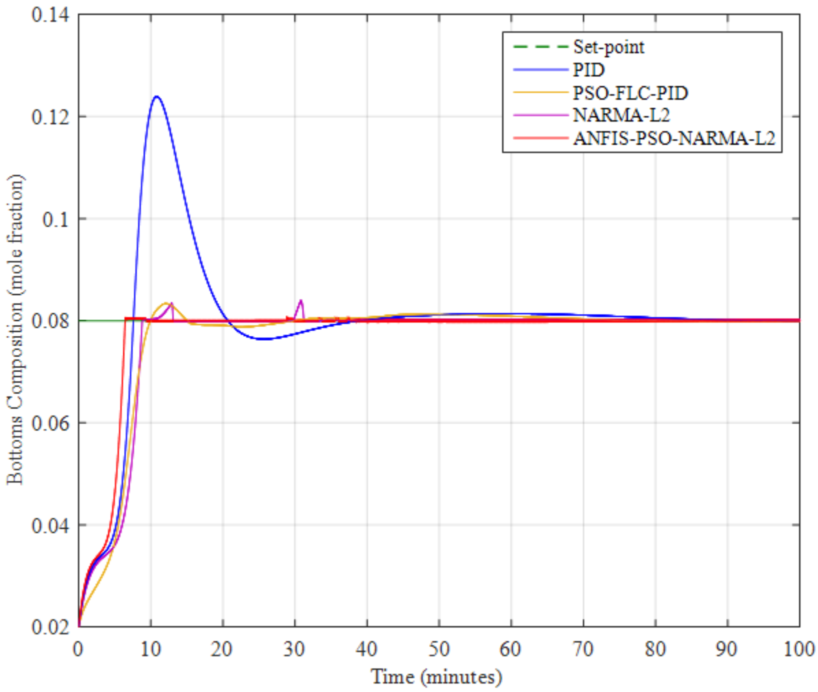

(b) Bottoms product

Figure 5.22 Step response of the various controllers of the binary distillation column

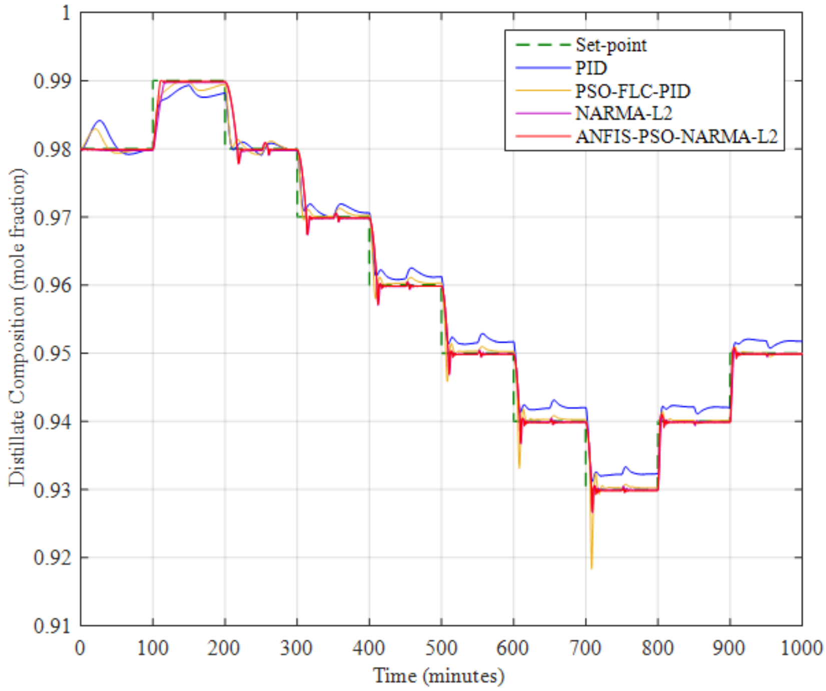

(a) Distillate product

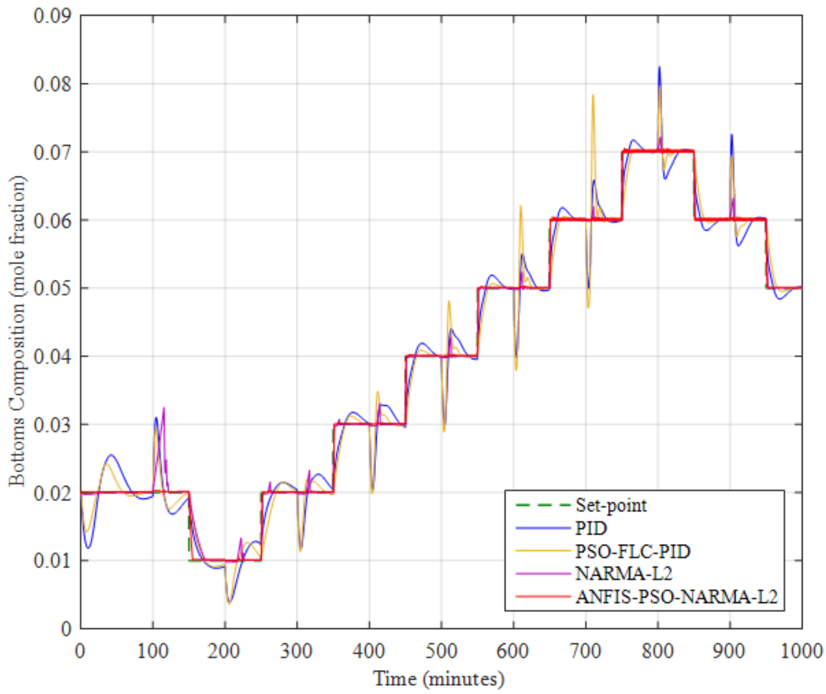

(b) Bottoms product

Figure 5.23 Changing-step response of the various controllers of the binary distillation column

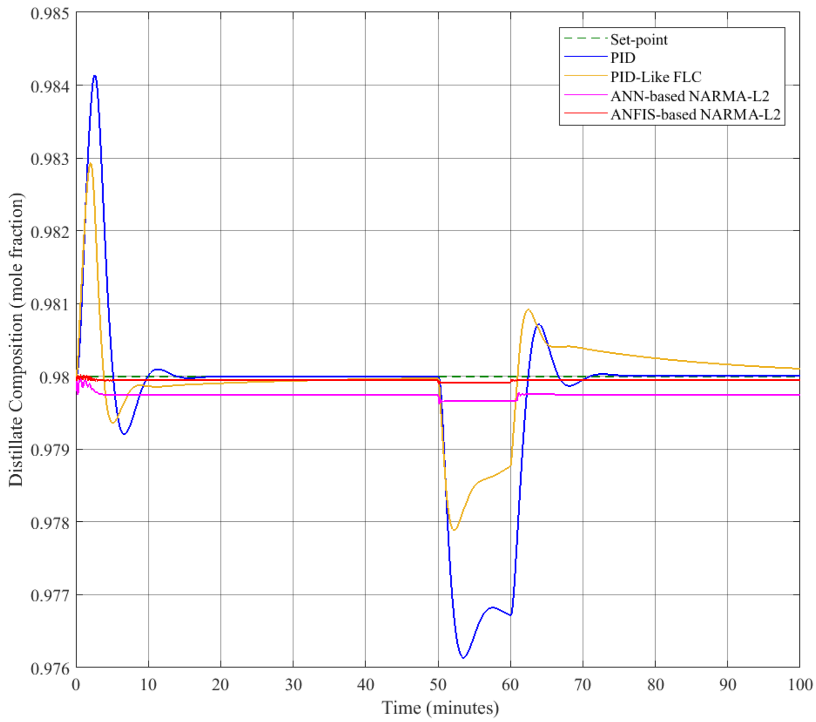

(a) Distillate product

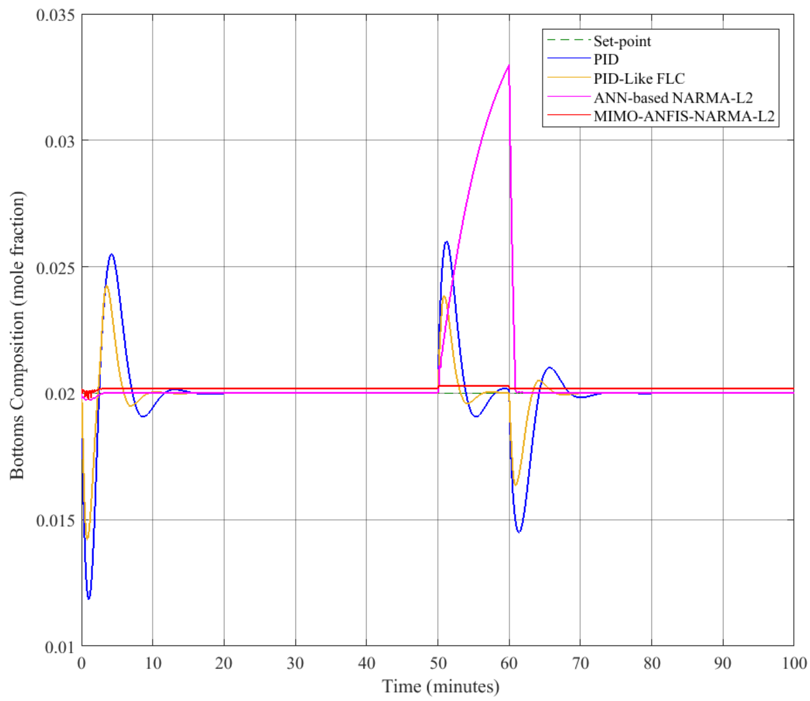

(b) Bottoms product

Figure 5.24 Effects of +50% of feed flow rate as a disturbance on the controlled (a) distillate composition and (b) bottoms composition

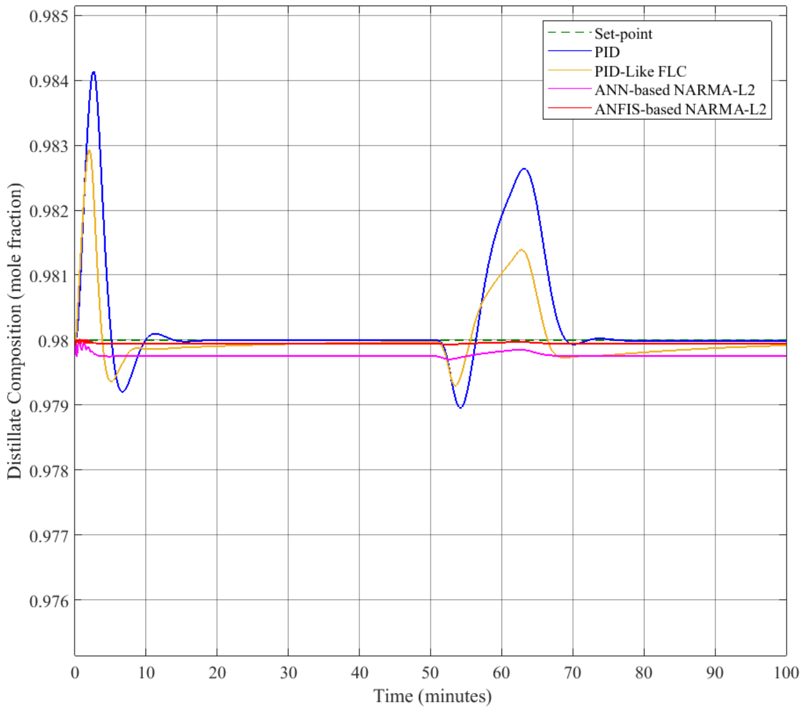

(a) Distillate product

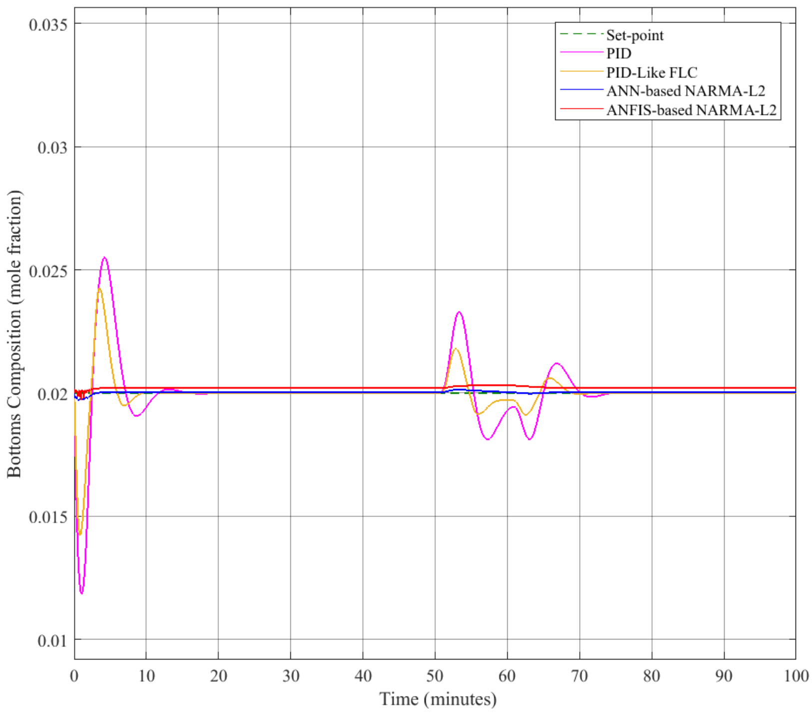

(b) Bottoms product

Figure 5.25 Effects of +50% of feed composition as a disturbance on the controlled (a) distillate composition and (b) bottoms composition

5.5 Summary

In this chapter, various intelligent controllers have been designed to control both distillate and bottoms composition products of the simulated binary distillation column. In order to compare various controllers, several configurations have been investigated and implemented, which are as follows:

1. Traditional PID controller;
2. Fuzzy controllers including PI- PD- and PID-like FLC;
3. ANN-based NARMA-L2;
4. ANFIS-based NARMA-L2.

GA and PSO have been employed to tune FLCs by finding the optimal set of the scaling factors that trigger the controllers to achieve optimum performance. PSO has shown its advantages in terms of attainment of the best objective function and computational time efficiency compared to GA. Then, PSO was used as an overlapping optimiser, the outer PSO being employed to find the best model structure and the inner one to tune the FISs of the ANFIS-based NARMA-L2 identification model. The ANFIS-based NARMA-L2 controller was subsequently designed by rearranging the FISs obtained at the identification phase.

All the controllers were assessed according to two performance indexes, i.e. ISE and ITAE, at different test scenarios. These test scenarios comprised tracking constant set-points, and asynchronous set-points, as well as disturbance tests being conducted to check the robustness and stability of the designed controllers. The feed flow rate and feed composition were chosen as expected disturbances variables since they are unlikely to be constant while the binary distillation column is in operation. All the results have clearly indicated that ANFIS-based NARMA-L2 outperformed the other controllers in terms of best transient response and fewer errors for all test scenarios.

Chapter 6

Modelling and Control of a Multicomponent Distillation Column

6.1 Introduction

Nowadays, many of the distillation procedures deal with multicomponent mixtures [121] and for separating these mixtures the process behaviour is becoming increasingly more complex than for binary ones. In response, much innovative work has been undertaken to achieve this kind of distillation using various configurations of columns. The columns used for multicomponent distillation are designed mainly to produce pure chemicals with as little energy usage as possible.

In the 1930s and 40s, many patents were issued that proposed a novel strategy of dividing wall distillation columns [138, 139]. Later, in 1965, Petlyuk and co-authors proposed a new configuration of thermally coupled columns that could separate ternary mixtures based on thermodynamic properties. Despite their innovative study being revolutionary for the distillation process industry regarding energy saving and capital cost reduction, these researchers' work took around 20 years to come to the attention of the industry. In 1985, the first dividing wall was implemented by the German chemical company Baden Aniline and Soda Factory (BASF), and nowadays it is recognised as the leader in operating multicomponent distillation columns. In 1987, Kaibel introduced new design with the purpose of separating multicomponent mixtures with further energy efficiency and with a minimum use of equipment for separation in one column [140]. One study presented a comparison of the energy usage of a Kaibel column with a conventional column arrangement and demonstrated that the former provides an energy reduction of 33% [141]. There are also other benefits from operating Kaibel columns than just energy investments. For instance, the distillation process can be achieved by only one shell, which leads to less capital cost compared to conventional arrangements. Since it involves of a single unit, the space required in a distillation plant is correspondingly reduced [142]. Implementing of energy-efficient columns has been increasing in recent years in the industry, hence nowadays, many studies in academia have involved focusing on operating and controlling these columns with optimal performance [31].

In this chapter, a brief theoretical introduction to the configuration and arrangement of multicomponent distillation columns is provided. Also, the modelling and control of a 4-product distillation (Kaibel) column using the proposed ANFIS-based NARMA-L2 controller are covered. Then, the results are presented and comparisons made, which is followed by a conclusion.

6.1.1 Multicomponent Distillation Columns Types

For multicomponent mixture separation, a sequence of distillation columns is often utilised to produce pure products. For instance, two columns at least are required to separate three components [31], for which the direct and indirect sequences should include four heat exchangers (two reboilers and two condensers), as depicted in Figure 6.1. The state-task to separate mixture F that contains chemicals A, B and C is shown in Figure 6.2.

Petlyuk et al. pioneered an alternative arrangement that notably reduces the consumed energy and capital cost [143]. In their superior proposal, the so-called Petlyuk configuration, two columns are thermally coupled, whilst the streams of vapour and liquid leaving the main column (the second) are directly linked with the prefractionator (the first column). This joined configuration is commonly known as the Fully Thermally Coupled Distillation Column (FTCDC), in which, a condenser and a reboiler are efficiently replaced by thermal coupling

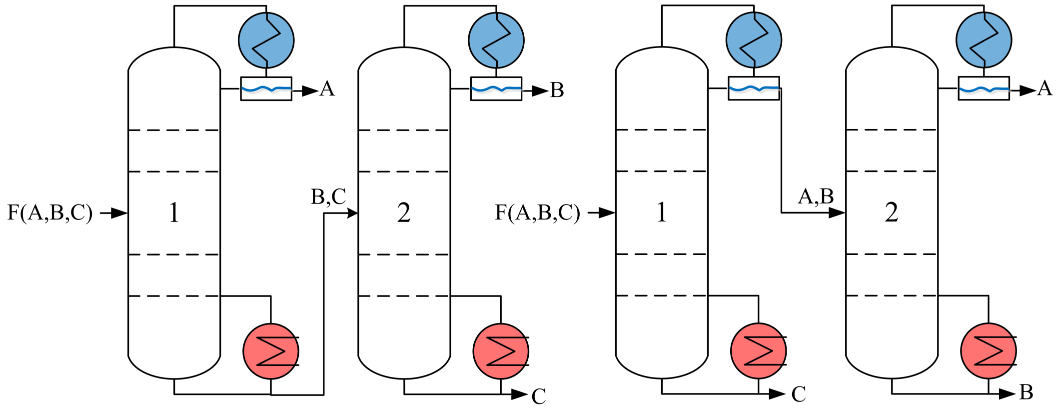

Figure 6.1 Column sequences for the separation of a three components mixture: indirect (left) and direct (right)

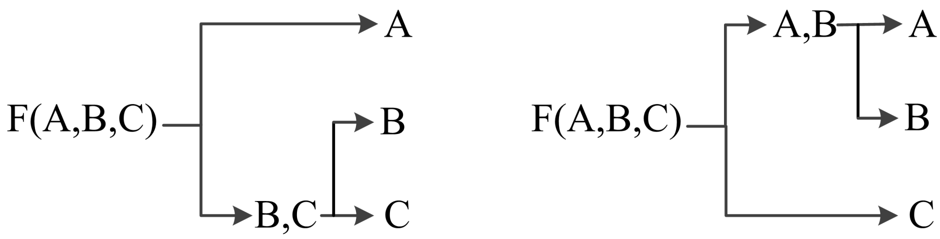

Figure 6.2 State-task network for the separation of a three components mixture: indirect (left), direct (right)

of the prefractionator with the main column, whilst the remaining condenser and reboiler are involved to the main column [124], as shown in Figure 6.3. The notable improvement in the thermal efficiency of the Petlyuk configuration reduces the amount of heat and cooling energy required to achieve and maintain the distillation process. It was reported about one-third of energy is saved compared to the direct and indirect sequences to separate the same mixture [144]. The avoidance of remixing of steam inside the column is considered the main reason for applying the Petlyuk configuration. In addition, the thermodynamic inefficiency indicated as a result of mixing and remixing of the mixture compositions, which is unavoidably escorted by the entropy of the mixing construction [145]. Kaibel went further with regards to energy saving and capital cost reduction by implementing distillation of a multicomponent mixture by only one column. The schematic setup of the Kaibel column, also known as the dividing-wall column, is illustrated in Figure 6.4.

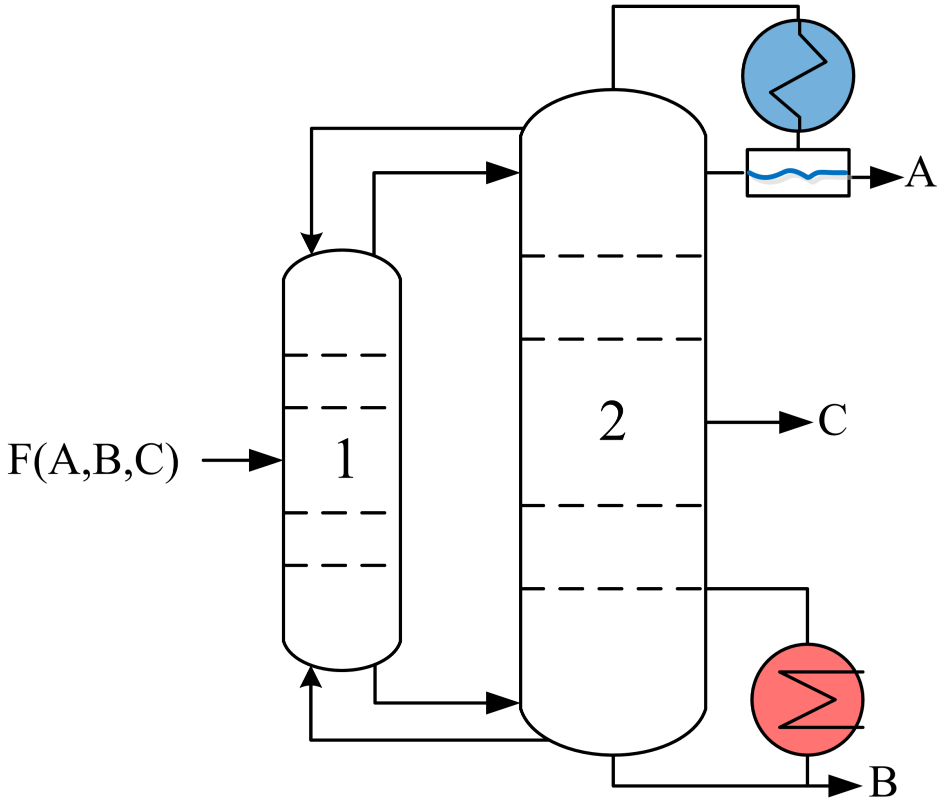

Figure 6.3 Petlyuk's distillation column configuration

Less attention has been paid by researchers in academia to the dividing wall configuration columns than to the Petlyuk arrangement. Figure 6.5 presents a graphical comparison between the number of published papers on the Kaibel column and those on Petlyuk column, the data having been retrieved from the Scopus® database index. To address this imbalance, the Kaibel column configuration was chosen for the second case study in the thesis with regards to modelling, simulation, and control, all of which is presented in this chapter.

6.2 Multicomponent Distillation

For the modelling of the dividing-wall column to separate four chemicals based on Kaibel configuration, a stage-by-stage model has been utilised with following simplification assumptions:

1. Constant molar flows inside the column;

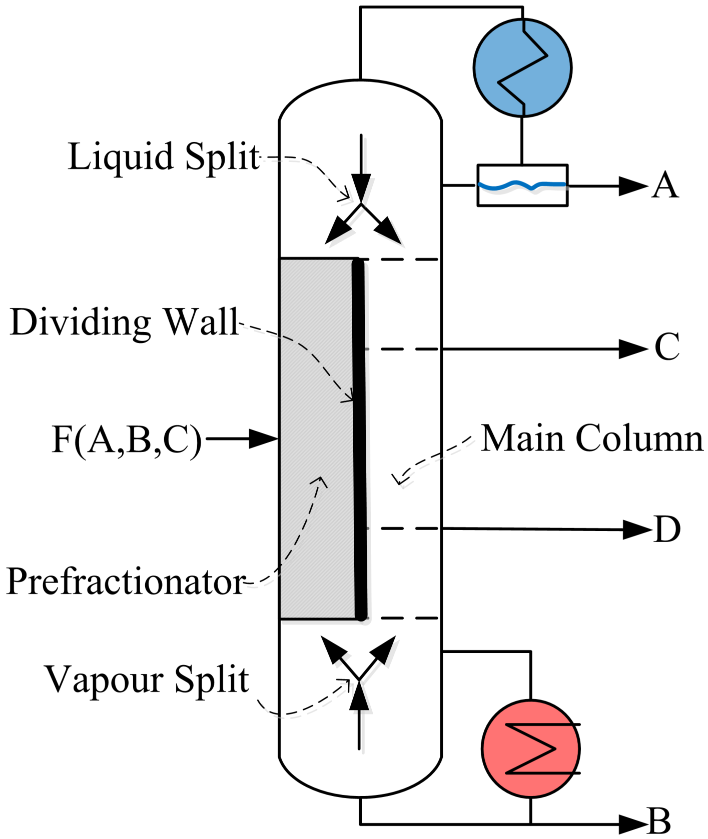

Figure 6.4 The schematic setup of the Kaibel Column

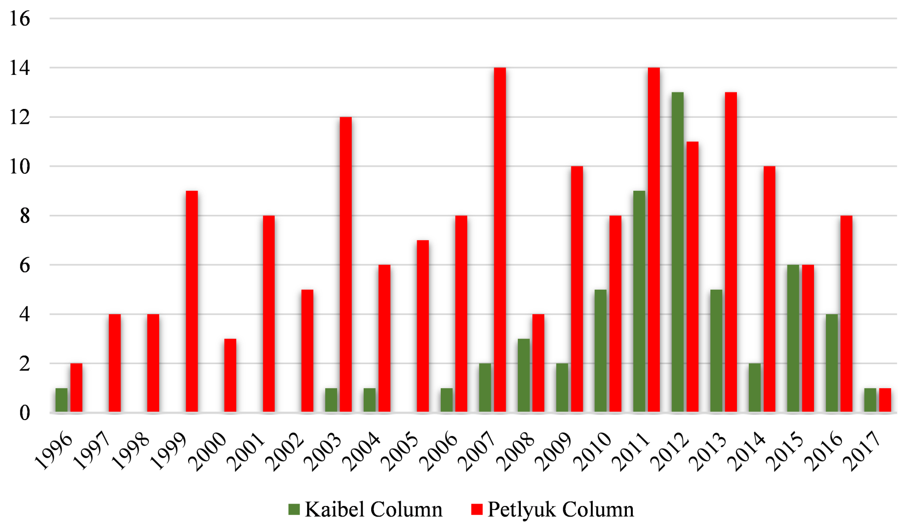

Figure 6.5 Published papers on Kaibel column versus Petlyuk column

2. Constant pressure;
3. Equilibrium on each stage;
4. Linear relationship of flow dynamics;
5. No heat transfer between the prefractionator and the main column.

6.2.1 Modelling of a Multicomponent Distillation Column

Basically, three of different differential equations describe the behaviour of the Kaibel column as follows:

1. Mass balance;
2. Mole fraction balance;
3. Updating of stage temperatures inside the column.

The physical and chemical data of the Kaibel's column used in this thesis are based on the lab-scale column implemented in the Department of Chemical Engineering at the Norwegian University of Science and Technology. Researchers from the university used this model for investigating the operational and control properties of the column [146, 147].

The simulated multicomponent distillation model in this thesis has seven sections and 64 stages in total (industrial size); two for the prefractionator and five sections for the main column. The detailed Kaibel column is depicted in Figure 6.6 showing the sections and stage numbering. The steady state data and the notation variables of the column used in the modelling and simulation are illustrated in Table 6.1. The nominal values of the temperature stages are shown in Table A.2.

The modelled and simulated column uses alcohols (butanol, ethanol, methanol and propanol) as a feed mixture. Methanol, as the lightest composition in the feed, is streamed at the top of column D, while ethanol and propanol are drained from the side stream 1 and 2, respectively. Lastly, the bottoms product is butanol. The three main equations the govern in the simulation model can be written as:

Table 6.1 Inputs and the nominal values of the Kaibel column used in the modelling and simulation

Symbol	Description	Value	Unit
D	Distilled flow rate	0.2508	mol/min
L	Reflux flow rate	2.8492	mol/min
V	Vapour flow rate	3	mol/min
R_L	Liquid split ratio	0.2572	$\cdots$
R_V	Vapour split ratio	0.377	$\cdots$
S_1	Side stream (1) flow rate	0.2494	mol/min
S_2	Side stream (2) flow rate	0.2497	mol/min
F	Feed flow rate	1	mol/min
z_D	Distilled mole composition ratio in the feed	25%	$\cdots$
z_{S1}	Side stream (1) mole fraction ratio in the feed	25%	$\cdots$
z_{S2}	Side stream (2) mole fraction ratio in the feed	25%	$\cdots$
z_B	Bottoms mole fraction ratio in the feed	25%	$\cdots$
zq	Liquid fraction ratio of the feed	90%	$\cdots$
B	Bottoms product flow rate	0.2503	mol/min

- **The mass balance:**

$$\frac{dM_i}{dt} = L_{i+1} + V_{i-1} - L_i - V_i. \tag{6.1}$$

- **The mole fraction balance:**

  To calculate mole fraction x of each component j at each stage i:

$$M_i \frac{dx_{i,j}}{dt} = L_{i+1}(x_{i,j+1} - x_{i,j}) + V_{i-1}(y_{i-1} - x_{i,j}) - V_i(y_{i,j} - x_{i,j}). \tag{6.2}$$

There is a need to compute $y_{i,j}$,the vapour mole fraction of component j at stage i, using the modified Raoult's Law as:

$$y_{i,j} = \frac{x_{i,j}\gamma_{i,j}p^*_{i,j}}{P_i}, \tag{6.3}$$

where, P_i is the pressure at stage i, $\gamma_{i,j}$ is activity coefficient and $p^*_{i,j}$ is the vapour pressure of a pure component i. Whilst the Antoine equation is used to calculate vapour pressure as:

$$p^*_{i,j} = e^{(A_i \frac{B_i}{T+C_i})}, \tag{6.4}$$

where, A_i, B_i and C_i are Antoine constants, which can be found in chemicals handbooks [148], and T is the temperature at which vapour pressure is to be calculated. Also, the pressure at stage i is computed by:

$$P_i(x_{i,j}, T) = \sum_{i=1}^{N_c} x_{i,j}\gamma_{i,j}p^*_{i,j}T_i. \tag{6.5}$$

- **Update stage temperature:**
  Update the temperature inside the column with an open vent, in order to let the pressure inside the column reach an atmospheric value of P_o. The temperature is updated to make sure that the pressure given in Equation 6.6 converges to P_o, which is just a numerical adjustment with no physical interpretation. However, it assures that the pressure calculated via Raoult's law and Wilson's model meets to the correct the atmospheric pressure P_o [146]. The differential update equation is:

$$\frac{dT_i}{dt} = \theta\Big(P_o - P_i(x_{i,j}, T_i)\Big), \tag{6.6}$$

where, θ is a positive constant that chooses the convergence rate.

The flowchart of the model simulation steps, according to the mathematical description mentioned earlier, is given in Figure 6.7 and the model is represented by a Simulink® block diagram, as shown in Figure B.7 in Appendix B.

6.2.2 Validation of the Simulated and Modelled Column

Validation of the modelled column is conducted after being simulated by MATLAB® and Simulink®. This done by comparing the outputs of the column with published papers that implemented optimal operation and different types of controllers on the same chemical and physical properties of the Kaibel column used in the thesis. The open-loop response of the column to the nominal inputs is demonstrated in Figure 6.8, which shows reasonable accuracy of 99.63% in comparison with [146, 147], as shown in Table 6.2.

Table 6.2 Comparison of the simulated model outputs with [145], [146].

Temperature stage	**Output temperatures in [145], [146] (K)**	**Output temperatures in the simulated column (K)**	**Overall accuracy =99.63%**
T17	368.29	368.31	99.99%
T30	341.97	338.49	98.98%
T49	379.64	380.43	99.79%
T59	355.83	355.035	99.77%

The temperature profile of the column is shown in Figure 6.9. The steady-state optimal composition profile of the simulated Kaibel column is demonstrated in Figure 6.10 for the prefractionator, sections 1 and 2, including stages 1 to 24, versus the mole fraction ratio of the output products. While Figure 6.11 shows the composition profile of the main column, sections 3 to 7, including stages 25 to 64.

6.2.3 Identification of the Multicomponent Distillation Column

As in Chapter 5, the first step of design the proposed controller, ANFIS-based NARMA-L2, is to identify the column to be controlled. The approximator submodels in the NARMA-L2 model should be trained first to represent the forward dynamics of the column. Obtaining input/output data is achieved after deciding which are the manipulated inputs and outputs of the column being controlled. In [146, 147] it has been shown that the manipulated inputs of a Kaibel column are:

$$U = [L \quad S_1 \quad S_2 \quad R_L]\,. \tag{6.7}$$

The column outputs can be selected freely. However, often the temperatures along the column are often measured and then, a controller is implemented to maintain temperatures at preferred set-points to keep the column's temperature stable [149]. The temperatures at each stage has a good relationship with the respective mole fraction and thus, the controlled outputs are the temperatures of stages 17, 30, 59 and 49:

$$Y = [T_{17} \quad T_{30} \quad T_{59} \quad T_{49}]. \tag{6.8}$$

In order to collect sufficient information for creating a good model that represents the column behaviour as well capturing the importance of column dynamics, the inputs are selected as PRBS within the operating range. The collected dataset is presented in Figure 6.12, showing the inputs and respective outputs of the simulated column for 2,000 minutes.

The collected dataset has been divided into 70% and 30% for training and testing the subset, respectively. The structure of the approximation submodels was selected, where, as stated earlier, an identification problem normally comprises ten or even more potential inputs to the proposed model. Consequently, a heuristic approach may be employed for governing swiftly these important candidate inputs and applying them accordingly. The lag space of the inputs and outputs in the NARMA-L2 was selected by PSO. For simplicity, the time delay assumed to be in the range of inputs and outputs is (1-3) to form the model input candidates as:

$$\begin{aligned} M(t) = \Big(&u_1(t-1), u_1(t-2), u_1(t-3), \cdots, u_4(t-1), u_4(t-2), u_4(t-3), \\ &y_1(t-1), y_1(t-2), y_1(t-3), \cdots, y_4(t-1), y_4(t-2), y_4(t-3)\Big). \end{aligned} \tag{6.9}$$

While the predicted output is:

$$\hat{Y}(t) = [\hat{y_1}(t) \quad \hat{y_2}(t) \quad \hat{y_3}(t) \quad \hat{y_4}(t)]. \tag{6.10}$$

PSO is implemented to find the best combination of inputs from the candidates set in Equation 6.9, and then another PSO is used to tune the approximation ANFIS submodels, as undertaken in Chapter 5. Table 6.3 shows the results of the performance of identification RMSE against the best combination of inputs. Since finding the ANFIS parameters for a large number of inputs is time-consuming, ANFIS models for various combinations of inputs that have been constructed by a few iterations. Then, it chooses that with the best RMSE and proceeds to engender further optimisation. The input selection approach assumes that the ANFIS model with the minimum RMSE after one iteration of adjustment has a greater potential of achieving a lower RMSE when given more iterations of adjustment. This assumption is not undeniably accurate, but it is heuristically sensible [150]. Figure 6.13 shows bar charts of the best number of inputs to the model for identifying the column outputs (temperatures) y_1, y_2, y_3 and y_4, respectively. Accordingly, Figure 6.14 shows the predicted versus simulated temperatures of the identified Kaibel column.

Table 6.3 RMSE of the different NARMA-L2 model structures

Predicted output	The best number of input	The best combination	RMSE	
			Training	Testing
$\hat{Y}_1$	7	$\big(u_1(t-1), u_2(t-1), y_1(t-1), y_1(t-2), y_1(t-3), y_2(t-1), y_2(t-2)\big)$	0.001825	0.00345
$\hat{Y}_2$	8	$\big(u_1(t-1), u_2(t-1), y_1(t-1), y_2(t-1), y_2(t-2), y_2(t-3), y_3(t-1), y_3(t-2)\big)$	0.015934	0.02167
$\hat{Y}_3$	6	$\big(u_2(t-1), u_3(t-1), y1(t-1), y_2(t-1), y_3(t-1), y_3(t-2)\big)$	0.001523	0.00193
$\hat{Y}_4$	7	$\big(u_3(t-2), u_4(t-1), y_2(t-1), y_3(t-1), y_4(t-1), y_4(t-2), y_4(t-3)\big)$	0.004213	0.00532

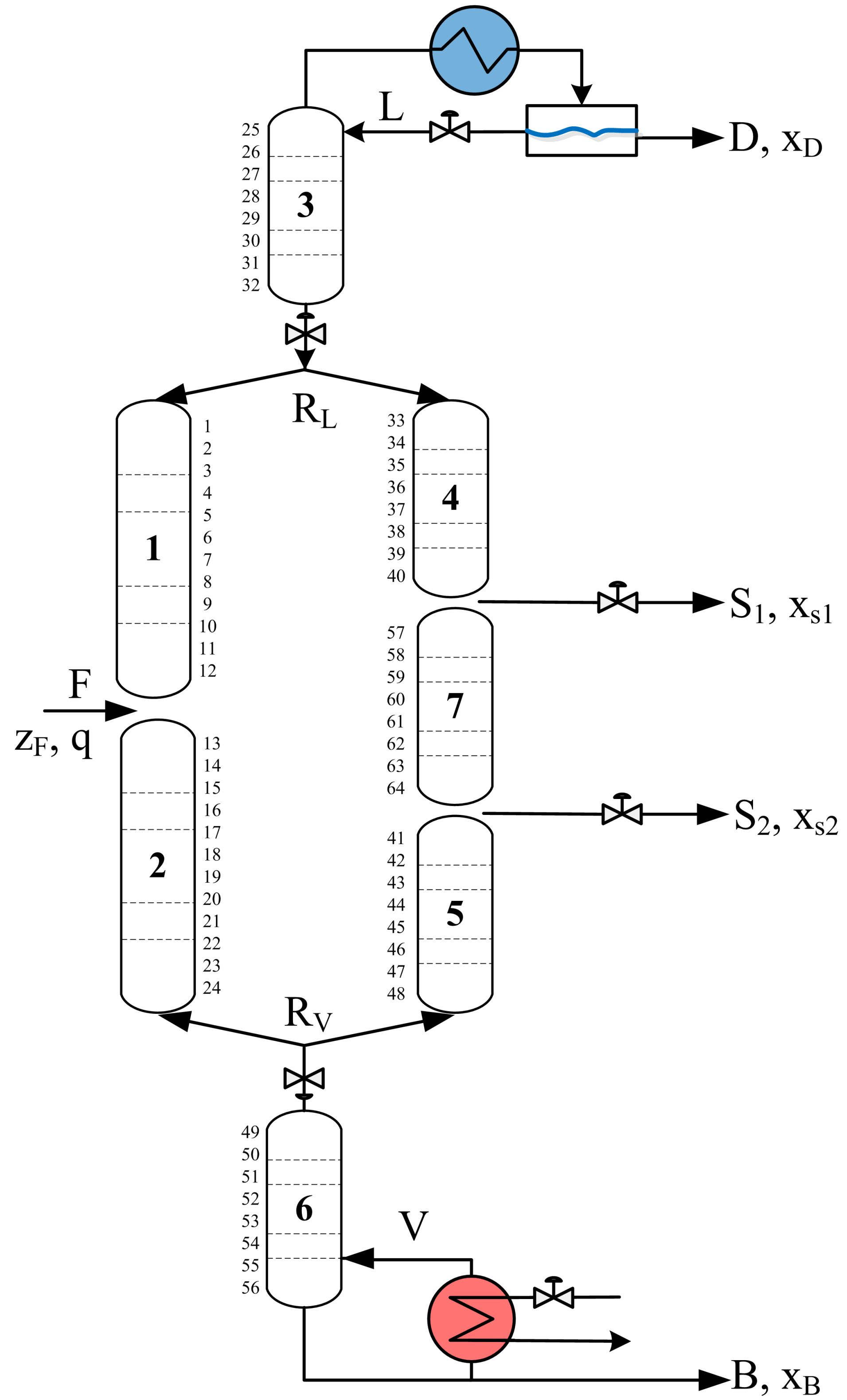

Figure 6.6 Sections and stage numbering of the modelled Kaibel column

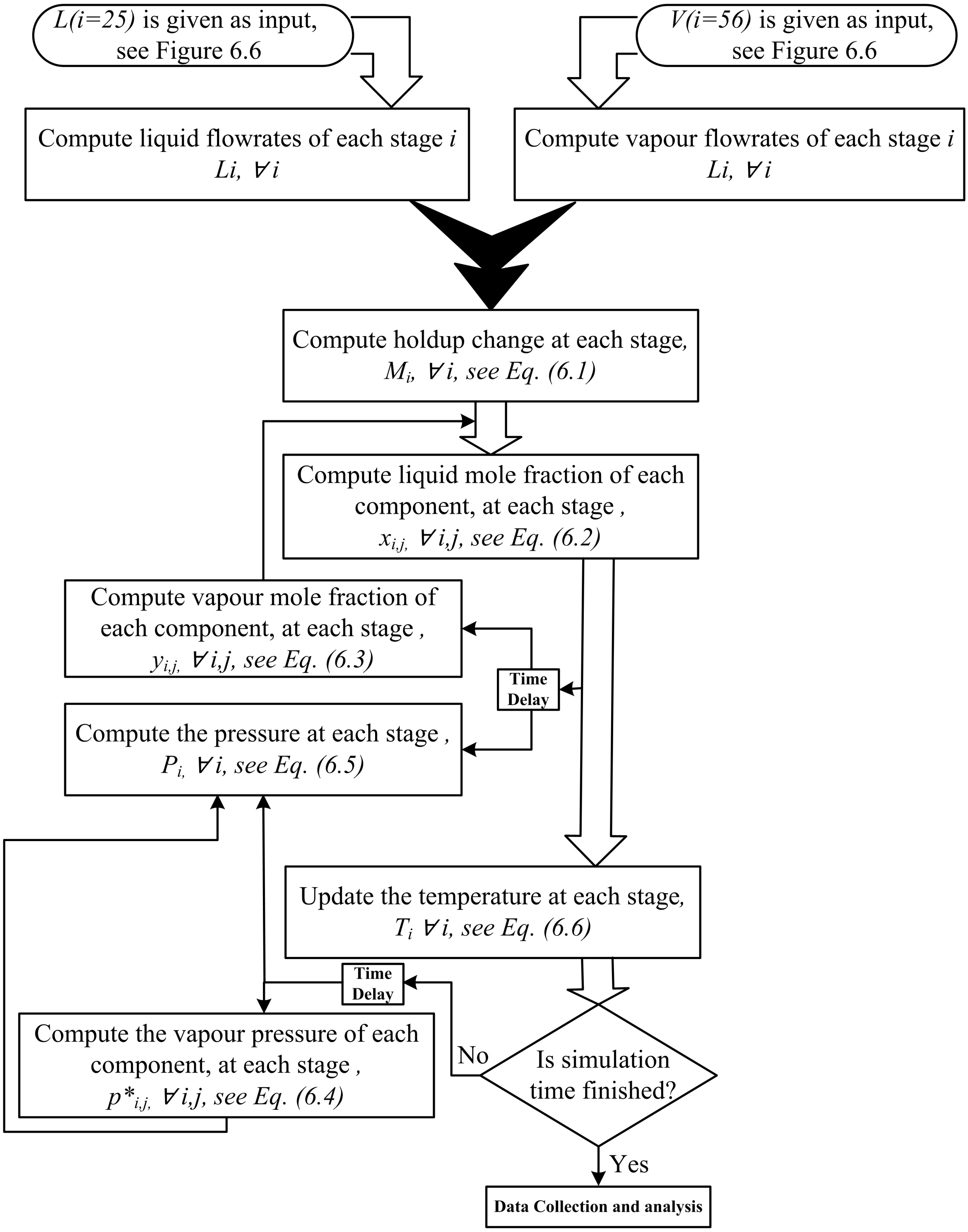

Figure 6.7 Model simulation steps flowchart

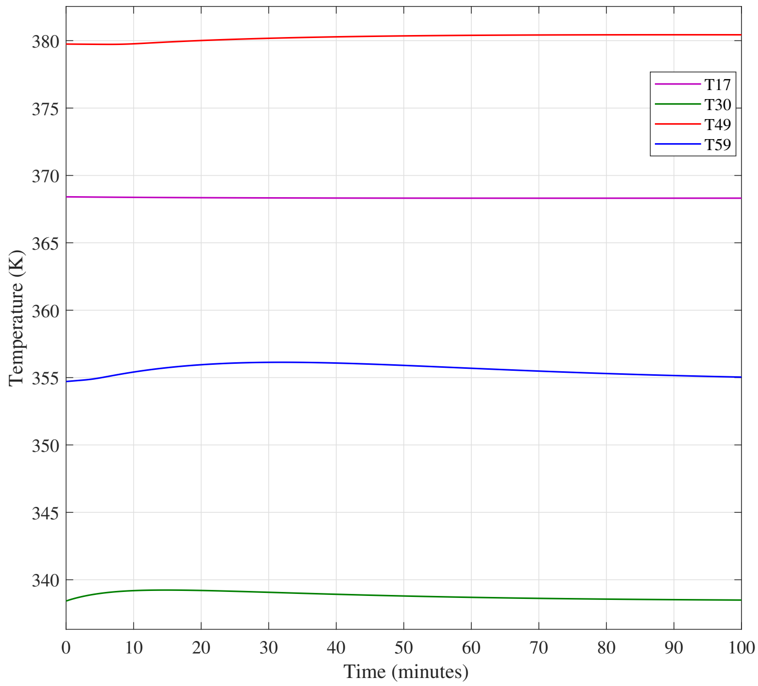

Figure 6.8 Open-loop response of the simulated column to the nominal inputs

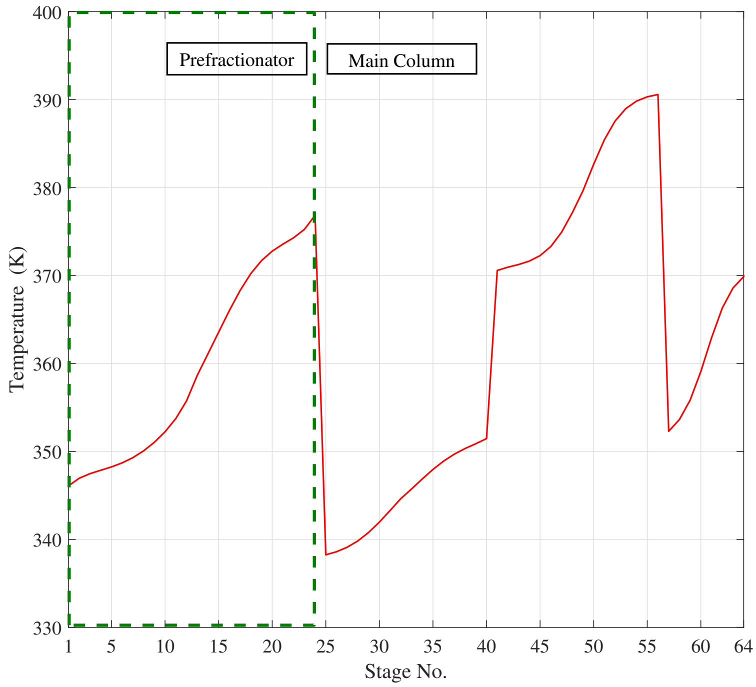

Figure 6.9 Temperature profile of the simulated column

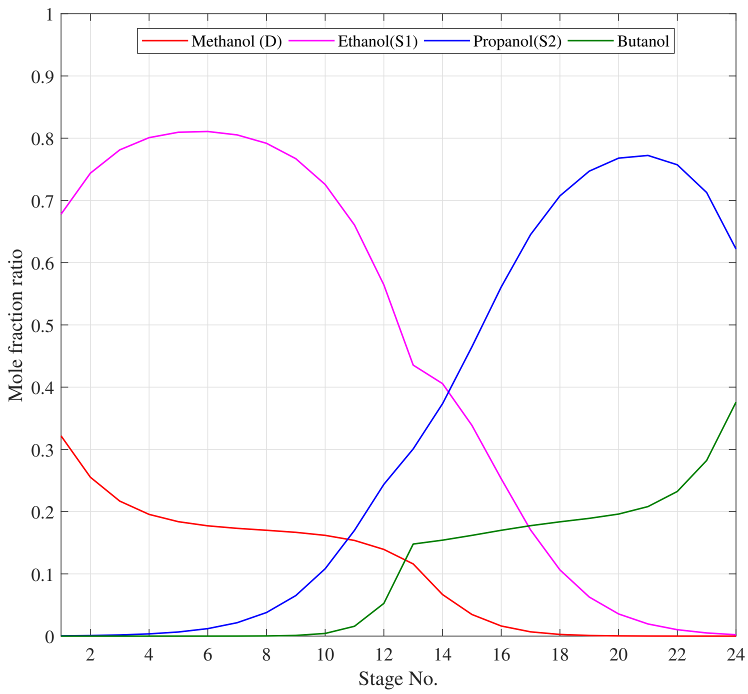

Figure 6.10 Prefractionator optimal composition profile

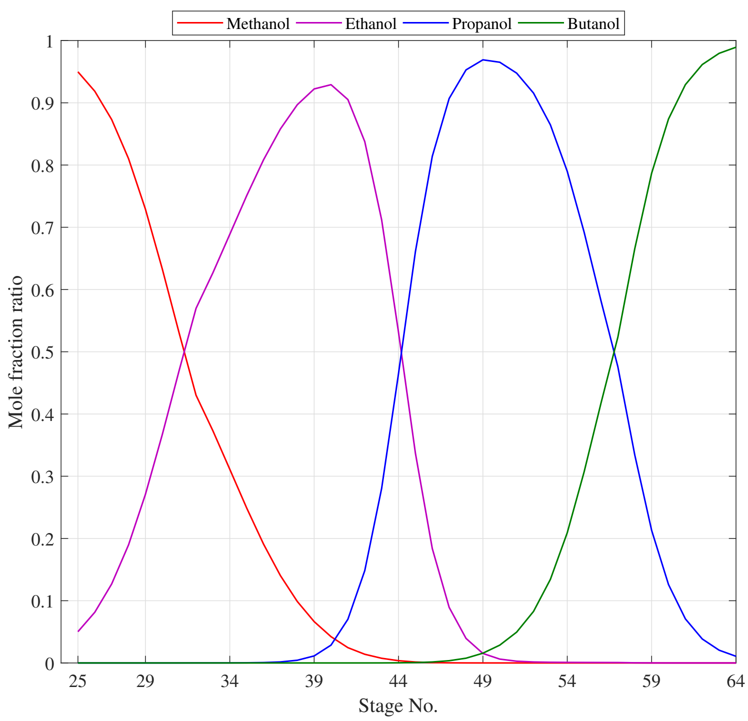

Figure 6.11 Main column optimal composition profile

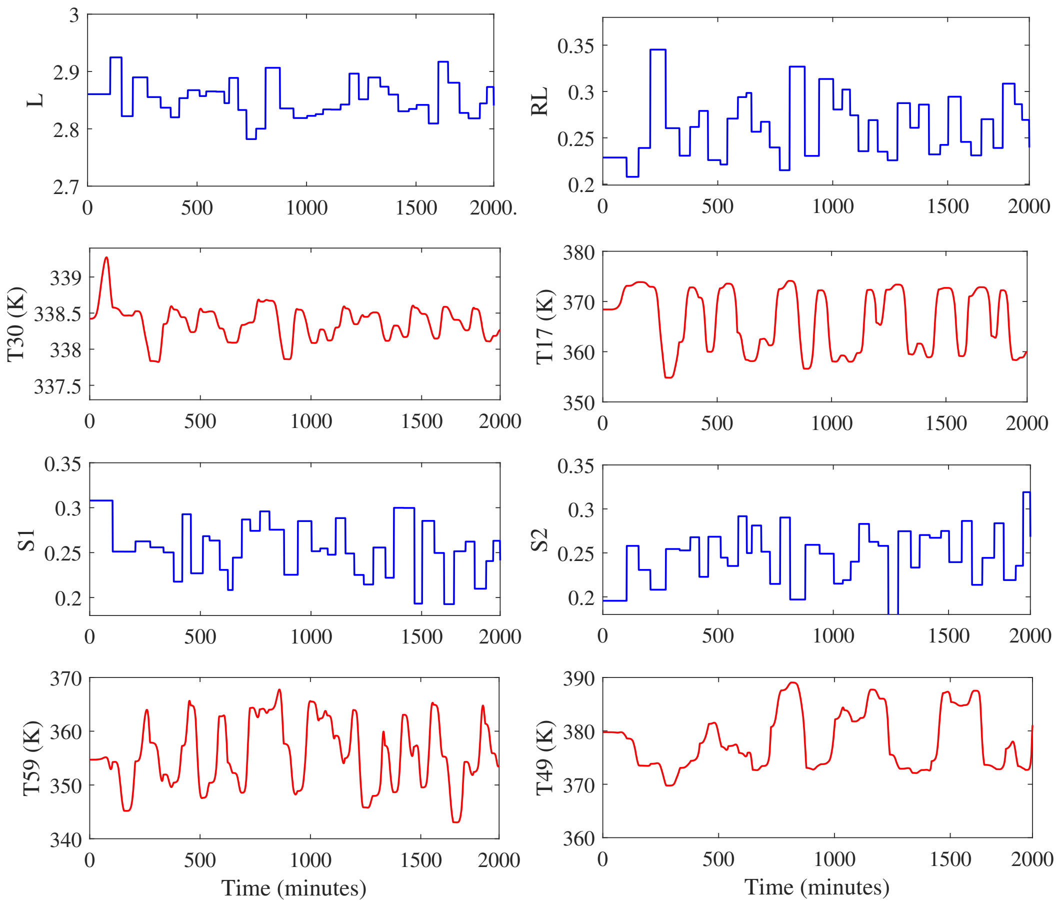

Figure 6.12 Open-loop response of the simulated Kaibel column

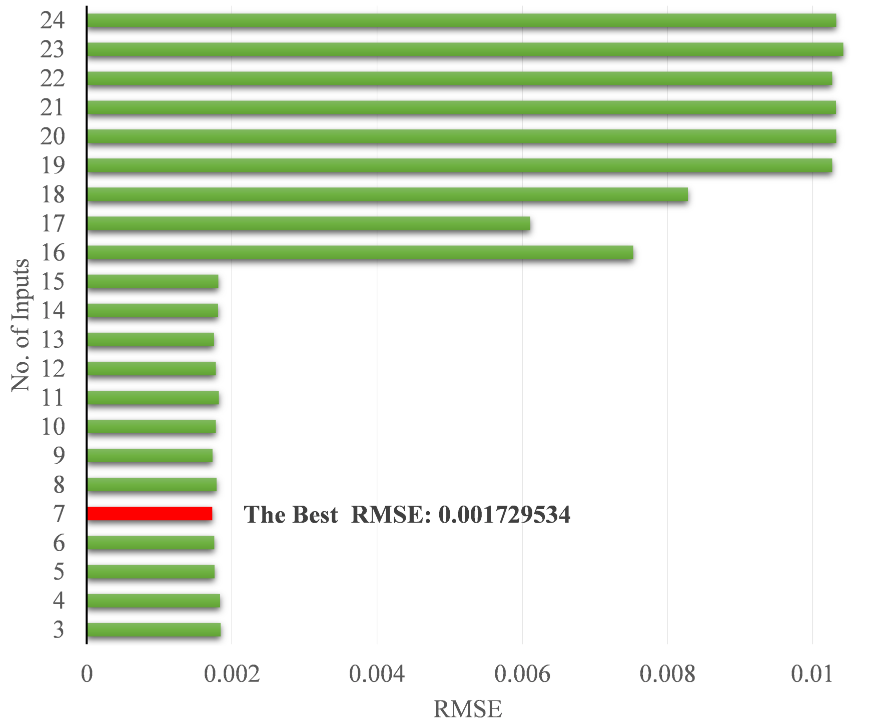

(a) RMSE (y_1)

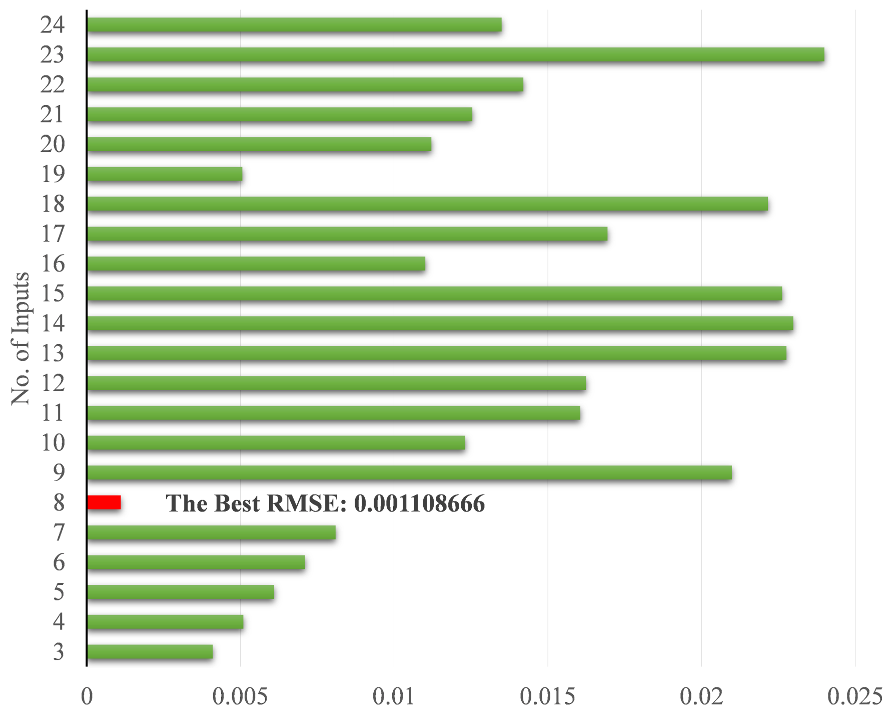

(b) RMSE (y_2)

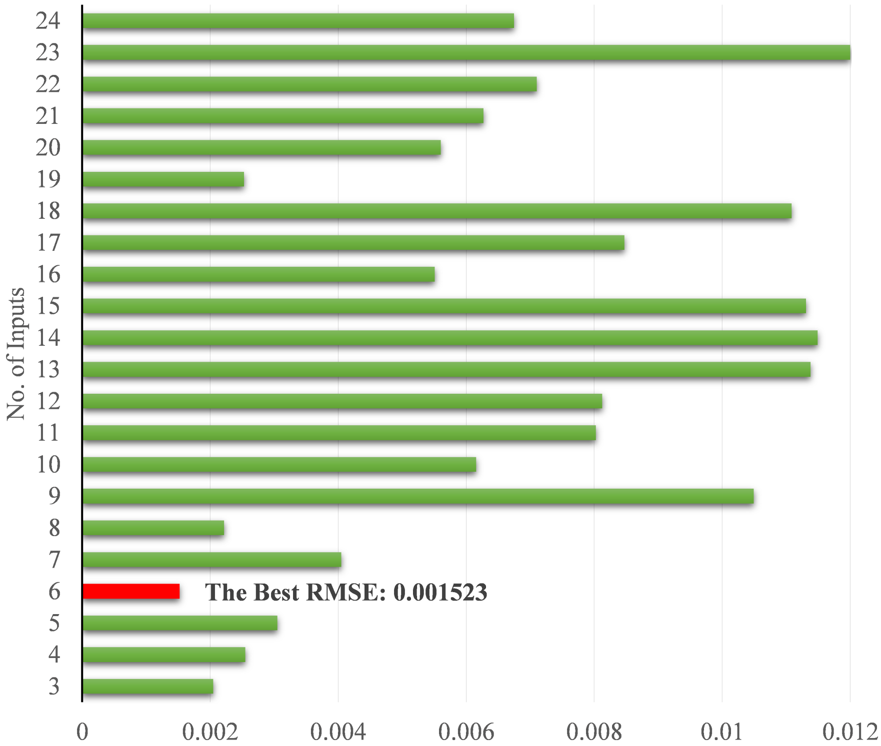

(c) RMSE (y_3)

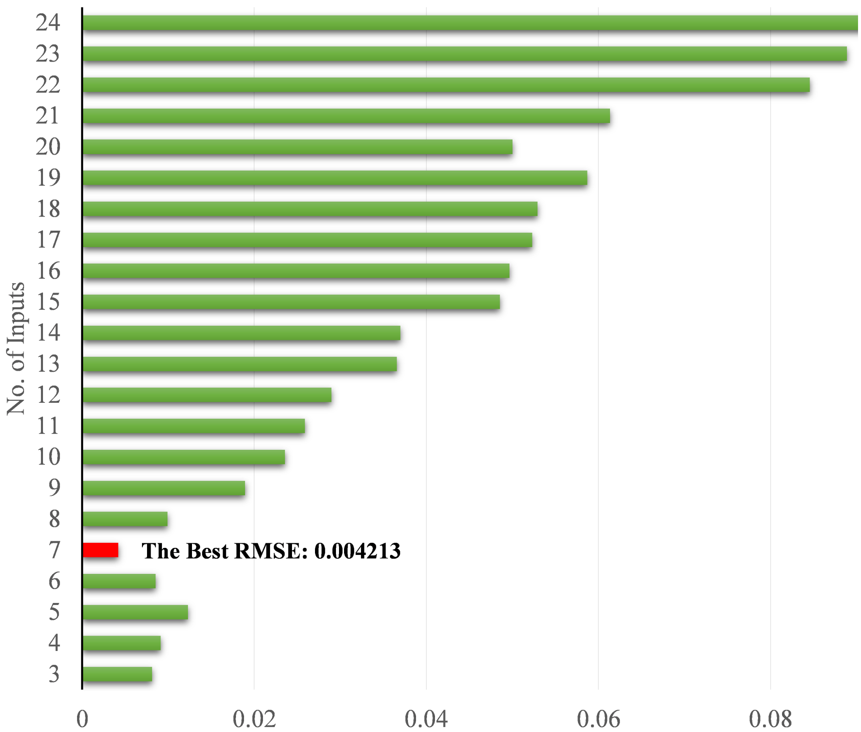

(d) RMSE (y_4)

Figure 6.13 Best number of inputs to the model for identifying the column outputs (y_1, y_2, y_3 and y_4)

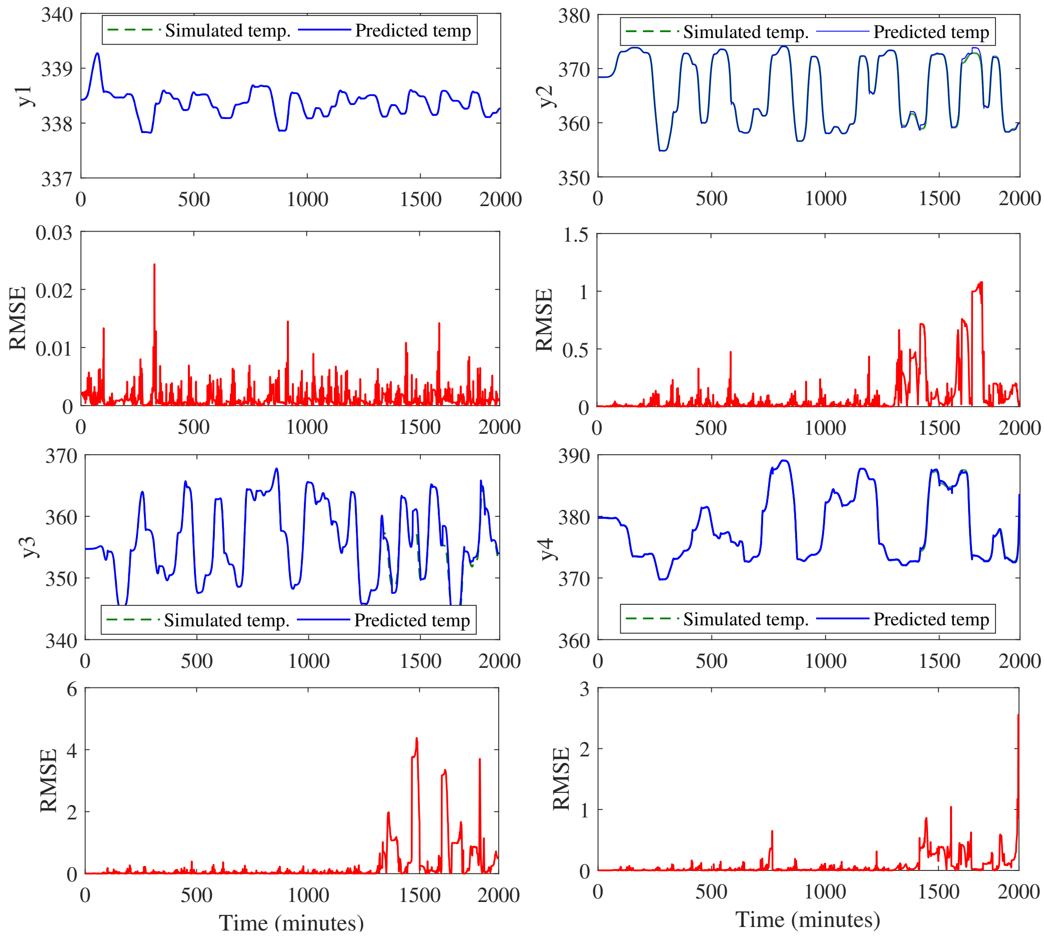

Figure 6.14 Predicted vs. simulated temperatures of the identified Kaibel column

6.3 Control System Design for the Multicomponent Distillation Column

Similar to control the binary distillation column, the ANFIS-based NARMA-L2 controller is formed by rearrangement of the identification model. For validation and comparison purposes, a PID controller also has been applied to the simulated Kaibel column. As mentioned earlier, it is often the case that the distillation process is controlled by using specific stage temperatures, which give a reasonable indication of their respective compositions [146].

Skogestad, in his review [151] about the control of distillation, indicated some advantages of applying temperatures to control distillation columns. Some of those benefits are as follows:

1. Setting the compositions profile at a steady state level along the column;
2. Lessening the requirement of level control, because it gives indirect level control;
3. Reducing the interaction problem of the remaining composition and consequently, making it likely to have good two-point composition control. In addition, it reduces the nonlinearity of the column behaviour.

As indicted previously in Section 6.2.3, Strandberg et al. investigated the optimal operation and control of Kaibel column. The manipulated inputs, including reflux flow rate, liquid split ratio, and both side stream flow rates $(L, R_L, S_1$ and $S_2)$, are selected to control specific temperatures. The chosen temperatures $(T_{17}, T_{30}, T_{49}$ and $T_{59})$ are controlled to specified set-points that automatically makes the column operate at the optimal steady state function [152]. Figure 6.15 shows the decentralised control loops of the simulated Kaibel column.

6.3.1 Control Performance Evaluation

For the purpose of comparison and evaluation, PID controllers have been applied to the simulated Kaibel column as well as the ANFIS-based NARMA-L2 control design. The controlled column performance is assessed against disturbances rejection, for certain inputs,

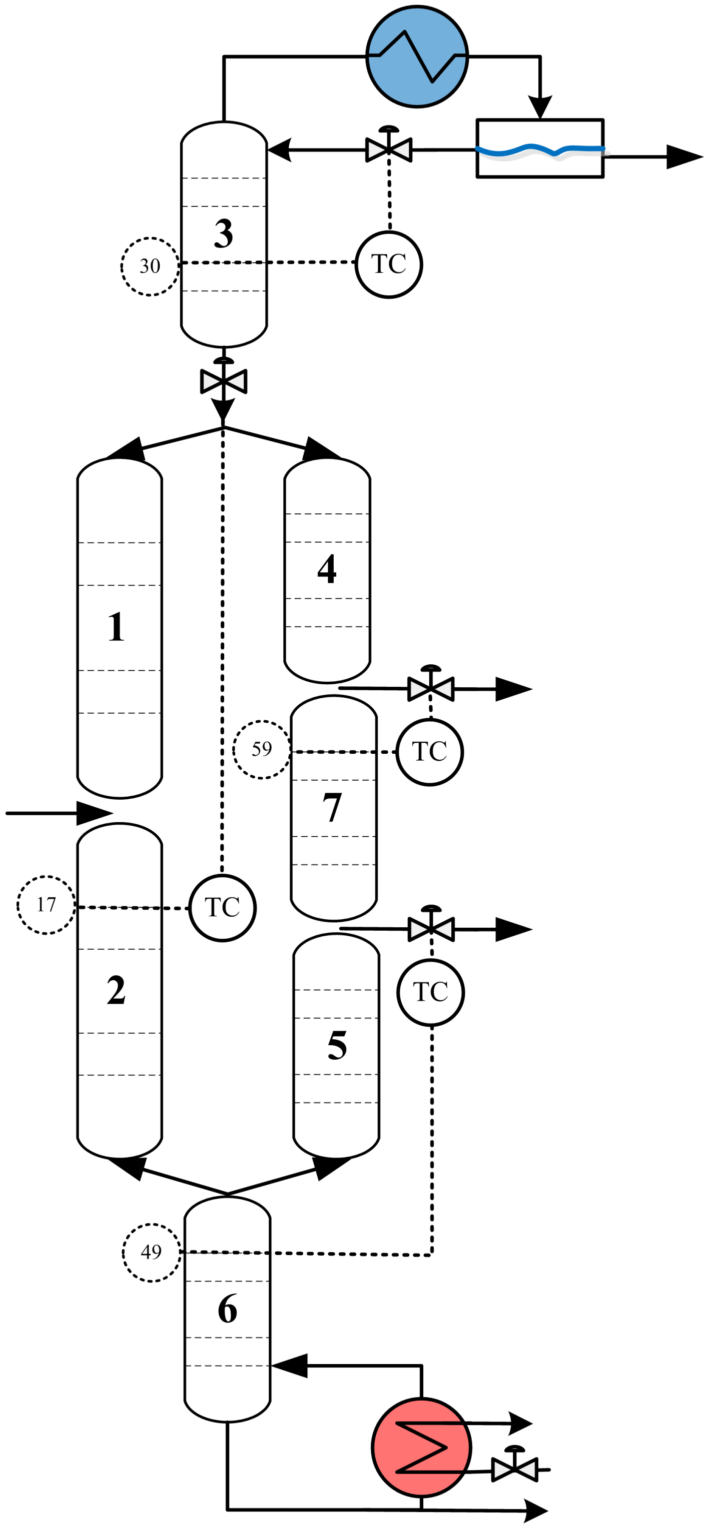

Figure 6.15 Temperature control loops of the simulated Kaibel column

to ensure the superiority of the ANFIS-based NARMA-L2 control layout. The inputs that are used to change owing to disturbances are the feed flow rate, mole fraction ratio of the product S_1 and the vapour split ratio. It important that those disturbances should be handled as much as possible by the controlled column. Since the feed flow rate is computed by other sections of the process plant where the column is in operation [153], it is extremely improbable that this rate is kept at a constant level at all operation times of the column. In addition, the liquid composition in the mixture similarly changes and will be conducted in the assessment. Lastly, the vapour split is featured with high uncertainty and thus, contained within the disturbance inputs. The simulation was carried out for 2,000 minutes, with the disturbances test of various inputs being applied separately to the controlled column (at 500 minutes) to check its ability of to handle the disturbances. The performance indexes of the controllers under the disturbances tests are shown in Table 6.4.

Figure 6.16 depicts the graphical behaviour of the controlled column by showing the set-points temperatures and the selected temperature outputs. It is clear that the ANFIS-based NARMA-L2 handles the disturbances more efficiently than the PID control design, which thus provides evidence of the robustness of the proposed controller.

Table 6.4 Performance indexes of PID and ANFIS-based NARMA-L2 controllers under various disturbances tests

Disturbance type	Control Design	Performance index	
		ISE	ITAE$\times 10^3$
Feed flow rate	PID	9.333	9.530
+30%	ANFIS-based NARMA-L2	1.576	1.515
Liquid composition	PID	10.451	9.971
in the mixture +20%	ANFIS-based NARMA-L2	1.206	1.041
Liquid split ratio	PID	7.317	7.835
+10%	ANFIS-based NARMA-L2	1.249	1.134

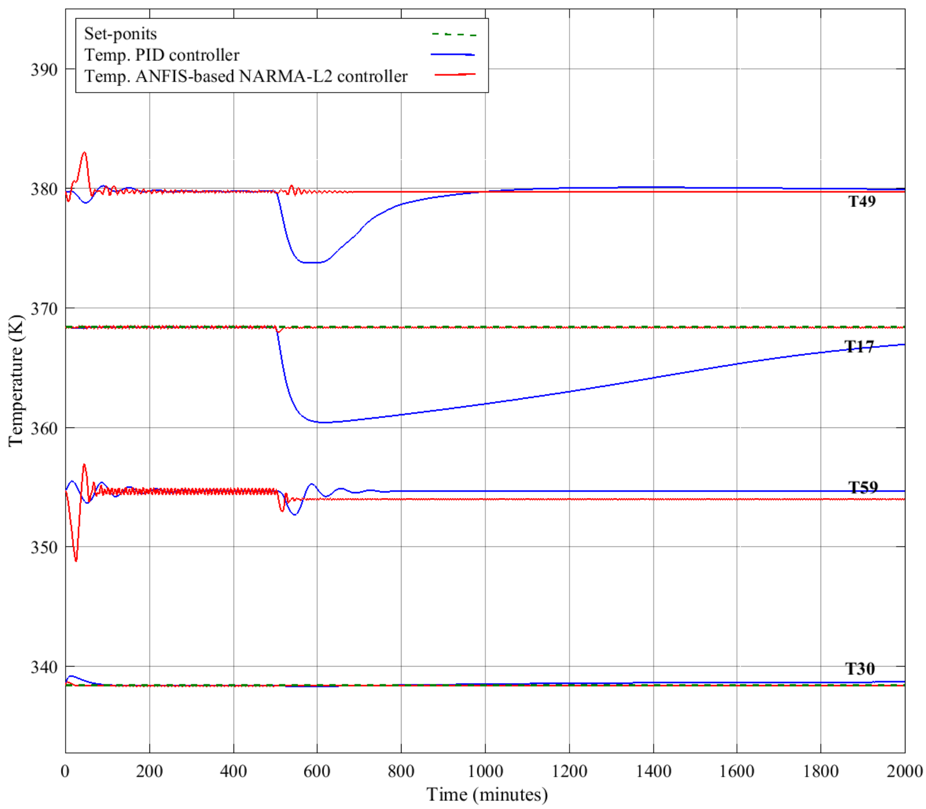

(a) $F + 30\%$

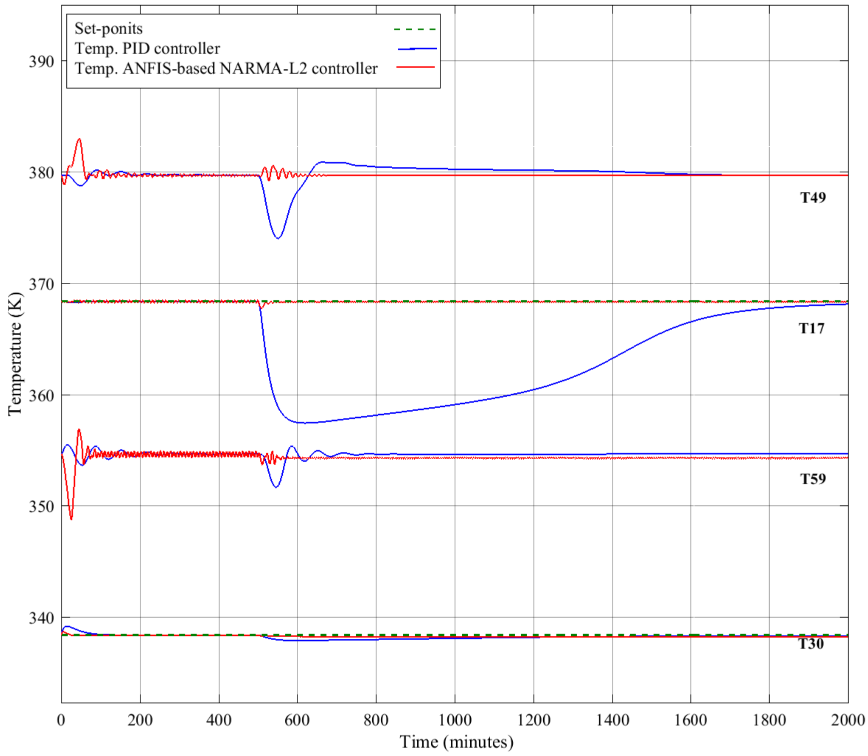

(b) $zq + 30\%$

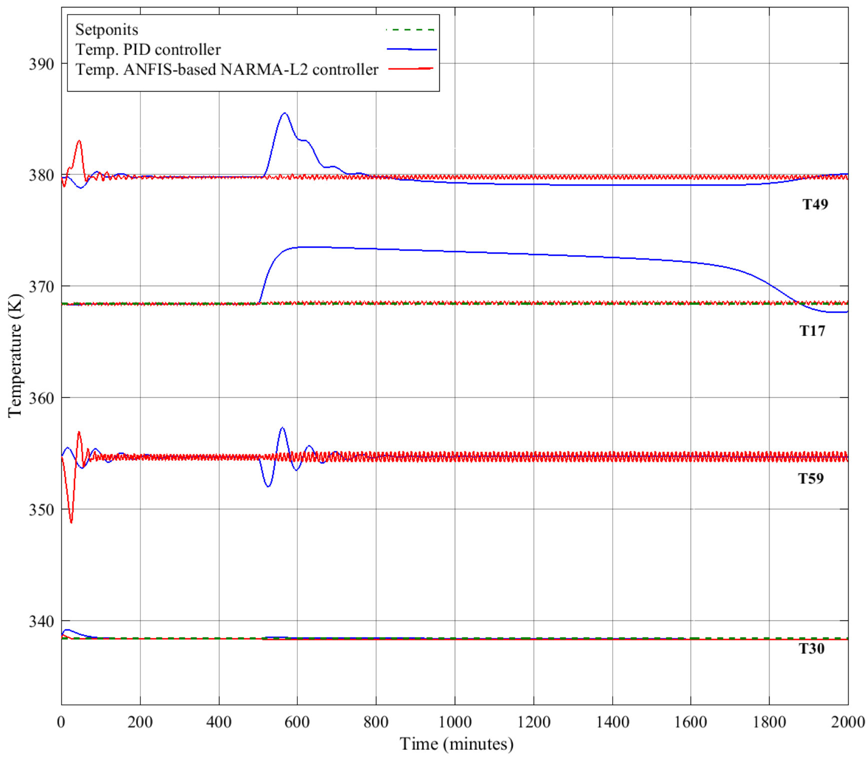

(c) $R_v + 10\%$

Figure 6.16 Effects of the selected disturbances on the controlled temperatures of Kaibel's column

6.4 Summary

In this chapter, a brief history of the multicomponent distillation process has been provided, as well as different types of column designs and arrangements being depicted. Nowadays, the most used configuration for separating four products, namely Kaibel column, has been modelled and simulated via MATLAB® and Simulink® using mathematical representations that characterise the behaviour of the column with seven sections and 64 stages, in total. The simulated model of the column was verified by comparing the steady state values of the selected temperature with previous studies in the literature.

In the identification phase, many of candidate inputs have been examined using PSO in order to select the most potential set of inputs that reflect the behaviour of the column. RMSE was chosen as an objective function to decide the best set of inputs of the ANFIS-based NARMA-L2 model. The trained model was rearranged to design the ANFIS-based NARMA-L2 controller to control the selected temperatures of the column. PID was applied as well for comparison purposes. The robustness of both controllers was examined using disturbances tests, with the results showing the superiority of the proposed controller for handling disturbances efficiently with less ISE and ITAE, which are used as performance indexes. The new proposed ANFIS-based NARMA-L2 controller has proven its robust performance for controlling a 4×4 multicomponent distillation process.

Chapter 7

Conclusions and Future Works

7.1 Summary of the Thesis

The increased complication and stringent requirements of today's industrial process plants demand more advanced control designs capable of achieving better and more flexible performance. New control designs can be implemented when coping with demanding process control requirements. The main focus of this thesis has been to design an intelligent controller for a distillation process using different intelligent-based approaches. Various intelligent controllers have been implemented, to control the product compositions of the distillation columns, including:

- Traditional PID controller, for comparison evaluation purposes;
- FLC design in different configurations, such as PD- and PI- and PID-like;
- ANN-based NARMA-L2;
- A new proposed ANFIS-based NARMA-L2

GA and PSO have been employed to optimise FLCs by selecting the best scaling factors, separately. In addition, PSO has been used to find the best model structure of the proposed ANFIS-based NARMA-L2 design as well as to tune several FISs used to approximate the submodels. The above listed intelligent controllers have been implemented to control a binary distillation column used to separate two products. While PID and the new proposed controller have been employed to control a 4-product Kaibel distillation column.

7.2 Conclusions

The main findings of the thesis can be concisely put as follows.

- All the implemented controllers have passed the transient response requirements with various performance indexes. However, the NARMA-L2 configuration design, using ANNs and ANFIS separately, showed its superiority over the fuzzy and PID controllers. Moreover, ANFIS-based indicated a better performance of all the controllers in the different test scenarios. Those scenarios included tracking a constant step and changing the steps of the desired outputs of the simulated binary distillation column. In addition, there were disturbances tests for both the binary and multicomponent distillation columns.

- PSO outperformed GA when used to tune the scaling factors of the fuzzy controllers in terms of the best objective function and the time requirement for the optimisation process.

- The new proposed control design involves using PSO to find the best model structure of the identification phase to approximate the simulated binary and multicomponent distillation columns.

- For the multicomponent distillation column, the proposed controller was applied to provide stability and robustness in the presence of the expected disturbances.

7.3 Suggestions and Recommendations for Future Work

Whilst strenuous effort has been made to ensure a satisfactory level of accuracy when conducting this research study, it was unavoidable that compromises had to be made. In addition, given the analytical nature of the investigation undertaken regarding the new proposed controller, it was necessary for time and cost purposes that its performance should initially be verified using a simulated environment. As the tests results from the simulations appear promising, the following logical step is to assess the proposed controller in a real environment. This could be done, first, by utilising a laboratory-scale or a pilot-scale process and then proceeding to the industrial-scale level.

Through the research, real-coded PSO and GA have been employed with combination with other integrant approaches and new swarm optimisation techniques could be used to seek even better performance of intelligent controllers by speeding up the tuning process of the scaling factors, such as glowworm swarm optimisation. Moreover, Support Vector Machine (SVM) could be employed to approximate submodel structure in order to identify the optimal MIMO NARMA model and control. Finally, other types of distillation could be investigated for modelling and control by implementing the new proposed ANFIS-based NARMA-L2 control design, such as reactive distillation in which a chemical reaction occurs during the process.

References

[1] J. A. Karl and P. Kumar, "Control: A perspective," *Automatica*, vol. 50, no. 1, pp. 3–43, 2014.

[2] M. Mahfouf, S. Kandiah, and D. Linkens, "Fuzzy model-based predictive control using an arxstructure with feedforward," *Fuzzy Sets and Systems*, vol. 125, no. 1, pp. 39–59, 2002.

[3] A. Gani, A. Siddiqa, S. Shamshirband, and F. Hanum, "A survey on indexing techniques for big data: taxonomy and performance evaluation," *Knowledge and Information Systems*, vol. 46, no. 2, pp. 241–284, feb 2016.

[4] R.-E. Precup and H. Hellendoorn, "A survey on industrial applications of fuzzy control," *Computers in Industry*, vol. 62, no. 3, pp. 213–226, 2011.

[5] M. Chandrasekaran, M. Muralidhar, C. M. Krishna, and U. Dixit, "Application of soft computing techniques in machining performance prediction and optimization: a literature review," *The International Journal of Advanced Manufacturing Technology*, vol. 46, no. 5-8, pp. 445–464, 2010.

[6] S. Shamshirband, N. B. Anuar, M. L. M. Kiah, V. A. Rohani, D. Petković, S. Misra, and A. N. Khan, "Co-fais: cooperative fuzzy artificial immune system for detecting intrusion in wireless sensor networks," *Journal of Network and Computer Applications*, vol. 42, pp. 102–117, 2014.

[7] C. Caraveo, F. Valdez, and O. Castillo, "Optimization of fuzzy controller design using a new bee colony algorithm with fuzzy dynamic parameter adaptation," *Applied Soft Computing*, vol. 43, pp. 131–142, 2016.

[8] L. Amador-Angulo, O. Mendoza, J. R. Castro, A. Rodríguez-Díaz, P. Melin, and O. Castillo, "Fuzzy sets in dynamic adaptation of parameters of a bee colony optimization for controlling the trajectory of an autonomous mobile robot," *Sensors*, vol. 16, no. 9, p. 1458, 2016.

[9] S. Fabri and V. Kadirkamanathan, *Functional adaptive control: an intelligent systems approach*. Springer Science & Business Media, 2012.

[10] D. White, D. Sofge, and T. Samad, “Handbook of intelligent control: neural, fuzzy, and adaptive approaches,” *IEEE Transactions on Automatic Control*, vol. 39, no. 7, pp. 1534–1534, 1994.

[11] A. J. Isaksson, “Some aspects of industrial system identification,” *IFAC Proceedings Volumes*, vol. 46, no. 32, pp. 153–159, 2013.

[12] G. Szederkényi, R. Lakner, and M. Gerzson, *Intelligent control systems: an introduction with examples*. Springer Science & Business Media, 2006, vol. 60.

[13] P. J. Antsaklis, “Intelligent control,” *Wiley Encyclopedia of Electrical and Electronics Engineering*, 1999.

[14] M. Mahfouf, M. F. Abbod, and D. A. Linkens, “A survey of fuzzy logic monitoring and control utilisation in medicine,” *Artificial intelligence in medicine*, vol. 21, no. 1, pp. 27–42, 2001.

[15] D. Montgomery, “The present state of industrial statistics,” *Quality and Reliability Engineering International*, vol. 16, no. 4, pp. 253–254, 2000.

[16] M. M. Gupta and G. N. Saridis, *Fuzzy automata and decision processes*. North Holland, 1977.

[17] S. Kamalasadan, “A new high performance intelligent speed controller for induction motor based on supervisory loops,” in *Power and Energy Society General Meeting-Conversion and Delivery of Electrical Energy in the 21st Century, 2008 IEEE*. IEEE, 2008, pp. 1–7.

[18] C.-H. Chen, C.-M. Lin, and T.-Y. Chen, “Intelligent adaptive control for mimo uncertain nonlinear systems,” *Expert Systems with Applications*, vol. 35, no. 3, pp. 865–877, 2008.

[19] Y. Fu and T. Chai, “Intelligent decoupling control of nonlinear multivariable systems and its application to a wind tunnel system,” *IEEE Transactions on Control Systems Technology*, vol. 17, no. 6, pp. 1376–1384, 2009.

[20] H. Lam, “Sampled-data fuzzy-model-based control systems: stability analysis with consideration of analogue-to-digital converter and digital-to-analogue converter,” *IET control theory & applications*, vol. 4, no. 7, pp. 1131–1144, 2010.

[21] M. R. Adaryani and H. Afrakhte, “Narma-l2 controller for three-area load frequency control,” in *Electrical engineering (ICEE), 2011 19th Iranian conference on*. IEEE, 2011, pp. 1–6.

[22] A. M. Kassem, “Mppt control design and performance improvements of a pv generator powered dc motor-pump system based on artificial neural networks,” *International Journal of Electrical Power & Energy Systems*, vol. 43, no. 1, pp. 90–98, 2012.

[23] P. Menghal and A. J. Laxmi, "Adaptive neuro fuzzy based dynamic simulation of induction motor drives," in *Fuzzy Systems (FUZZ), 2013 IEEE International Conference on*. IEEE, 2013, pp. 1–8.

[24] H. Li, X. Jing, H.-K. Lam, and P. Shi, "Fuzzy sampled-data control for uncertain vehicle suspension systems," *IEEE Transactions on Cybernetics*, vol. 44, no. 7, pp. 1111–1126, 2014.

[25] A. Sallama, M. Abbod, and G. Taylor, "Supervisory power system stability control using neuro-fuzzy system and particle swarm optimization algorithm," in *Power Engineering Conference (UPEC), 2014 49th International Universities*. IEEE, 2014, pp. 1–6.

[26] J. Darvill, A. Tisan, and M. Cirstea, "An anfis-pi based boost converter control scheme," in *Industrial Informatics (INDIN), 2015 IEEE 13th International Conference on*. IEEE, 2015, pp. 632–639.

[27] I. Pan and S. Das, "Fractional order fuzzy control of hybrid power system with renewable generation using chaotic pso," *ISA transactions*, vol. 62, pp. 19–29, 2016.

[28] N. Mahmud, A. Zahedi, and A. Mahmud, "A cooperative operation of novel pv inverter control scheme and storage energy management system based on anfis for voltage regulation of grid-tied pv system," *IEEE Transactions on Industrial Informatics*, 2017.

[29] S. Skogestad, "Dynamics and control of distillation columns-a critical survey," *IFAC Proceedings Volumes*, vol. 25, no. 5, pp. 11–35, 1992.

[30] A. Gorak and H. Schoenmakers, *Distillation: Operation and applications*. Academic Press, 2014.

[31] Ö. Yildirim, A. A. Kiss, and E. Y. Kenig, "Dividing wall columns in chemical process industry: a review on current activities," *Separation and Purification Technology*, vol. 80, no. 3, pp. 403–417, 2011.

[32] N. Sharma and K. Singh, "Control of reactive distillation column: a review," *International Journal of Chemical Reactor Engineering*, vol. 8, no. 1, 2010.

[33] W. Luyben, "Feedback control of distillation columns by double differential temperature control," *Industrial & Engineering Chemistry Fundamentals*, vol. 8, no. 4, pp. 739–744, 1969.

[34] W. Luyben., "Profile position control of distillation columns with sharp temperature profiles," *AIChE Journal*, vol. 18, no. 1, pp. 238–240, 1972.

[35] R. Wood and M. Berry, "Terminal composition control of a binary distillation column," *Chemical Engineering Science*, vol. 28, no. 9, pp. 1707–1717, 1973.

[36] C. Fuentes and W. L. Luyben, "Control of high-purity distillation columns," *Industrial & Engineering Chemistry Process Design and Development*, vol. 22, no. 3, pp. 361–366, 1983.

[37] S. Skogestad and M. Morari, "Lv-control of a high-purity distillation column," *Chemical Engineering Science*, vol. 43, no. 1, pp. 33–48, 1988.

[38] C. A. Ruiz, I. Cameron, and R. Gani, "A generalized dynamic model for distillation columns—iii. study of startup operations," *Computers & chemical engineering*, vol. 12, no. 1, pp. 1–14, 1988.

[39] M. V. Finco, W. L. Luyben, and R. E. Polleck, "Control of distillation columns with low relative volatilities," *Industrial & engineering chemistry research*, vol. 28, no. 1, pp. 75–83, 1989.

[40] C. A. Muhrer, M. A. Collura, and W. L. Luyben, "Control of vapor recompression distillation columns," *Industrial & engineering chemistry research*, vol. 29, no. 1, pp. 59–71, 1990.

[41] T. Mejdell and S. Skogestad, "Estimation of distillation compositions from multiple temperature measurements using partial-least-squares regression," *Industrial & Engineering Chemistry Research*, vol. 30, no. 12, pp. 2543–2555, 1991.

[42] P. S. Fruehauf and D. P. Mahoney, "Distillation column control design using steady state models: Usefulness and limitations," *ISA Transactions*, vol. 32, no. 2, pp. 157–175, 1993.

[43] M. Barolo, G. Guarise, S. Rienzi, and A. Trotta, "On-line startup of a distillation column using generic model control," *Computers & chemical engineering*, vol. 17, pp. S349–S354, 1993.

[44] S. Ganguly and D. N. Saraf, "Startup of a distillation column using nonlinear analytical model predictive control," *Industrial & engineering chemistry research*, vol. 32, no. 8, pp. 1667–1675, 1993.

[45] T. Mejdell and B.-O. Andersson, "Using temperature profile for product quality estimation on a distillation column," *ISA Transactions*, vol. 33, no. 1, pp. 27–34, 1994.

[46] M. Barolo, G. B. Guarise, S. A. Rienzi, and A. Trotta, "Nonlinear model-based startup and operation control of a distillation column: an experimental study," *Industrial & engineering chemistry research*, vol. 33, no. 12, pp. 3160–3167, 1994.

[47] J. C. MacMurray and D. Himmelblau, "Modeling and control of a packed distillation column using artificial neural networks," *Computers & chemical engineering*, vol. 19, no. 10, pp. 1077–1088, 1995.

[48] S. Ramchandran and R. R. Rhinehart, "A very simple structure for neural network control of distillation," *Journal of Process Control*, vol. 5, no. 2, pp. 115–128, 1995.

[49] R. Luo, H. Shao, and Z. Zhang, "Fuzzy-neural-net-based inferential control for a high-purity distillation column," *Control Engineering Practice*, vol. 3, no. 1, pp. 31–40, 1995.

[50] I. J. Halvorsen and S. Skogestad, "Optimizing control of petlyuk distillation: Understanding the steady-state behavior," *Computers & chemical engineering*, vol. 21, pp. S249–S254, 1997.

[51] P. Dutta and R. R. Rhinehart, "Application of neural network control to distillation and an experimental comparison with other advanced controllers," *ISA transactions*, vol. 38, no. 3, pp. 251–278, 1999.

[52] R. Henry and I. Mujtaba, "Distillation column control: the use of feed temperature to respond to modest variations in feed composition," *Computers & Chemical Engineering*, vol. 23, pp. S265–S268, 1999.

[53] A. M. F. Fileti, L. S. Pedrosa, and J. A. Pereira, "A self tuning controller for multicomponent batch distillation with soft sensor inference based on a neural network," *Computers & Chemical Engineering*, vol. 23, pp. S261–S264, 1999.

[54] R. Ross, V. Bansal, J. Perkins, E. Pistikopoulos, G. Koot, and J. Van Schijndel, "Optimal design and control of an industrial distillation system," *Computers & Chemical Engineering*, vol. 23, pp. S875–S878, 1999.

[55] J. F. de Canete, T. Cordero, D. Guijas, and J. Alarcon, "An adaptive neuro-fuzzy approach to control a distillation column," *Neural Computing & Applications*, vol. 9, no. 3, pp. 211–217, 2000.

[56] M. Mahfouf, D. Linkens, and M. Abbod, "Adaptive fuzzy tsk model-based predictive control using a carima model structure," *Chemical Engineering Research and Design*, vol. 78, no. 4, pp. 590–596, 2000.

[57] H. Bloemen, C. Chou, T. Van den Boom, V. Verdult, M. Verhaegen, and T. Backx, "Wiener model identification and predictive control for dual composition control of a distillation column," *Journal of Process control*, vol. 11, no. 6, pp. 601–620, 2001.

[58] M. Alpbaz, S. Karacan, Y. Cabbar, and H. Hapoğlu, "Application of model predictive control and dynamic analysis to a pilot distillation column and experimental verification," *Chemical Engineering Journal*, vol. 88, no. 1, pp. 163–174, 2002.

[59] D. Osorio, R. Pérez-Correa, A. Belancic, and E. Agosin, "Rigorous dynamic modeling and simulation of wine distillations," *Food Control*, vol. 15, no. 7, pp. 515–521, 2004.

[60] U. Volk, D.-W. Kniese, R. Hahn, R. Haber, and U. Schmitz, "Optimized multivariable predictive control of an industrial distillation column considering hard and soft constraints," *Control Engineering Practice*, vol. 13, no. 7, pp. 913–927, 2005.

[61] V. Singh, I. Gupta, and H. Gupta, "Ann based estimator for distillation—inferential control," *Chemical Engineering and Processing: Process Intensification*, vol. 44, no. 7, pp. 785–795, 2005.

[62] A. N. Fard, M. Shahbazian, and M. Hadian, "Adaptive fuzzy controller based on cuckoo optimization algorithm for a distillation column," in *Computational Intelligence and Applications (ICCIA), 2016 International Conference on*. IEEE, 2016, pp. 93–97.

[63] T. T. Tuan, L. D. Tufa, M. I. A. Mutalib, and A. F. M. Abdallah, "Control of depropanizer in dynamic hysys simulation using mpc in matlab-simulink," *Procedia Engineering*, vol. 148, pp. 1104–1111, 2016.

[64] S. Tututi-Avila, L. A. Domínguez-Díaz, N. Medina-Herrera, A. Jiménez-Gutiérrez, and J. Hahn, "Dividing-wall columns: Design and control of a kaibel and a satellite distillation column for btx separation," *Chemical Engineering and Processing: Process Intensification*, vol. 114, pp. 1–15, 2017.

[65] B. Shi, X. Yang, and L. Yan, "Optimization of a crude distillation unit using a combination of wavelet neural network and line-up competition algorithm," *Chinese Journal of Chemical Engineering*, 2017.

[66] P. Antsaklis *et al.*, "Defining intelligent control," *Report of the Task Force on Intelligent Control, IEEE Control Systems*, pp. 0272–1708, 1994.

[67] K. M. Passino, "Intelligent control: An overview of techniques," pp. 104–133, 2001.

[68] T. N. Nguyen and H. E. Stephanou, "An introduction to intelligent and autonomous control," *Kluwer Academic Publishers*, pp. 319–347, 1993.

[69] A. T. Azar and S. Vaidyanathan, *Advances in chaos theory and intelligent control*. Springer, 2016, vol. 337.

[70] Y.-Z. Lu, *Industrial intelligent control: fundamentals and applications*. John Wiley & Sons, 1996.

[71] D. E. Rumelhart, J. L. McClelland, P. R. Group *et al.*, *Parallel distributed processing*. MIT press Cambridge, MA, USA:, 1987, vol. 1.

[72] G. C. Goodwin, S. F. Graebe, and M. E. Salgado, "Control system design," *Upper Saddle River*, 2001.

[73] W. He, Y. Chen, and Z. Yin, "Adaptive neural network control of an uncertain robot with full-state constraints," *IEEE Transactions on Cybernetics*, vol. 46, no. 3, pp. 620–629, 2016.

[74] M. A. Hussain, "Review of the applications of neural networks in chemical process control—simulation and online implementation," *Artificial intelligence in engineering*, vol. 13, no. 1, pp. 55–68, 1999.

[75] A. Khosravi, S. Nahavandi, D. Creighton, and A. F. Atiya, "Comprehensive review of neural network-based prediction intervals and new advances," *IEEE Transactions on neural networks*, vol. 22, no. 9, pp. 1341–1356, 2011.

[76] A. Afram, F. Janabi-Sharifi, A. S. Fung, and K. Raahemifar, "Artificial neural network (ann) based model predictive control (mpc) and optimization of hvac systems: A state of the art review and case study of a residential hvac system," *Energy and Buildings*, vol. 141, pp. 96–113, 2017.

[77] M. Hagan, *Neural network design*. Martin Hagan, 2014.

[78] M. H. Beale, M. T. Hagan, and H. B. Demuth, *Neural network toolbox user's guide*. MathWork, 2017.

[79] D. W. Patterson, *Artificial neural networks: theory and applications*. Prentice Hall PTR, 1998.

[80] K. J. Hunt, D. Sbarbaro, R. Żbikowski, and P. J. Gawthrop, "Neural networks for control systems—a survey," *Automatica*, vol. 28, no. 6, pp. 1083–1112, 1992.

[81] P. M. Nørgård, O. Ravn, N. K. Poulsen, and L. K. Hansen, *Neural Networks for Modelling and Control of Dynamic Systems-A Practitioner's Handbook*. Springer-London, 2000.

[82] K. S. Narendra and S. Mukhopadhyay, "Adaptive control using neural networks and approximate models," *IEEE Transactions on neural networks*, vol. 8, no. 3, pp. 475–485, 1997.

[83] L. A. Zadeh, "Fuzzy logic," *Computer*, vol. 21, no. 4, pp. 83–93, 1988.

[84] K. Uçak and G. Ö. Günel, "A novel adaptive narma-l2 controller based on online support vector regression for nonlinear systems," *Neural Processing Letters*, vol. 44, no. 3, pp. 857–886, 2016.

[85] L. A. Zadeh., "Fuzzy sets," *Information and control*, vol. 8, no. 3, pp. 338–353, 1965.

[86] R. E. Precup, H. Hellendoorn, R. Jain, N. Sivakumaran, and T. K. Radhakrishnan, "World Economic and Social Survey 2013," *Computers in Industry*, vol. 38, no. 3, pp. 1–175, 2011.

[87] K. Tai, A.-R. El-Sayed, M. Biglarbegian, C. I. Gonzalez, O. Castillo, and S. Mahmud, "Review of recent type-2 fuzzy controller applications," *Algorithms*, vol. 9, no. 2, p. 39, 2016.

[88] K. Lochan and B. Roy, "Control of two-link 2-dof robot manipulator using fuzzy logic techniques: A review," in *Proceedings of Fourth International Conference on Soft Computing for Problem Solving*. Springer, 2015, pp. 499–511.

[89] T. Takagi and M. Sugeno, "Fuzzy identification of systems and its applications to modeling and control," *IEEE transactions on systems, man, and cybernetics*, no. 1, pp. 116–132, 1985.

[90] I. MathWorks, *Fuzzy Logic ToolboxTM User's Guide*. Mathworks, Incorporated, 2017.

[91] E. H. Mamdani and S. Assilian, "An experiment in linguistic synthesis with a fuzzy logic controller," *International journal of man-machine studies*, vol. 7, no. 1, pp. 1–13, 1975.

[92] M. Sugeno, *Industrial applications of fuzzy control*. Elsevier Science Inc., 1985.

[93] K. M. Passino, S. Yurkovich, and M. Reinfrank, *Fuzzy control*. Addison-wesley Reading, MA, 1998, vol. 20.

[94] L.-X. Wang, "Fuzzy systems are universal approximators," in *Fuzzy Systems, 1992., IEEE International Conference on*. IEEE, 1992, pp. 1163–1170.

[95] W. Z. Qiao and M. Mizumoto, "Pid type fuzzy controller and parameters adaptive method," *Fuzzy sets and systems*, vol. 78, no. 1, pp. 23–35, 1996.

[96] J.-S. R. Jang *et al.*, "Fuzzy modeling using generalized neural networks and kalman filter algorithm." in *AAAI*, vol. 91, 1991, pp. 762–767.

[97] J.-S. R. Jang, C.-T. Sun, and E. Mizutani, *Neuro-fuzzy and soft computing: a computational approach to learning and machine intelligence*. prentice hall, 1997.

[98] R. T. Marler and J. S. Arora, "Survey of multi-objective optimization methods for engineering," *Structural and multidisciplinary optimization*, vol. 26, no. 6, pp. 369–395, 2004.

[99] Y. C. Shin and C. Xu, *Intelligent systems: modeling, optimization, and control*. CRC press, 2008, vol. 30.

[100] J. H. Holland, *Adaptation in natural and artificial systems: an introductory analysis with applications to biology, control, and artificial intelligence*. MIT press, 1992.

[101] L. J. Fogel, *Intelligence through simulated evolution: forty years of evolutionary programming*. John Wiley & Sons, Inc., 1999.

[102] M. Maarouf, A. Sosa, B. Galván, D. Greiner, G. Winter, M. Mendez, and R. Aguasca, "The role of artificial neural networks in evolutionary optimisation: a review," in *Advances in Evolutionary and Deterministic Methods for Design, Optimization and Control in Engineering and Sciences*. Springer, 2015, pp. 59–76.

[103] Z. Michalewicz, *Genetic algorithms+ data structures= evolution programs*. Springer Science & Business Media, 2013.

[104] R. Kennedy, "J. and eberhart, particle swarm optimization," in *Proceedings of IEEE International Conference on Neural Networks IV, pages*, vol. 1000, 1995.

[105] M. Dorigo and L. M. Gambardella, "Ant colony system: a cooperative learning approach to the traveling salesman problem," *IEEE Transactions on evolutionary computation*, vol. 1, no. 1, pp. 53–66, 1997.

[106] B. Sun, L. Li, and H. Chen, "Shortest path routing optimization algorithms based on genetic algorithms," *Computer Engineering*, vol. 31, no. 6, pp. 142–144, 2005.

[107] H. Tamaki, H. Kita, and S. Kobayashi, "Multi-objective optimization by genetic algorithms: A review," in *Evolutionary Computation, 1996., Proceedings of IEEE International Conference on*. IEEE, 1996, pp. 517–522.

[108] M. Srinivas and L. M. Patnaik, "Genetic algorithms: A survey," *computer*, vol. 27, no. 6, pp. 17–26, 1994.

[109] J. Zhang, J. Zhuang, H. Du *et al.*, "Self-organizing genetic algorithm based tuning of pid controllers," *Information Sciences*, vol. 179, no. 7, pp. 1007–1018, 2009.

[110] H. B. Gürocak, "A genetic-algorithm-based method for tuning fuzzy logic controllers," *Fuzzy sets and systems*, vol. 108, no. 1, pp. 39–47, 1999.

[111] F. Herrera, M. Lozano, and J. L. Verdegay, "Tuning fuzzy logic controllers by genetic algorithms," *International Journal of Approximate Reasoning*, vol. 12, no. 3-4, pp. 299–315, 1995.

[112] I. Pan, S. Das, and A. Gupta, "Tuning of an optimal fuzzy pid controller with stochastic algorithms for networked control systems with random time delay," *ISA transactions*, vol. 50, no. 1, pp. 28–36, 2011.

[113] T. L. Seng, M. Khalid, and R. Yusof, "Self-tuning neuro-fuzzy controller by genetic algorithm with application to a coupled-tank," *IFAC Proceedings Volumes*, vol. 30, no. 25, pp. 29–34, 1997.

[114] R. Eberhart and J. Kennedy, "A new optimizer using particle swarm theory," in *Micro Machine and Human Science, 1995. MHS'95., Proceedings of the Sixth International Symposium on*. IEEE, 1995, pp. 39–43.

[115] R. C. Eberhart, Y. Shi, and J. Kennedy, *Swarm intelligence*. Elsevier, 2001.

[116] V. Kothari, J. Anuradha, S. Shah, and P. Mittal, "A survey on particle swarm optimization in feature selection," *Global Trends in Information Systems and Software Applications*, pp. 192–201, 2012.

[117] Y.-M. Jau, K.-L. Su, C.-J. Wu, and J.-T. Jeng, "Modified quantum-behaved particle swarm optimization for parameters estimation of generalized nonlinear multi-regressions model based on choquet integral with outliers," *Applied Mathematics and Computation*, vol. 221, pp. 282–295, 2013.

[118] J. Kennedy, "Bare bones particle swarms," in *Swarm Intelligence Symposium, 2003. SIS'03. Proceedings of the 2003 IEEE*. IEEE, 2003, pp. 80–87.

[119] L.-Y. Chuang, S.-W. Tsai, and C.-H. Yang, "Chaotic catfish particle swarm optimization for solving global numerical optimization problems," *Applied Mathematics and Computation*, vol. 217, no. 16, pp. 6900–6916, 2011.

[120] Y. Zhang, S. Wang, and G. Ji, "A comprehensive survey on particle swarm optimization algorithm and its applications," *Mathematical Problems in Engineering*, vol. 2015, 2015.

[121] C. L. Smith, *Distillation control: An engineering perspective*. John Wiley & Sons, 2012.

[122] W. L. Luyben, "Design and control of dual condensers in distillation columns," *Chemical Engineering and Processing: Process Intensification*, vol. 74, pp. 106–114, 2013.

[123] A. R. C. Charles H. Corwin, *Introductory Chemistry: Concepts & Connections, 5th Edition*, 5th ed. Pearson, 2008.

[124] A. A. Kiss, *Advanced distillation technologies: design, control and applications*. John Wiley & Sons, 2013.

[125] W. L. Luyben, *Process modeling, simulation and control for chemical engineers*. McGraw-Hill Higher Education, 1989.

[126] H. Klee, *Simulation of dynamic systems with MATLAB and Simulink*. CRC Press, 2007.

[127] S. Skogestad, "Dynamics and control of distillation columns: A tutorial introduction," *Chemical Engineering Research and Design*, vol. 75, no. 6, pp. 539–562, 1997.

[128] K. K. Tan, Q.-G. Wang, and C. C. Hang, *Advances in PID control*. Springer Science & Business Media, 2012.

[129] D. E. Seborg, D. A. Mellichamp, T. F. Edgar, and F. J. Doyle III, *Process dynamics and control*. John Wiley & Sons, 2010.

[130] J. G. Ziegler and N. B. Nichols, "Optimum settings for automatic controllers," *trans. ASME*, vol. 64, no. 11, 1942.

[131] L. Zheng, "A practical guide to tune of proportional and integral (pi) like fuzzy controllers," in *Fuzzy Systems, 1992., IEEE International Conference on*. IEEE, 1992, pp. 633–640.

[132] C. Batur and V. Kasparian, "Predictive fuzzy expert controllers," *Computers & industrial engineering*, vol. 20, no. 2, pp. 199–209, 1991.

[133] A. Ollero and A. Garcia-Cerezo, "Direct digital control, auto-tuning and supervision using fuzzy logic," *Fuzzy Sets and Systems*, vol. 30, no. 2, pp. 135–153, 1989.

[134] P. Xian-Tu, "Generating rules for fuzzy logic controllers by functions," *Fuzzy sets and systems*, vol. 36, no. 1, pp. 83–89, 1990.

[135] Z.-W. Woo, H.-Y. Chung, and J.-J. Lin, "A pid type fuzzy controller with self-tuning scaling factors," *Fuzzy sets and systems*, vol. 115, no. 2, pp. 321–326, 2000.

[136] S. Aksoy and R. M. Haralick, "Feature normalization and likelihood-based similarity measures for image retrieval," *Pattern recognition letters*, vol. 22, no. 5, pp. 563–582, 2001.

[137] Y. Al-Dunainawi, M. F. Abbod, and A. Jizany, "A new mimo anfis-pso based narma-l2 controller for nonlinear dynamic systems," *Engineering Applications of Artificial Intelligence*, vol. 62, pp. 265–275, 2017.

[138] Monro, "USA Patent," 1933.

[139] R. Wright, "USA Patent," 1949.

[140] G. Kaibel, "Distillation columns with vertical partitions," *Chemical engineering & technology*, vol. 10, no. 1, pp. 92–98, 1987.

[141] I. J. Halvorsen and S. Skogestad, "Minimum Energy for the four-product Kaibel-column," *AIChE Annual Meeting Conference Proceedings*, pp. 216d/1 – 216d/8, 2006.

[142] M. Ghadrdan, I. J. Halvorsen, and S. Skogestad, "Optimal operation of Kaibel distillation columns," *Chemical Engineering Research and Design*, vol. 89, no. 8, pp. 1382–1391, 2011.

[143] D. Petlyuk, FB and Platonov, VM and Slavinskii, "Thermodynamically optimal method for separating multicomponent mixtures," *Int. Chem. Eng.*, vol. 5, pp. 555–561, 1965.

[144] M. A. Schultz, D. G. Stewart, J. M. Harris, S. P. Rosenblum, M. S. Shakur, and D. E. O'BRIEN, "Reduce costs with dividing-wall columns," *Chemical engineering progress*, vol. 98, no. 5, pp. 64–71, 2002.

[145] I. Dejanović, L. Matijašević, and Ž. Olujić, "Dividing wall column—a breakthrough towards sustainable distilling," *Chemical Engineering and Processing: Process Intensification*, vol. 49, no. 6, pp. 559–580, 2010.

[146] J. Strandberg, S. Skogestad, and I. J. Halvorsen, "Practical control of dividing wall columns," *Proceedings of distillation and Absorption*, pp. 527–532, 2010.

[147] M. Kvernland, I. Halvorsen, and S. Skogestad, "Model predictive control of a kaibel distillation column," *IFAC Proceedings Volumes*, vol. 43, no. 5, pp. 553–558, 2010.

[148] R. Perry, D. Green, and J. Maloney, "Perry's chemical engineers' handbook. mcgrw-hill," 2008.

[149] J. Strandberg and S. Skogestad, "Stabilizing operation of a 4-product integrated kaibel column," in *Institution of Chemical Engineers Symposium Series*, vol. 152. Institution of Chemical Engineers; 1999, 2006, p. 638.

[150] J.-S. Jang, "Input selection for anfis learning," in *Fuzzy Systems, 1996., Proceedings of the Fifth IEEE International Conference on*, vol. 2. IEEE, 1996, pp. 1493–1499.

[151] S. Skogestad, "The dos and don'ts of distillation column control," *Chemical Engineering Research and Design*, vol. 85, no. 1, pp. 13–23, 2007.

[152] J. P. Strandberg, *Optimal operation of dividing wall columns*. Norges teknisk-naturvitenskapelige universitet, Fakultet for naturvitenskap og teknologi, Institutt for kjemisk prosessteknologi, 2011.

[153] M. A. Mutalib and R. Smith, "Operation and control of dividing wall distillation columns: Part 1: Degrees of freedom and dynamic simulation," *Chemical Engineering Research and Design*, vol. 76, no. 3, pp. 308–318, 1998.

Appendix A

The Nominal Values of the Simulated Distillation Columns

Table A.1 The nominal values of liquid composition at every stage of the simulated binary distillation column

Stage	x_i	**Stage**	x_i
$Boiler(xB)$	0.02000	11	0.51526
1	0.03500	12	0.56295
2	0.57149	13	0.61896
3	0.08885	14	0.68052
4	0.13180	15	0.74345
5	0.18622	16	0.80319
6	0.24951	17	0.85603
7	0.31618	18	0.89995
8	0.37948	19	0.93458
9	0.43391	20	0.96079
10	0.47688	$Condenser(xD)$	0.98000

Table A.2 The nominal values of temperature at every stage of the simulated multicomponent distillation column

Stage	Temp. (K)	Stage	Temp. (K)	Stage	Temp. (K)	Stage	Temp. (K)
1	346.10741	17	368.29441	33	345.73055	49	379.63715
2	346.95961	18	370.21714	34	346.86868	50	382.65678
3	347.47748	19	371.69589	35	347.95288	51	385.44185
4	347.86275	20	372.77083	36	348.90728	52	387.5712
5	348.24305	21	373.57299	37	349.69666	53	388.98319
6	348.70195	22	374.29894	38	350.3337	54	389.83418
7	349.29754	23	375.23959	39	350.87971	55	390.31786
8	350.06888	24	376.84166	40	351.45713	56	390.58366
9	351.03997	25	338.2498	41	370.57766	57	352.29346
10	352.23668	26	338.59788	42	370.95086	58	353.62579
11	353.73443	27	339.11085	43	371.25386	59	355.83088
12	355.74109	28	339.8337	44	371.64387	60	359.09124
13	358.63891	29	340.79227	45	372.26695	61	362.92439
14	361.0945	30	341.96901	46	373.29941	62	366.29955
15	363.56288	31	343.28873	47	374.914	63	368.58295
16	366.01519	32	344.63256	48	377.12501	64	369.87997

Appendix B

The Tuned MFs and Surfs of the ANFIS_based NARMA-L2 Controller

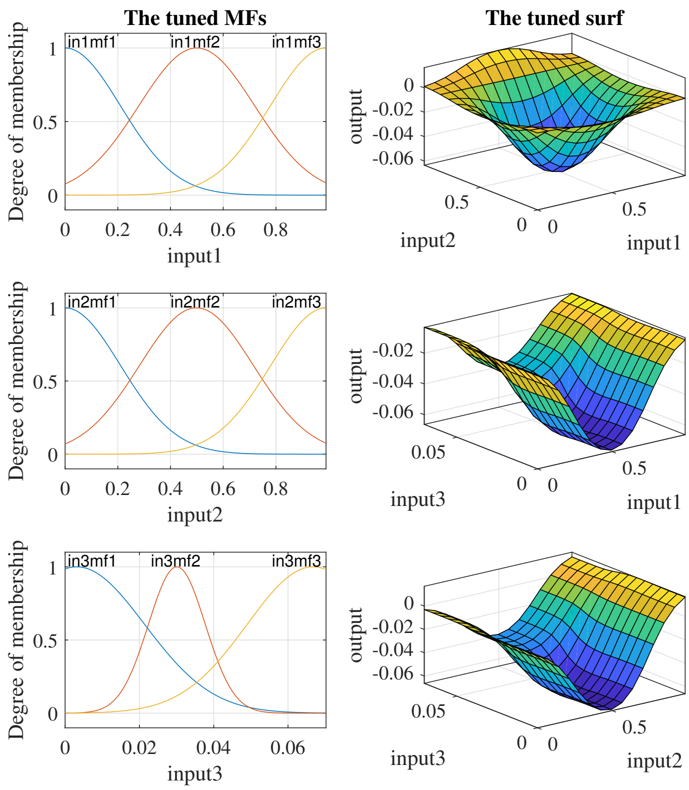

Figure B.1 PSO-tuned MFs and surf of FIS_2

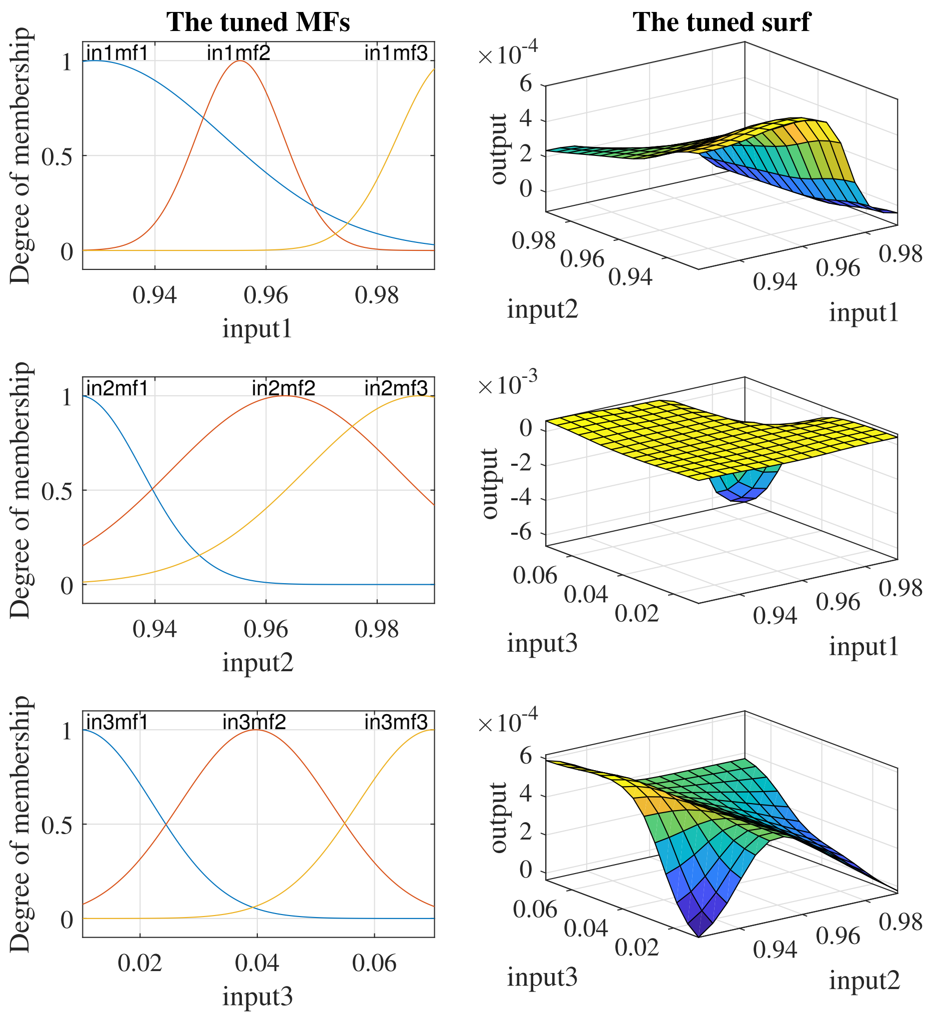

Figure B.2 PSO-tuned MFs and surf of FIS_3

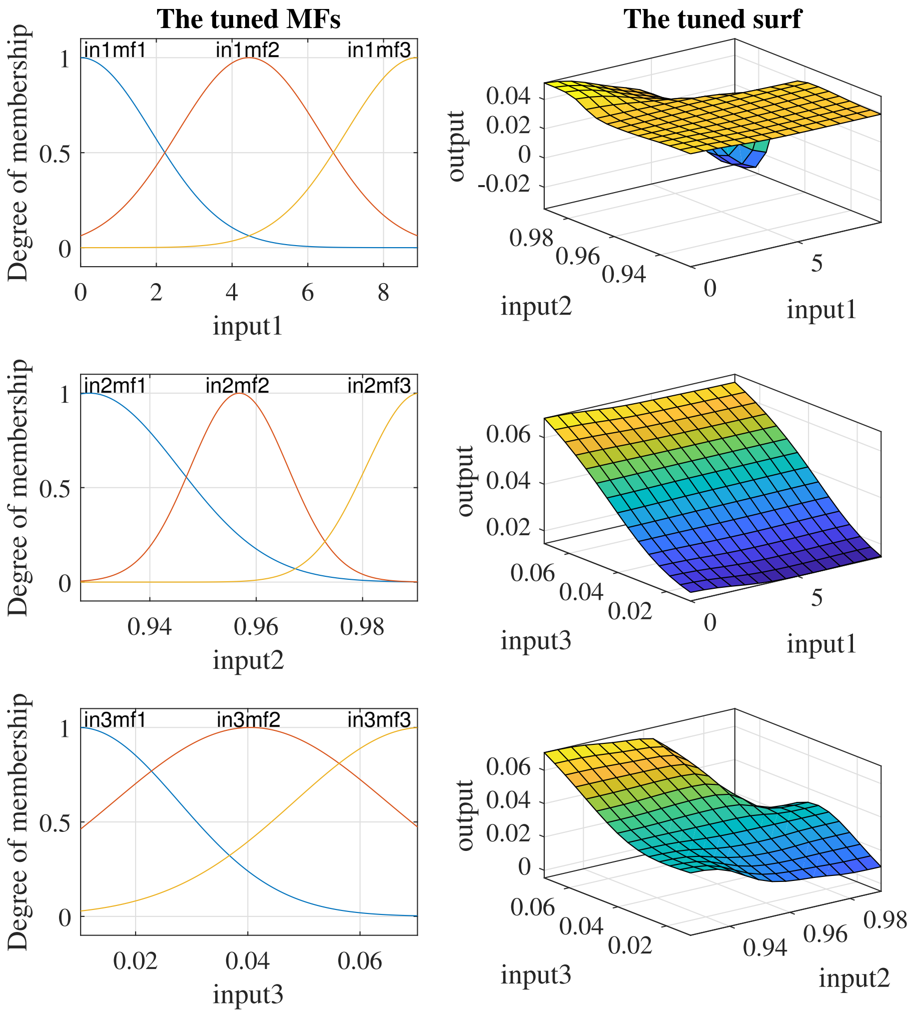

Figure B.3 PSO-tuned MFs and surf of FIS_4

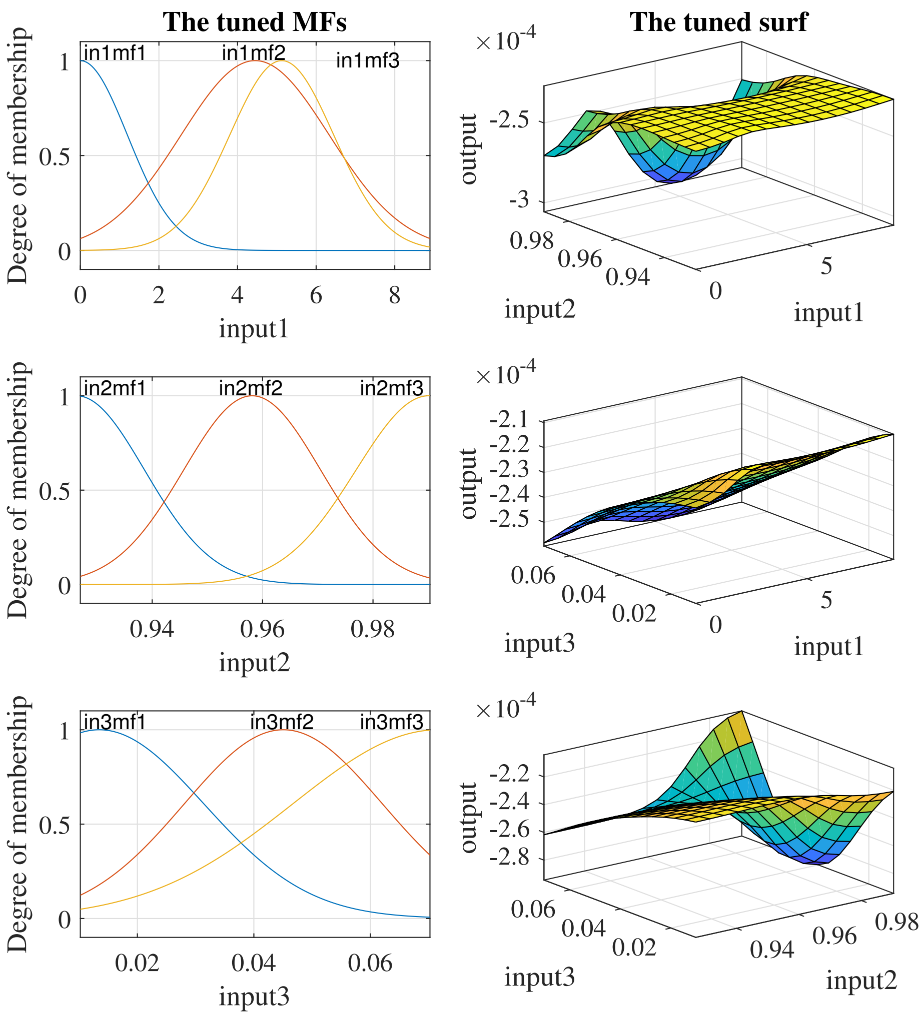

Figure B.4 PSO-tuned MFs and surf of FIS_5

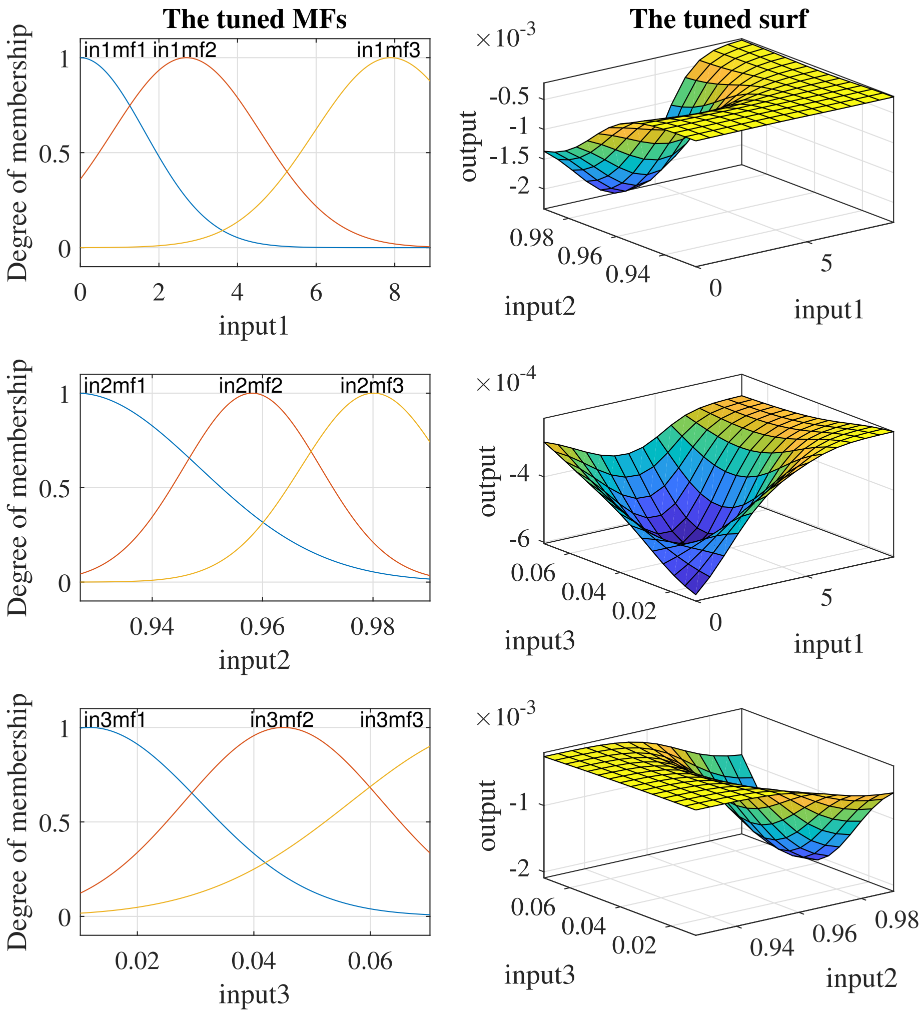

Figure B.5 PSO-tuned MFs and surf of FIS_6

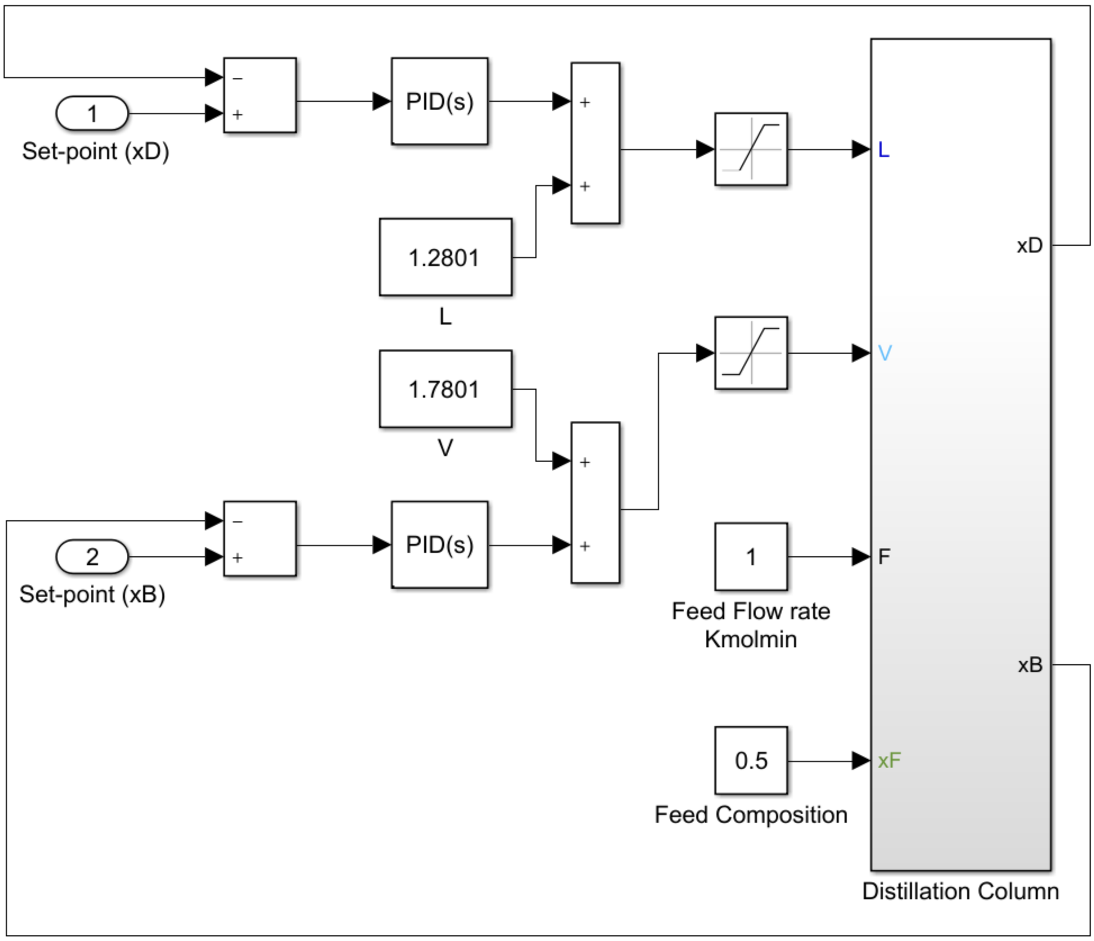

Figure B.6 Simulation of a binary distillation column controlled by PID controllers

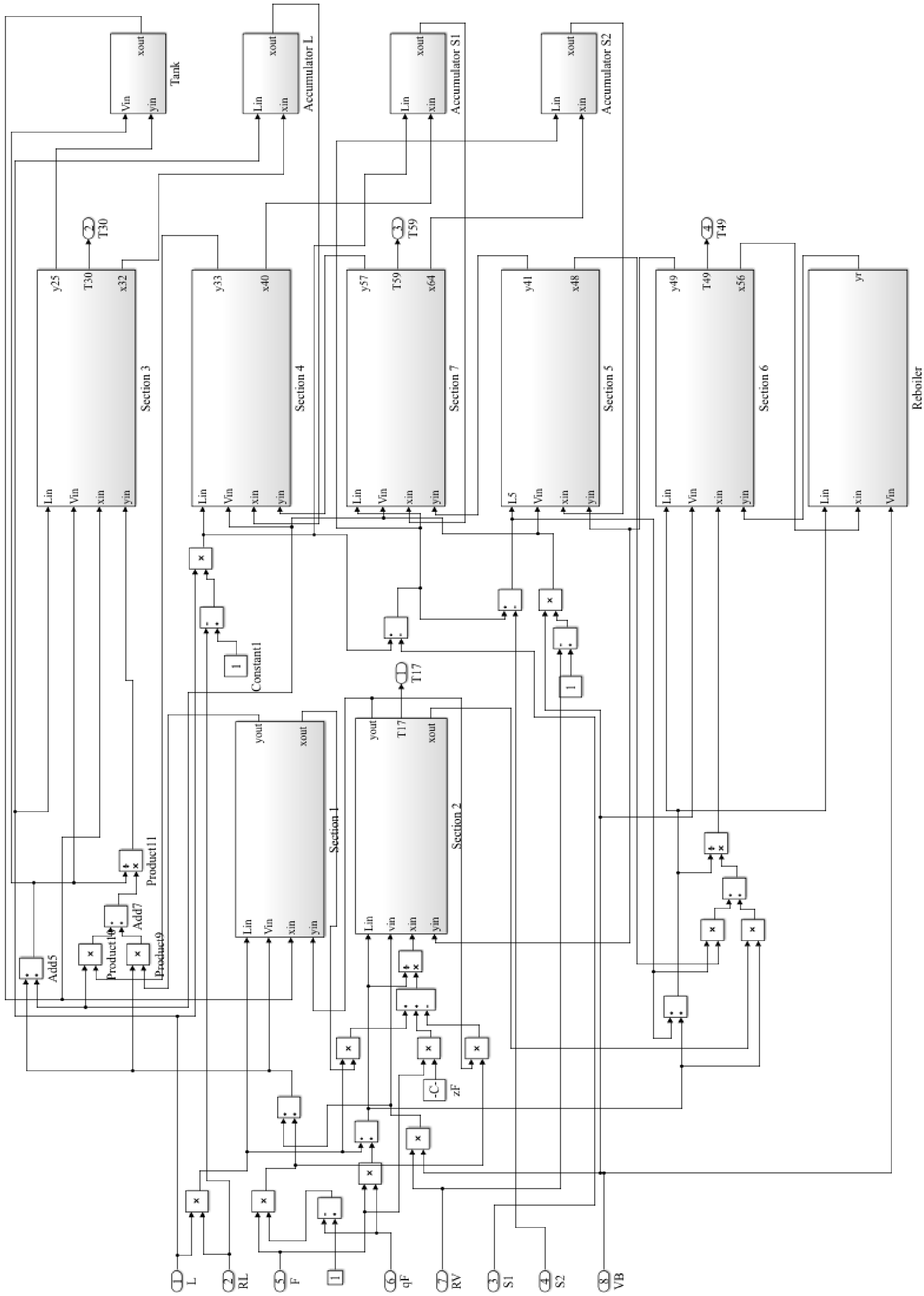

Figure B.7 Simulink block diagram of the Kaibel distillation column